RESEARCH & DEVELOPMENT

Protocol for Outlet Analysis at Highway Sites

William F. Hunt III, PhD, PE, D.WRE

Sarah Waickowski, PE

Department of Biological and Agricultural Engineering

North Carolina State University

Technical Report Documentation Page

1. Report No. 2019-02	2. Government Accession No.	3. Recipient's Catalog No.
4. Title and Subtitle Protocol for Outlet Analysis at Highway Sites		5. Report Date January 16, 2023 6. Performing Organization Code
7. Author(s) William F. Hunt III, PhD, PE, D.WRE Sarah Waickowski, PE		8. Performing Organization Report No.
9. Performing Organization Name and Address Department of Biological and Agricultural Engineering North Carolina State University Raleigh, NC 27695-7625		10. Work Unit No. (TRAIS) 11. Contract or Grant No. FHWA/NC/20YY-NN
12. Sponsoring Agency Name and Address North Carolina Department of Transportation Research and Development Unit 104 Fayetteville Street Raleigh, North Carolina 27601		13. Type of Report and Period Covered Final Report August 2018- October 2022 14. Sponsoring Agency Code
Supplementary Notes:		

16. Abstract

Stormwater conveyance networks contribute to stream degradation and instability either through direct discharges of sediment or by eroding gullies downslope of pipe outlets. To limit erosion downslope of pipe outlets, current regulations require the 10-yr, 24-hr peak velocity discharged to a vegetated area to be less than the downslope soils' permissible velocity. Otherwise, the conveyance system must be redesigned. The effectiveness of this design standard has not been evaluated. North Carolina State University assessed 60 pipe outlets in the Piedmont and Mountain physiographic regions of North Carolina to identify which watershed and downslope characteristics influence the severity of erosion caused by pipe outlets. The effectiveness of the current standard was also assessed. Six assessed sites in Raleigh were additionally monitored for hydrologic, hydraulic, and water quality impacts. These data were also used to evaluate the effectiveness of a swale with (1) rip-rap, (2) well-established vegetation, (3), check dams with mowed turf grass, and (4) check dams with well-established vegetation to limit downslope erosion. The results indicate the current standard does not limit downslope erosion, and designers should consider limiting the 1-yr, 24-hr peak velocity to the permissible velocity. Designers should also consider the downslope soil and vegetative conditions to reduce the potential for gully erosion. Designers can use the predictive tools developed from the data to help determine the optimal discharge point for pipe outlets. Preliminary results suggest turf grass swales with check dams may mitigate the potential for erosion downslope of pipe outlets. However, this design should be validated with field-scale studies before standards for pipe outlets are revised.

17. Key Words	18. Distribution Statement
Erosion, pipe outlets, bank stability, permissible velocity	

19. Security Classif. (of this report)	20. Security Classif. (of this page)	21. No. of Pages	22. Price
Unclassified	Unclassified	395	

Form DOT F 1700.7 (8-72) **Reproduction of completed page authorized**

DISCLAIMER

The contents of this report reflect the views of the author(s) and not necessarily the views of the University. The author(s) are responsible for the facts and the accuracy of the data presented herein. The contents do not necessarily reflect the official views or policies of either the North Carolina Department of Transportation or the Federal Highway Administration at the time of publication. This report does not constitute a standard, specification, or regulation.

Acknowledgements

North Carolina State University would like to thank NCDOT for funding this project, Erin Cartner for her assistance with data collection and analysis, Thomas Stephenson for his assistance with monitoring equipment installation, and the Center for Applied Aquatic Ecology for performing the water quality analyses. North Carolina State University would also like to thank Drs. Castro-Bolinaga, Doll, Fox, Griffith, and Heitman for their expertise and support given throughout the project.

Executive Summary

Sediment pollution is a worldwide concern, and stormwater conveyance networks contribute to stream degradation and instability either through direct discharges of sediment or by eroding gullies downslope of pipe outlets. To limit erosion downslope of pipe outlets, current North Carolina regulations require designers to limit the peak velocity for the 10-yr, 24-hr storm to the permissible velocity for the downslope soils'; otherwise the conveyance system must be redesigned. This study assessed 60 pipe outlets draining highway and non-highway areas in the Piedmont and Mountain physiographic regions of North Carolina to identify which watershed and downslope characteristics influence the severity of erosion caused by pipe outlets. The effectiveness of the current standard was also assessed. Six assessed sites in Raleigh were additionally monitored for hydrologic, hydraulic, and water quality impacts.

Results from the assessments suggest the current practice of limiting the 10-yr, 24-hr velocity to the permissible velocity does not sufficiently protect against downslope erosion. Forty-eight of the 60 pipe outlets had erosion from the pipe outlet to the outfall (stream). The 12 sites that exhibited little to no erosion had heavy stands of mixed herbaceous and grassed vegetation, a lack of clustered trees, and a large percentage (> 50%) of moderately permeable hydrologic soil group (HSG) B soils downslope of the outlets. A decision tree identifying a gully's stage of degradation was developed using the assessment data. Influential predictors included the ratio between the cross-sectional area at the top of bank and the corresponding bankfull area, radial distance from the pipe outlet to the stream, percentage of HSG C soils downslope of the pipe outlet, and the estimated elevation difference between the pipe outlet and outfall (departure). The decision tree had an accuracy of 39%, which suggests the tree needs more data to correctly predict the true stage of degradation. The assessment data were further used to develop regression equations and decision trees to predict the magnitude of erosion. The magnitude of erosion was defined in terms of the (1) estimated total volume of eroded soil normalized by the channel length and (2) the cross-sectional area, width, and maximum depth at the top of bank normalized by the respective bankfull characteristic. The normalized root means square errors (NRMSEs) for the decision trees and regression equations ranged from 0.07 to 0.24. Values closer to zero indicate a better fit to the data. Additional predictors, such as the age of the pipe installation at the time of assessment, could improve model performance.

Hydrologic data collected from the six sites were modeled in HEC-RAS 6.2 to quantify the hydraulic impacts. The potential maximum ε from steady flow analyses ranged from

$6.06*10^{-4}$ to 0.04 in/s per storm event and indicate designers should include the erodibility of the soils downslope of pipe discharge points in their hydraulic analyses. The mean peak velocities ranged from 1.80 to 10.72 ft/s and exceeded the permissible velocity at least 10 times during the 13-month monitoring period, despite none of the storms exceeding the sites' 10-yr, 24-hr rainfall depth. The gullies downslope of the pipe outlets eroded between 22 and 774 yd^3 of soil. Given the magnitude of erosion downslope of the pipes and reoccurring exceedance of the permissible velocity, limiting the peak velocity for the 1-yr, 24-hr storm event to the permissible velocity may be a more effective standard to protect against downslope erosion. Mean TSS concentrations ranged from 15.1 to 219 mg/L, and concentrations from four outlets exceeded the state's water quality standard for non-trout waters (20 mg/L) by more than 50% of the time. These results indicate pipe outlets draining highway and non-highway areas require additional treatment to meet regulations. four proposed designs were evaluated for the potential to mitigate erosion downslope of pipe outlets using 1D steady and quasi-unsteady HEC-RAS 6.2 models with BSTEM. The designs included a swale with (1) rip-rap, (2) well-established vegetation, (3), check dams with mowed turf grass, and (4) check dams with well-established vegetation. The swales were designed using existing design regulations and tools. Preliminary results suggest turf grass swales with check dams may mitigate potential erosion downslope of pipe outlets. Ultimately, field-scale studies should validate these results before design standards for pipe outlets draining highway and non-highway areas are revised.

Table of Contents

List of Tables

List of Figures

Introduction

Background

Sediment pollution is a worldwide concern, and excess sediment discharged to streams increases turbidity, eutrophication, and the degradation of aquatic health and habitat (Bledsoe et al., 2012; Liu et al., 2015; Marshall et al., 2010; Paul & Meyer, 2001; Shields et al., 2010; Simon & Rinaldi, 2000, 2006; Williams et al., 2022). Causes of excess sediment in water bodies includes streambank erosion exacerbated by stormwater runoff, construction, timber harvesting, and gullies transporting sediment from overland erosion to streams (Bennett et al., 2000; Bledsoe, 2002; Bracken & Croke, 2007; Litschert & MacDonald, 2009; Nehrke & Roesner, 2004; Pomeroy et al., 2008; Roesner et al., 2001; Rohrer & Roesner, 2006; Schueler et al., 2009; Valentin et al., 2003; Vietz et al., 2014; Voli et al., 2013; Walsh et al., 2016; Walsh et al., 2005). In 2022, over 40 waterbodies in North Carolina were impaired for turbidity (NC DEQ, 2022), despite state regulations requiring the total suspended solids (TSS) concentration is no more than 10 mg/L in trout waters and 20 mg/L for other water bodies (*15A NCAC 02B .0101*, 2019). Additional efforts limiting sediment pollution include requiring the use of primary stormwater control measures (SCMs) for stormwater treatment (NC DEQ, 2017). A primary designation indicates the SCM meets the North Carolina Department of Environmental Quality's (NC DEQ) highest thresholds for effluent TSS concentrations. In North Carolina, Voli et al. (2013) found streambank erosion caused by stormwater runoff was the main contributor of excess sediment in three streams that discharge into Falls Lake.

Primary sources of excess sediment

Stormwater runoff and streambank erosion

The detrimental impacts of stormwater runoff on streams is well documented, and urbanization exacerbates these impacts (Bledsoe, 2002; Nehrke & Roesner, 2004; O'Driscoll et al., 2010; Roesner et al., 2001; Schueler et al., 2009; Walsh et al., 2005). Urbanization increases the occurrence and magnitude of runoff, decreases lag times for peak discharges, and alters stream sediment supply, which results in changes to stream geomorphology and macroinvertebrate health. The primary large-scale source driving this degradation are hydraulically efficient stormwater drainage networks.

Previous studies have quantified the threshold for stream degradation in terms of total impervious area (TIA) and directly connected impervious area (DCIA). O'Driscoll et al. (2010) reviewed studies quantifying the impacts of urbanization on streams in the southern United

States and found degradation occurred in watersheds with as little as 6% TIA. Morse et al. (2003) reported similar results for streams draining 20 catchments in Maine. Vietz et al. (2014) evaluated 17 streams in Melbourne, Australia, with varying degrees of TIA and DCIA, for geomorphic changes (e.g., sediment bedload depth, bank stability). Vietz et al. (2014) reported DCIA was a better predictor for degradation compared to TIA, and geomorphic changes occurred in watersheds with at least 3% DCIA. Baruch et al. (2018) evaluated the impacts of directly connected roadways on macroinvertebrate health in seven streams located throughout the Raleigh-Durham metropolitan area in North Carolina. The roads accounted for 7 to 16% of the watersheds and had a surface density between 9.3 and 17 mi/mi^2; the density of conveyance systems directly discharging into the streams was between 0.06 and 4.29 mi/mi^2. Baruch et al. (2018) found macroinvertebrate health decreased with increasing DCIA, and the density of drainage networks and roads were better predictors than TIA for aquatic ecosystem health.

Overland erosion and gullies

Because stormwater conveyance networks concentrate flow, they also degrade streams through the formation of migrating headcuts that result in gullies or channels downslope of pipe outlets. Gullies are typically narrow channels with depths between 1.5 and 98 ft and usually cannot be restored with farming equipment (Bennett & Wells, 2019; Bull & Kirkby, 1997). Headcuts are the result of concentrated flow exceeding the soil's critical shear stress (τ_c), often either creating a waterfall and plunge pool situation or eroding to an impermeable layer (Bennett & Wells, 2019; Douglas-Mankin et al., 2020; Flores-Cervantes et al., 2006). Headcuts will migrate upwards when a backwards eddy forms and forces flow against the foot of the soil's headwall. Migration stops once the soil's resistance to detachment exceeds the flow's shear stress (τ). Soil characteristics that influence the resistance to detachment include the fraction of organic material (OM), clay content, structure, texture, water content (w), permeability and vegetative cover (Allen et al., 2018; Hillel, 2003; Clark & Wynn, 2007; Liu et al., 1999; McCool & Williams, 2008; Smith et al., 2021). The erosion caused by the headcut contributes excess sediment to streams; gullies will help transport sediment caused by upland erosion to receiving channels (Bennett et al., 2000; Bracken & Croke, 2007; Litschert & MacDonald, 2009; Valentin et al., 2003).

Liu et al. (2015) monitored sediment discharge in the South Tobacco Creek watershed in central Canada and found up to 40% of the discharged sediment was the result of upland erosion. Valentin et al. (2003) conducted a literature review of gully erosion rates (ε) and found

gully erosion throughout the United States can result in the loss of 0.22 to 16 ton/ac-yr of soil. This accounts for between 18 to 81% of the total soil lost in the United States each year. Vanmaercke et al. (2016) also evaluated studies quantifying gully ε in terms of volumetric soil loss. Throughout the world, gullies erode between 0.07 and $1.67*10^6$ ft^3/yr; the median ε is 78 ft^3/yr. Valentin et al. (2003) and Vanmaercke et al. (2016) found watershed area and rainfall intensity significantly influence gully ε. Both studies recommended future research to evaluate how soil and vegetative characteristics influence ε as well as determine the thresholds for gully initiation.

Zaimes & Schultz (2012) investigated the impacts of riparian land management on gully erosion in the central, northeastern, and southeastern regions of Iowa. Gully erosion was quantified in terms of length and bank area. The total length of the gullies associated with row-cropped field and grazed pasture management strategies ranged from 56 to 3,530 ft, and the total area of eroding banks was between 43 and 5,038 ft^2. For reaches adjacent to grass filters and riparian forest buffers, the total gully length and eroding bank areas was from 0 to 1,099 ft and 43 and 291 ft^2, respectively.

Zaimes et al. (2009) conducted a similar study in the Southern Iowa Drift Plain of Iowa. Mean ε and eroding bank areas were quantified for three channels adjacent to sections of continuous, rotational, or intensive rotational grazed pastures. The total lengths and eroded bank areas for the continuous, rotational, and intensive rotational reaches were 1,201, 2,251, and 1,322 ft and 2,734, 4,176, and 861 ft^2, respectively. The measured ε for the monitoring period (17 months) for the continuous, rotational, and intensive rotational reaches were 9.65, 5.31, and 4.76 in, respectively.

Dabney et al. (2004) assessed how well switchgrass (Panicum virgatum *L.*) hedges mitigate gully erosion. The hedges were planted at 1.5 ft vertical intervals within one naturally occurring and two constructed gullies. Runoff was simulated during the dormant period of the second growing season to quantify the preliminary design's effectiveness. Erosion was mitigated if the bed slope was less than 33%, and flow depths were less than 1 ft. Results from Dabney et al. (2004), Zaimes & Shultz (2012), and Zaimes et al. (2009) indicate vegetation and channel slope influence the severity of gully erosion.

Quantifying gully erosion

The Universal Soil Loss Equation (USLE) (Wischmeier & Smith, 1978) and its successors, the Revised Universal Soil Loss Equation (RUSLE) (Renard et al., 1997) (Equation 1) and RUSLE2, serve as the basis for models developed specifically for ephemeral gully

erosion (Douglas-Mankin et al., 2020). USLE, RUSLE, and RUSLE2 predict long-term (e.g., 20 years) average annual ε while accounting for climate, soil, topography and land use factors that affect erosion. These models inherently calculate inter-rill and rill erosion but do not allow for the formation of ephemeral gullies, small channels that re-form in the same location after being filled in; rill erosion consists of randomly occurring channels with minimal depth (< 1.5 ft) that can be repaired by typical farming equipment (Bryan, 2000; Owoputi & Stolte, 1995).

$$A = R*K*L*S*C*P \qquad \text{Equation 1}$$

Where:
A = soil loss per unit area in unit time
R = rainfall erosivity factor
K = soil erodibility factor
L = slope length factor
S = slope steepness factor
C = cover management factor
P = soil conservation practice factor

Kinnell (2017) compared erosion simulated by USLE and RUSLE2 to measured erosion from three sites in the central United States. The models' performance was assessed using the Nash-Sutcliffe Efficiency (NSE) metric, where a value of 0.65 or higher indicates the model is good fit to the data (Ritter & Muñoz-Carpena, 2013). The NSEs for the USLE models ranged from 0.47 to 0.67 and were between 0.48 and 0.65 for the RUSLE2 models. The modified USLE (USLE-M) models with observed runoff data had NSEs between 0.55 and 0.89. These results suggest these existing models reliably predict erosion. RUSLE2 and USLE-M allow for the prediction of daily sediment loss and account for sediment deposition; however, these models do not directly include runoff as a factor and assume only one erosive storm event occurs on days with precipitation (Kinnell, 2017).

The Chemicals, Runoff, and Erosion from Agricultural Management Systems (CREAMS) was the first model developed for ephemeral gully erosion. The model uses an iterative process and factors such as drainage area, runoff curve number (CN), evapotranspiration, percolation, seepage, confining layer, length of the gully, ρ_b, and τ_c to calculate sediment loads. The Ephemeral Gully Erosion Model (EGEM) is similar to the CREAMS model but uses regression equations consisting of the peak flow rate (Q_p), gully slope, and τ_c to estimate the final gully's dimensions and sediment load. EGEM also assumes the gully is rectangular, has a constant depth, and the maximum depth to the confining layer is 18 in. Woodward (1999) simulated ε for

over monitored 400 ephemeral gullies across the United States using EGEM. The percent difference between the predicted and measured ε ranged from 4 to 250%. Nachtergaele et al. (2001) compared EGEM simulations for the total volume of eroded soil and cross-sectional changes to data collected from 86 ephemeral gullies located in Portugal and Spain. The relationship between the predicted and measured volumes of eroded soil had a R^2 value of 0.88. However, Nachtergaele et al. (2001) found the relationship between the measured and modeled channel cross-sections only had an R^2 value of 0.27. These studies indicate EGEM is not a reliable predictor for ephemeral gully ε.

The Watershed Erosion Prediction Project (WEPP) directly includes runoff as a factor but requires extensive data and is not considered user-friendly (Ismail & Ravichandran, 2008). Laflen et al. (1997) compared measured annual soil losses to WEPP simulations using data from 544 USLE runoff plots located across the United States. The overall percent difference between the measured and predicted annual soil losses was 10%. Laflen et al. (1997) reported WEPP simulations were the most accurate for plots smaller than 12 ac.

The Revised Ephemeral Gully Erosion Model (REGEM) in Annualized Agricultural Non-Point Source (AnnAGNPS) builds upon CREAMS and EGEM by accounting for plunge pool erosion and headcut retreat (Douglas-Mankin et al. 2020). REGEM does not require the user to specify an ephemeral gully length and treats channel dimensions as a function of discharge. This allows the user to predict channel dimensions at any point in time and space. Gordon et al. (2007) evaluated how well REGEM in AnnAGNPS predicts ephemeral gully length and width using data from four gullies located throughout Mississippi. The RMSEs for gully length and width were 31 and 52%, respectively. Taguas et al. (2010) simulated sediment losses from gullies located in olive orchards in Spain using REGEM in AnnAGNPS. The NSE for the event-based simulations was 0.70 while the NSE for monthly-based simulations was 0.79. Results from Gordon et al. (2007), Kinnell et al. (2017), and Taguas et al. (2010) suggest RUSLE2, USLE-M, and REGEM in AnnAGNPS reliably predict daily ephemeral gully erosion.

Allen et al. (2017) developed a model using the hydrologic results from the Soil & Water Assessment Tool (SWAT) to predict the advancement of gully headcuts. This simple model uses the gully height, total daily discharge, and an erodibility resistance component (Eh_c) to predict headcut migration. The Eh_c is based on a cover-root density factor (0 to 1.4) and the soil's k_d. Allen et al. (2017) found the model realistically predicts headcut migration and recommends using this model as an assessment tool for agricultural lands. Refer to Appendix A

for summary of factors influencing erosion and how existing form- and process-based models quantify streambank erosion.

Limiting erosion downslope of pipe outlets

To limit erosion and additional sediment loads discharged to streams, states such as Maryland provide pollutant removal credits for stabilizing gullies caused by pipe outlets (MDOT SHA, 2018). In North Carolina, engineers are required to limit the discharged peak 10-yr, 24-hr velocity to the maximum permissible velocity for the downslope soil conditions (*15A NCAC 04B .0109*, 1992; Fortier & Scobey, 1926); if the permissible velocity is exceeded, then the conveyance system must be redesigned. Recommended design modifications include energy dissipators, stormwater control measures (SCMs), and the replacement of impervious areas with vegetation. Additionally, efforts to retrofit eroding gullies with regenerative stormwater conveyances (RSCs) have increased over the years (Cizek et al., 2017, 2018; Koryto et al., 2017; Thompson et al., 2020). An RSC is a grade-control system that uses a series of pools riffles, and underlying media to stabilize eroding channels and provide water quality treatment. Through modeling, Thompson et al. (2018) has shown RSCs have the potential to minimize erosive velocities. However, field scale studies have not quantified how well RSCs reduce the potential for erosion.

Result of literature review

Previous research has shown stormwater conveyance systems impact stream stability and aquatic health either through direct discharges or gullies formed downslope of pipe outlets. Regulations exist to minimize the potential for erosion downslope of pipe outlets, but the success of these rules has yet to be quantified. Models predicting overland erosion do not simulate gully erosion, and studies quantifying gully erosion did not identify which watershed and downslope characteristics influence the severity of erosion. In addition, there lacks a form-based model to predict a gully's stage of degradation. Few, if any, studies have recommended design alternatives for pipe outlets to limit downslope erosion or quantify the hydraulic impacts of pipe outlets draining highway and non-highway areas. Several form- and processed-models have successfully determined stream instability. The study herein will use concepts and techniques discussed in the introduction and Appendix A (e.g., USLE, EGEM, bank erosion hazard index) to:

- Establish the current conditions of NCDOT-managed outlets and downslope receiving areas (Objective Two),

- Identify the outlet characteristics impacting the stability of downslope receiving areas (Objective Three),
- Develop and calibrate an outlet analysis protocol (Objective Four),
- Monitor a subset of field-assessed sites for water quality, hydrology, and landscape changes (Objective Five),
- Propose design standards for outlets that minimize overland erosion (Objective Six),
- Perform a cost analysis for the proposed design standards (Objective Seven), and
- Incorporate the project results into a Microsoft Excel-based tool (Objective Eight).

Methods

Objective Two

Study sites

A non-random sample of sixty pipe outlets draining highway and non-highway areas in the Piedmont (50) and Mountain (10) physiographic regions of North Carolina were assessed for downslope erosion (Figure 1). Non-highway refers to any area outside of the NCDOT right-of-way. Over 100 pipe outlets representing a range of watershed areas, downslope conditions, and pipe diameters were initially considered for assessment. Accessibility and safety determined which sites were assessed. At a minimum, conditions were assessed immediately downslope of the pipe outlet, at the adjacent property's furthermost boundary, and at the point of outfall to a receiving surface water. Hereinafter "intermediate" will refer to the adjacent property's furthermost boundary. Publicly available geographic information system (GIS) data for tax parcels determined the property boundaries. Additional evaluations occurred if there was a noticeable change in channel geometry and/or stability.

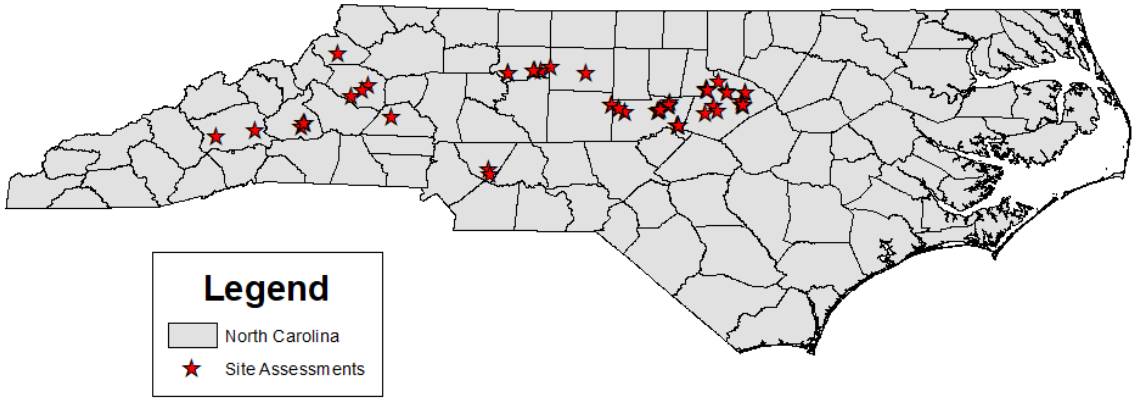

Figure 1. Map of assessed sites

Field measurements

Channel size, soil characteristics, erosion potential, and roughness were estimated immediately below the pipe outlet, at the intermediate location, and at the outfall just upstream of the receiving waterbody. Soil at the bank surface was collected from each visually different layer using a trowel and stored in sealed plastic bags until laboratory testing. Intact soil cores were collected using an AMS hammer corer (ring diameter of 2 in; AMS American Falls, Idaho) and capped with polyethylene lids. The samples were tested for bulk density (ρ_b) (ASTM D7263, 2021) and soil texture (ASTM D7928, 2021). Approximate unconfined compressive strength, the channel's potential for incision (depth to the confining layer) and bank erosion, and the channel's cross-sectional area were measured in the field. The approximate unconfined compressive strength was quantified by taking the median of five HM-500 pocket penetrometer readings (Gilson Company, Inc., Powell, OH) evenly spaced from the top of bank to the toe of slope. Soil measurements were repeated if there were visually different soil layers. Photos of the channel were taken to document vegetative conditions at the time of the assessment; the Manning's roughness coefficient (n) was estimated using these photos (Brunner, 2022). The channel bed's potential for incision or depth to the confining layer was estimated using a 4 ft long soil profile sampler that was hammered into the channel bed until the sampler no longer moved or the handle was flush with the ground. Note soil texture, ρ_b, and the depth to the confining layer were only found for the outlet, intermediate, and outfall cross-sections.

The future potential for bank erosion was estimated using the bank erosion hazard index (BEHI) assessment (Rosgen 2001). BEHI is one of the most common form-based models used to predict future bank erosion. This method consists of seven metrics and requires bank height and angle, root depth and density, and surface protection measurements to assess the bank's erodibility. This method also adjusts for streambank stratification, material, and location within the channel (e.g., pool, riffle, meander). The measurements and adjustments are converted from a score (0 to 50) into an erosion potential index that was developed from field observations of streambank instability. Appendix A includes a summary of these indices and a more in-depth discussion of this method. For these assessments, channel banks covered with rip-rap received BEHI scores 0 and soil texture measurements (ASTM D7928, 2021) were used to refine bank material adjustments. To measure the cross-sectional area, a level wind-up tape measure was secured at the top of bank and a handheld tape measure was placed perpendicular to flow at the height of the level wind-up measure (Harrelson et al., 1994). The depth of channel was

measured in 1 ft increments along the length of the wind-up tape measure. The total volume of eroded soil was estimated using the average end-area method (Equation 1).

$$V = 0.04 \sum_{i-1}^{n} L \frac{A_1 + A_2}{2} \quad \text{Equation 2}$$

Where:
V = total volume of eroded soil (yd^3)
L = channel length between cross-sections (ft^3)
A_1 = upslope cross-sectional area (ft^3)
A_2 = downslope cross-sectional area (ft^3)
n = number of cross-sections

Desktop analyses

Each pipe outlet's watershed area, composite curve number (CN), impervious and non-highway areas, percentage of downslope hydrologic soil groups (HSGs), radial distance from the nearby stream, departure, and peak discharge for the 1-yr and 10-yr, 24-hr storms were found using ArcGIS 10.7.1 (ESRI, 2019) and AutoCAD Civil3D 2020 (Autodesk, 2019) analyses (Homer et al., 2020; NC DPS, 2016; NOAA, 2006; USDA, 2015; USGS, 2018). Non-highway areas were quantified using the delineated watershed and NCDOT ROW GIS shapefiles (NCDOT, 2022). To account for the influence of slope on erosion, departure or the elevation difference between the channel bed at the pipe outlet and outfall was estimated using the most recent digital elevation model (DEM) data and the channel GIS shapefile (NC DPS, 2016). The radial distance of the pipe outlet to the stream was found by drawing a circle or buffer from the end of the pipe GIS shapefile to the nearest National Hydrography dataset (NHD) stream shapefile using the ArcGIS circle tool (Figure 2). The area within the buffer was used to identify the percentage of downslope HSGs. The duration of flow associated with the 1-yr and 10-yr, 24-hr storms were calculated using the equations included in Appendix B (Malcom, 1989; USDA-NRCS, 2004). Pipe slopes were estimated using ArcGIS shapefiles and DEM data (NC DPS, 2016).

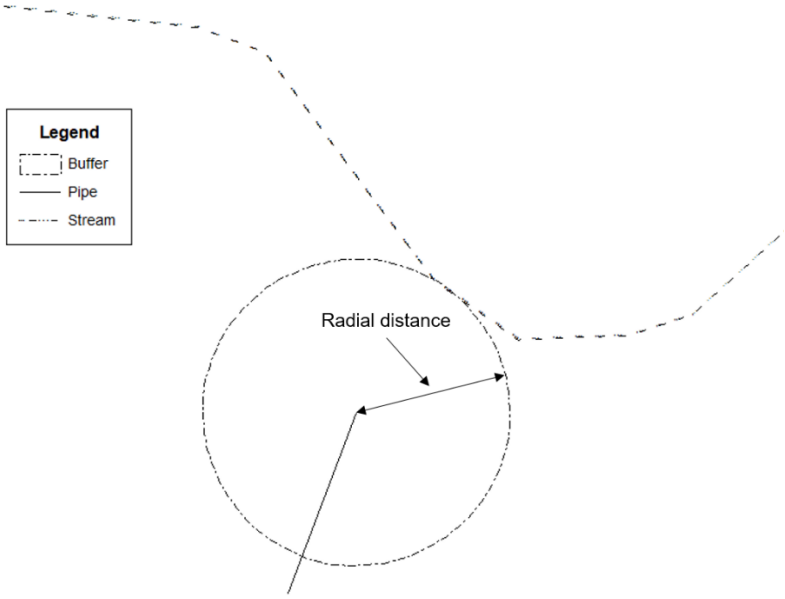

Figure 2. Radial distance from pipe outlet to stream (USGS, 2018)

Objectives Three and Four

The occurrence of erosion was evaluated using decision trees and principal components analysis (PCA) with logistic regression in RStudio™ (RStudio Team, 2021). Decision trees help identify patterns within datasets and create rules that partition the data into informative classification or regression models (Myles et al., 2004). Decision trees have low bias but may over-fit training data leading to high variance and low predictive accuracy (Hastie et al., 2009). PCA reduces the dimensionality of datasets without losing data variability or interpretability by linearly combining scaled and centered predictors into uncorrelated groups or principal components (PCs) (Faraway, 2016; James et al., 2000; Jollife & Cadima, 2016). The components are orthogonal predictors, and ideally the first component explains most of the data variability. Factor loadings or PC coefficients identify the importance or strength of correlation between predictors and PCs. PC coefficients are the eigenvectors scaled by the square root of the respective eigenvalues. Faraway (2016), James et al. (2000), and Jollife & Cadima (2016) provide more detailed discussions on how the PCs are formed. The components can be used as predictors in regression models to improve model fit; this is known as principal component regression (PCR). The PCR model's bias and variance decreases and increases as the number of components used increases, respectively (James et al., 2000). For this study, the number of components used in the model was determined through the proportion of the variance explained (PVE) by each component.

Twenty-two variables characterizing the pipe outlets' watershed and downslope soil conditions were used in the decision tree and PCR analyses to predict the occurrence of erosion stopping before reaching the outfall location. The predictors included the percentage of downslope HSG soils, median percentage of sand and clay content in the banks of the cross-section immediately below the pipe outlet, watershed area, and the durations of runoff for 1-yr and 10-yr, 24-hr storms. Erosion that stopped before reaching the outfall location was assigned a value of 1 or a "true" response while erosion that extended all of the way to the outfall was given a value of 0 or a "false" response. Both analyses used 85% of the data to build the decision tree and logistic regression models, and the remaining 15% of the data were used to calculate performance metrics such as accuracy, sensitivity, and specificity. The most commonly used splitting ratio is 80:20 although 70:30, 60:40, and 50:50 have been used in previous studies (Joseph, 2022). It is recommended that at least 70% of the data be allocated towards building or training models (Thien & Yeo, 2022). Appendix C provides a table summarizing the predictors and responses for each assessed site.

Previous studies quantifying erosion defined it in terms of volume and cross-sectional dimensions (Vanmaercke et al., 2016). For this study, the magnitude of erosion was defined in terms of the estimated total volume of eroded soil normalized by (1) the channel length ($Volume_{ERODED}/Length_{CHNL}$) and (2) the cross-sectional area, width, and maximum depth at the top of bank (TOB) normalized by the respective bankfull (BKFUL) characteristic ($Area_{TOB}/Area_{BKFUL}$; $Width_{TOB}/Width_{BKFUL}$; $Depth_{TOB}/Depth_{BKFUL}$). Bankfull refers to stable channel conditions that effectively move sediment loads and interact with the floodplain (Doll et al., 2002; Leopold & Maddock, 1953; Metcalf et al., 2009; Sweet & Geratz, 2003; Wolman & Miller, 1960). Bankfull geometry can be identified in the field or using regional curves that relate hydraulic geometry to drainage area (Harman et al., 1999, 2014) (Equation 2 through 7).

Piedmont- Rural

$A_{bkf} = 89.04A^{0.72}$ Equation 3

$W_{bkf} = 11.89A^{0.43}$ Equation 4

$D_{bkf} = 1.50A^{0.32}$ Equation 5

Mountain- Rural

$A_{bkf} = 22.1A^{0.67}$ Equation 6

$W_{bkf} = 19.9A^{0.36}$ Equation 7

$D_{bkf} = 1.1A^{0.31}$ Equation 8

Where:
A_{bkf} = bankfull cross-sectional area (ft^2)

W_{bkf} = bankfull width (ft)
D_{bkf} = bankfull mean depth (ft)
A = watershed area (mi^2)

Scaled and non-correlated variables fitted a generalized linear mixed effects model to predict the magnitude of erosion in terms of cross-sectional dimensions. The foundation for this model were the repeated measurements taken along the length of the channels downslope of the pipe outlets. Scaled and non-correlated variables also fit a generalized linear model to predict the magnitude of erosion in terms of volume. The final models were chosen using backwards selection, with a significance level of 0.05 ($\alpha = 0.05$). Q-Q plots of the residuals and normalized root mean square errors (NRMSEs) verified model legitimacy. NRMSEs are RMSEs divided by difference between the maximum and minimum data points; this normalization allows for models with different scales to be compared (Shcherbakov et al., 2013). Non-scaled variables fit decision trees predicting the magnitude of erosion in terms of cross-sectional dimensions and volume. These analyses also used 85% of the data to build the regression models and decision trees in RStudio™ (RStudio Team, 2021), and the remaining 15% to calculate the NRMSEs. Appendix C includes the predictor variables and responses used in the analyses for Objectives Three and Four.

Objective Five

Six previously assessed pipe outlets in Raleigh, North Carolina, were monitored for hydrology and TSS (Table 1; Figure 3). The watershed areas range from 0.75 to 29.4 ac and had CNs between 46 and 90.

Table 1. Summary of monitored pipe outlet characteristics

Parameter[a]	Site					
	MP458	**MP459**	**MP467**	**MP495**	**MP814**	**MP840**
Latitude, Longitude	35.9045, -78.6345	35.9032, -78.6321	35.8320, -78.5195	35.7934, -78.5142	35.7945, -78.7432	35.7558, -78.7162
Roadway	I-540				I-40	
Roadway functional class	Interstate					
Average annual daily traffic (vehicles/day)	98,500	98,500	62,500	62,500	114,000	114,000
Pipe diameter (ft)	3.5	3.5	3.0	2.0	4.0	2.5
Pipe outlet watershed area (ac)	8.47	17.3	0.75	1.84	29.4	4.72
Non-highway (offsite) area within pipe outlet watershed (ac)	6.14	15.4	0.16	0	24.6	4.06
Impervious area within pipe outlet watershed (ac)	0.89	4.43	0.25	0.79	15.4	1.82
Composite curve number (CN) for pipe outlet watershed	46	53	82	90	90	76
Watershed hydrologic soil groups	A: 61.2% B: 38.8% C: 0% D: 0%	A: 70.5% B: 29.5% C: 0% D: 0%	A: 0% B: 0% C: 100% D: 0%	A: 0% B: 0% C: 0% D: 100%	A: 0% B: 0% C: 0% D: 100%	A: 0.9% B: 65.6% C: 0% D: 33.5%
Monitoring equipment location	Pipe	Channel	Channel	Pipe	Pipe	Pipe
Average channel bed slope (ft/ft)	0.032	0.058	0.024	0.024	0.024	0.028
Channel roughness coefficient ($s/ft^{1/3}$)	0.05	0.04	0.04	0.04	0.04	0.04
Downslope channel length (ft)	2,450	237	592	99	230	1,222
Estimated volume of eroded soil (yd^3)	774	110	359	22	267	534

[a] Determined using ArcGIS (ESRI 2019), data from Homer et al. (2020), NCDOT (2022), NC DPS (2016), and USDA (2015)

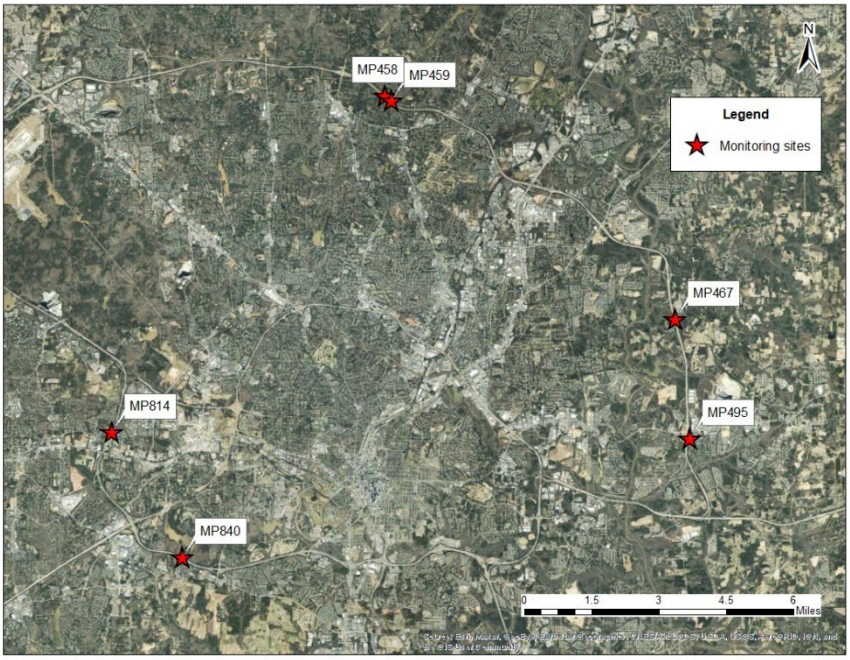

Figure 3. Map of monitoring sites

An ISCO 730™ bubbler flow module (Teledyne-ISCO™, Lincoln, Nebraska) and an automated ISCO 6712™ sampler (Teledyne-ISCO™, Lincoln, Nebraska) were installed at all of the sites to collect flow-paced water quality samples and hydrologic data every two minutes during storm events. Monitoring equipment was installed within the pipe or an area immediately downslope of the pipe if debris build-up was present (Figure 4). The equipment was located in areas that had minimal turbulence. Rainfall depth and intensity were recorded every two minutes by an ISCO 674™ (Teledyne-ISCO™, Lincoln, Nebraska) or 6466 Davis AeroCone (Davis Instruments, Hayward, California) automatic tipping bucket rain gauge. Efforts were made to install the rain gauges in areas (1) free of overhead obstructions and (2) that did not interfere with traffic. Storm events were defined as those that had a rainfall depth greater than or equal to 0.10 in with an antecedent dry period of at least six hours (Driscoll et al., 1989). Within 48 hours of a storm event, samples were collected, composited, and transported on ice to the Center for Applied Aquatic Ecology (CAAE) in Raleigh, North Carolina for TSS analysis (Std. Method 2540D) (APHA, 2005). After each storm event, the sample bottles were cleaned onsite using deionized water, and the monitoring equipment was calibrated.

Figure 4. Monitoring setup of bubbler and sampler tubing in pipe (left) and channel (right)

For pipes with free-flowing conditions, discharge was calculated using equations listed in Appendix A. Peak velocity was calculated by dividing the peak discharge by the corresponding cross-sectional area. Note if the measured water level exceeded the pipe diameter, the data were not included in the analyses. A rating curve was developed in a Hydrologic Engineering Center-River Analysis System (HEC-RAS) 6.2 model (USACE, 2022) to calculate discharge from the pipes with debris build-up. The HEC-RAS model was built using a total station survey of the channel downslope of the pipe outlet. Measured water levels in the channel were transformed into water surface elevations (WSEs) using the known elevation recorded by the bubbler. The VLOOKUP function in Excel was used to identify the discharges associated with the transformed WSEs. The VLOOKUP function was also used to estimate the peak velocity for each storm event using the channel velocities calculated from the HEC-RAS simulations.

The maximum potential ε for each storm event was estimated using Equation 8 (Hanson, 1990; Hanson & Cook, 1997; Partheniades, 1965). The maximum potential applied shear stress (τ_a) was quantified using steady and unsteady one-dimensional (1D) flow analyses in HEC-RAS 6.2 (USACE, 2022). 1D steady flow analyses calculate the water surface profiles by iteratively solving the energy equation (Equation 9) (Brunner, 2022). HEC-RAS uses the Manning's equation (Equation 10) to solve for discharge and velocity; τ_a is estimated using the energy grade line slope (S_f), unit weight of water, and the cross-section's hydraulic radius (Equation 13). 1D unsteady flow analyses iteratively solve the Saint-Venant equations for the conservation of mass (continuity) (Equation 11) and momentum (Equation 12) to calculate the water surface profiles; τ_a is solved using Equation 13. While unsteady flow analyses account for changes in flow over time, model stability is highly sensitive to channel geometry, roughness, and slope as

well as the computation interval and modeled flow rates. Brunner (2022) provides a more in-depth discussion regarding 1D steady and unsteady flow analyses.

$$\varepsilon = 12 * k_d * (\tau_a - \tau_c)^a$$ Equation 9

Where:
ε = erosion rate (in/s)
k_d = erodibility coefficient ($ft^3/lb*s$)
τ_a = applied shear stress (lb/ft^2)
τ_c = critical shear stress (lb/ft^2)
a = exponent typically assumed to be 1

$$Z_2 + Y_2 + \frac{\alpha_2 * V_2^2}{2g} = Z_1 + Y_1 + \frac{\alpha_1 * V_1^2}{2g} + h_e$$ Equation 10

Where:
Z = elevation of main channel invert (ft)
Y = depth of water at cross-section (ft)
V = average velocity at cross-section (ft/s)
α = velocity weighing coefficient (1)
g = gravitational constant (32.2 ft/s^2)
h_e = energy head loss (ft)

$$Q = \frac{1.49}{n} A R_h^{2/3} S_f^{1/2}$$ Equation 11

Where:
Q = discharge (ft^3/s)
n = Manning's roughness coefficient ($s/ft^{1/3}$)
A = flow cross-sectional area (ft^2)
R_h = cross-sectional hydraulic radius (ft)
S_f = frictional slope (ft/ft)

$$\frac{\partial Q}{\partial x} + \frac{\partial A}{\partial t} - q = 0$$ Equation 12

Where:
Q = discharge (ft^3/s)
x = channel distance (f)
A = flow cross-sectional area (ft^2)
t = time (s)
q = lateral inflow per unit length ($ft^3/s/ft$)

$$\frac{\partial Q}{\partial t} + \frac{\partial QV}{\partial x} + gA\left(\frac{\partial_z}{\partial_x} + S_f\right) = 0$$ Equation 13

Where:
Q = discharge (ft^3/s)
t = time (s)
V = average velocity at cross-section (ft/s)
x = channel distance (ft)
g = gravitational constant (32.2 ft/s^2)
A = flow cross-sectional area (ft^2)
z = water surface elevation (ft)
S_f = frictional slope (ft/ft)

$$\tau_a = \gamma R_h S_f$$ Equation 14

Where:
τ_a = applied shear stress (lb/ft^2)
γ = unit weight of water (62.4 lb/ft^3)
R_h = cross-sectional hydraulic radius (ft)
S_f = energy grade line slope (ft/ft)

For steady flow analyses, the measured discharge corresponding to each time step was simulated as a separate flow profile (Figure 5), and the measured hydrograph served as an upstream boundary condition for unsteady flow analyses. Both analyses only considered the potential τ_a at the first cross-section downslope of the pipe outlet. Visual inspections of the longitudinal and cross-section profiles verified model performance. The normal depth, estimated using the channel bed slope, served as the reach (steady) or downstream (unsteady) boundary condition. For unsteady flow analyses, the computational time step was one second, and the output intervals were two minutes. The measured durations of runoff determined the two-minute time steps. The potential τ_a was included in the analyses if the overall volume accounting error was one percent or less.

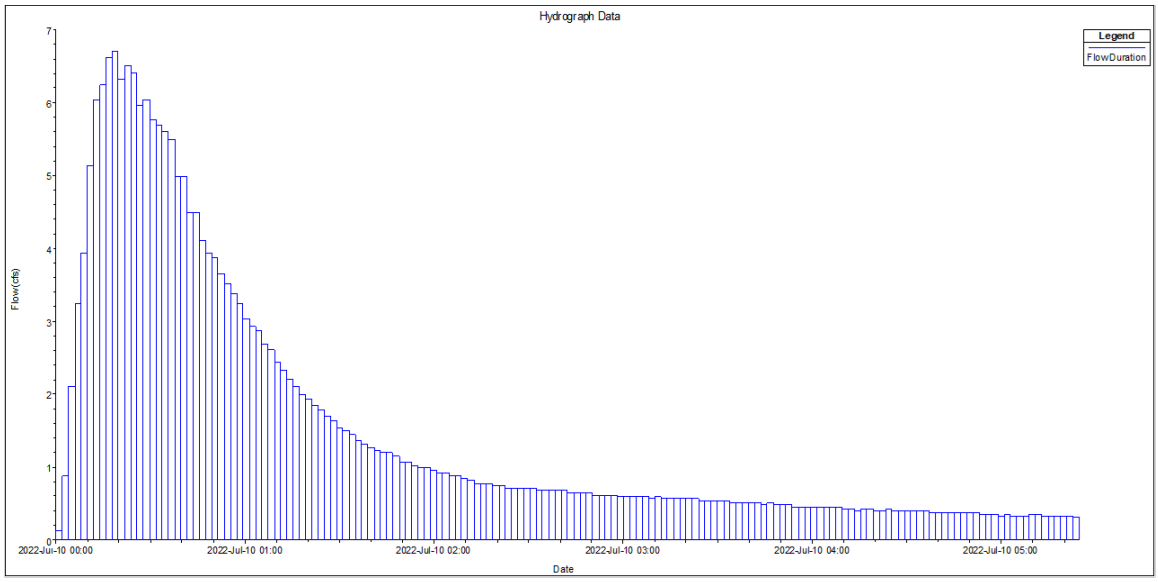

Figure 5. Measured hydrograph modeled as discrete profiles in steady flow analysis

The critical shear stress (τ_c) and erodibility coefficient (k_d) for the pipe outlets' channel banks were identified using a laboratory scale mini jet erosion test (JET) (Al-Madhhachi et al., 2013; Khanal et al., 2016; Khanal & Fox, 2017; Smith et al., 2021). The mini JET shoots a small jet of water into the soil sample at a constant pressure head, which causes the material to erode over time and create a scour hole. Depth measurements are taken over different time intervals and used to solve for τ_c and k_d using either the Blaisdell, Scour Depth, and or Iterative solutions in the JET Spreadsheet Tool version 2.1 (Daly et al., 2013). Appendix A includes a more detailed description of the JET apparatus and techniques used to solve for τ_c and k_d.

Efforts were made to collect soil samples free of roots and stones from the visually homogenous banks. The testing followed the protocol outlined by Khanal et al. (2016). The time intervals used during the tests were 0.25, 0.50, one, two, and five minutes, and time intervals were repeated until three consecutive depth measurements were achieved. Two consecutive measurements for the two- and five-minute intervals were deemed sufficient if the measurements were within 1 mm of the measurements taken during the one-minute intervals. Existing literature provides conflicting recommendations for solving for τ_c and k_d (Daly et al., 2013, 2015; Khanal et al., 2016; Mahalder et al., 2022; Wahl, 2021). Solutions for the Blaisdell method were used given the method's popularity and the linear assumption made for Equation 13. Particle size analyses (ASTM D7928, 2021) determined the permissible velocity (Fortier & Scobey, 1926) for the cross-section immediately downslope of the pipe outlet; the smallest

permissible velocity was used if the banks had different soil textures. Table 2 summarizes each site's τ_c , k_d, and permissible velocity.

Table 2.Summary of erodibility parameters and permissible velocity (Fortier & Scobey, 1926)

Site	Left bank		Right bank		Permissible velocity (ft/s)
	τ_c[1] (lb/ft^2)	k_d ($ft^3/lbf*s$)	τ_c (lb/ft^2)	k_d ($ft^3/lbf*s$)	
MP458	$2.30*10^{-3}$	$1.00*10^{-3}$	$3.34*10^{-3}$	$1.00*10^{-3}$	2.50
MP459	$2.53*10^{-3}$	$2.18*10^{-4}$	$1.09*10^{-2}$	$2.43*10^{-4}$	2.50
MP467	$4.18*10^{-4}$	$3.50*10^{-3}$	$1.42*10^{-2}$	$7.21*10^{-4}$	2.50
MP495	$1.46*10^{-3}$	$2.15*10^{-3}$	$2.67*10^{-2}$	$4.71*10^{-4}$	3.50
MP814	$1.27*10^{-2}$	$1.66*10^{-3}$	$5.01*10^{-2}$	$4.65*10^{-3}$	3.50
MP840	$9.19*10^{-3}$	$2.85*10^{-3}$	$7.73*10^{-3}$	$1.92*10^{-3}$	2.50

[1] τ_c, and k_d refers to the soil's critical shear stress, and erodibility coefficient, respectively.

Objective Six

Hydrologic, topographic, and soil data collected from the six monitoring sites were used to evaluate the four proposed designs to limit erosion downslope of pipe outlets. The proposed designs include a swale with (1) rip-rap (rip-rap swale), (2) well-established vegetation (vegetated swale), (3) check dams with mowed turf grass (maintained check dams), and (4) check dams with well-established vegetation (un-maintained check dams). Well-established vegetation refers to non-clumping grassed and herbaceous vegetation that is as tall as the flow depth. For each site, a peak discharge exceedance curve was calculated using methods from Helsel & Hirsch (1992). The storm events associated with the 12.5th, 25th, 75th, and 87.5th percentiles (peak discharges) as well as the 1-yr and 10-yr, 24-hr storms were simulated in HEC-RAS 6.2 models (USACE, 2022) representing the existing conditions and proposed designs (Figures 6 and 7; Table 2). These events ensure the proposed design standards are evaluated using a range of expected runoff conditions and the effectiveness of the standards can be compared across the sites. Refer to Objective Two for more details regarding how the design storm hydrographs were calculated.

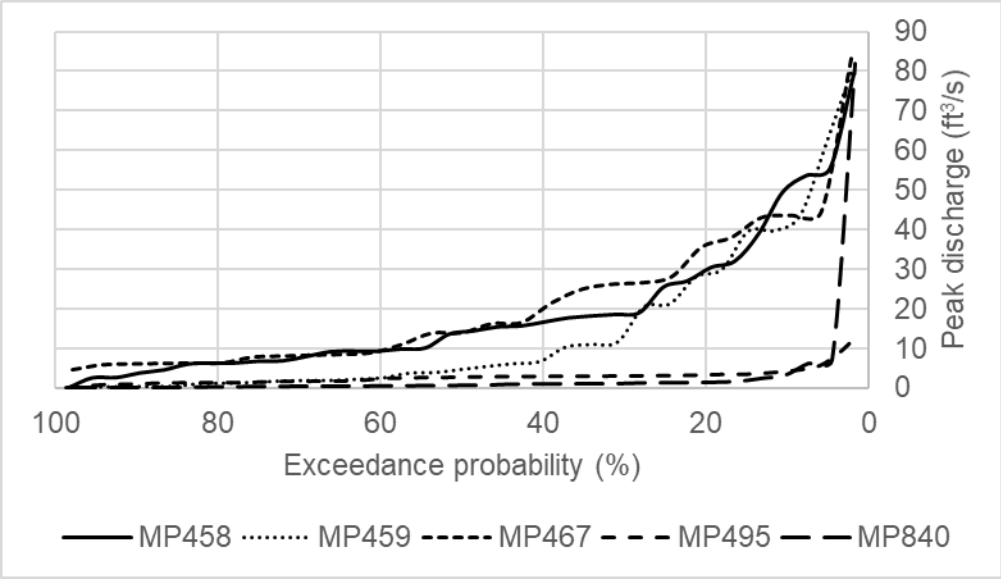

Figure 6. Flow exceedance curves (Helsel & Hirsch, 1992) for MP458, MP459, MP467, MP495, and MP840

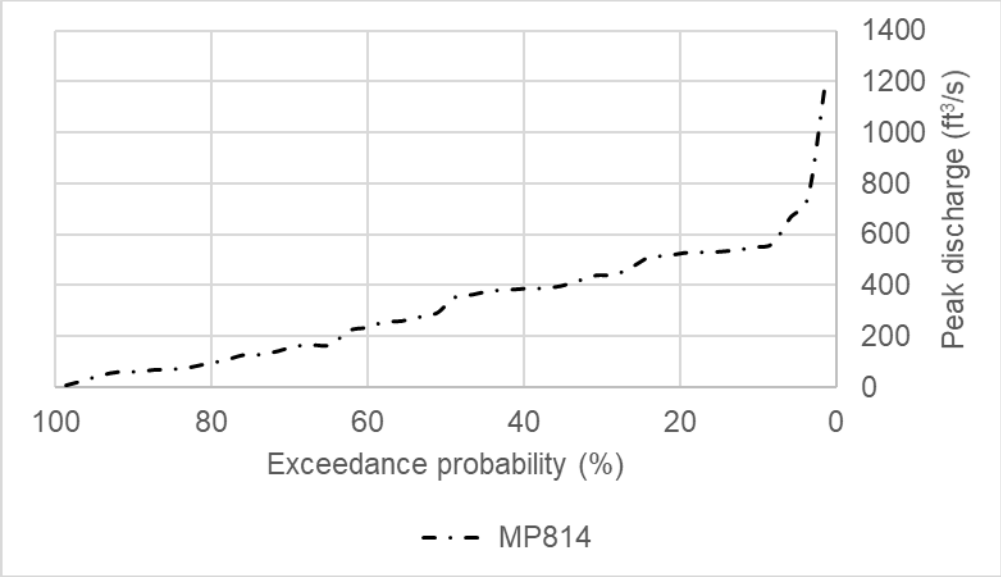

Figure 7. Flow exceedance curves (Helsel & Hirsch, 1992) for MP814

Table 3. Exceedance curve peak discharges

Site	87.5th (ft^3/s)	75th (ft^3/s)	50th (ft^3/s)	25th (ft^3/s)	12.5th (ft^3/s)	1-yr, 24-hr (ft^3/s)	10-yr, 24-hr (ft^3/s)
MP458	4.48	6.71	13.6	25. 5	39.0	$2.10*10^{-2}$	3.61
MP459	0.47	1.48	4.76	21.3	40.0	0.36	17.0
MP467	6.18	7.75	13.9	28.1	43.0	1.84	4.40
MP495	1.26	1.43	2.73	3.09	3.68	5.72	11.7
MP814	2.46	4.49	10.3	18.1	19.1	62.7	128
MP840	0.16	0.41	0.72	1.40	2.52	7. 5	20.5

The 1D steady and quasi-unsteady HEC-RAS models with BSTEM were built using the total station surveys, assessment data collected for Objective Two, and the erodibility parameters identified for Objective Five. Brunner (2022) recommends using 1D models for steep streams and/or when the terrain data are only available for specific cross-sections. Quasi-unsteady rather unsteady flow was simulated for the sediment transport analyses because Objective Five results indicated the models would be too unstable for 1D unsteady flow simulations. The banks' critical shear stresses (τ_c) ranges from $4.18*10^{-4}$ to $1.15*10^{-1}$ lb/ft^2 and the erodibility coefficients (k_d) are between $7.21*10^{-4}$ and $5.49*10^{-3}$ $ft^3/lb*s$ (Table 3). Soil data were collected at the pipe outlet and outfall (discharge point into a waterbody) as well as anywhere along the channel where there was a visible change in channel bed or bank material.

Table 4. Summary of bank characteristics (CEIWR-HEC, 2015)

Site	Assessment point	Left bank						Right bank					
		γ_{sat}[1] (lb/ft^3)	ϕ' (°)	c' (lb/ft^2)	ϕ^b (°)	τ_c (lb/ft^2)	k_d ($ft^3/lbf*s$)	γ_{sat}[1] (lb/ft^3)	ϕ' (°)	c' (lb/ft^2)	ϕ^b (°)	τ_c (lb/ft^2)	k_d ($ft^3/lbf*s$)
MP458	Outlet	115	26.6	89.8	15.0	$2.30*10^{-3}$	$1.00*10^{-3}$	115	26.6	89.8	15.0	$3.34*10^{-3}$	$1.00*10^{-3}$
	Intermediate	118	32.3	8.35	15.0	$1.73*10^{-2}$	$3.03*10^{-4}$	118	32.3	8.35	15.0	$1.73*10^{-2}$	$4.47*10^{-3}$
	Outfall	113	26.4	171	15.0	$3.55*10^{-3}$	$5.49*10^{-3}$	113	26.4	171	15.0	$3.55*10^{-3}$	$1.26*10^{-3}$
MP459	Outlet	118	32.3	8.35	15.0	$2.53*10^{-3}$	$2.18*10^{-4}$	118	32.3	8.35	15.0	$1.09*10^{-2}$	$2.43*10^{-4}$
	Outfall	118	32.3	8.35	15.0	$3.43*10^{-2}$	$2.59*10^{-4}$	118	32.3	8.35	15.0	$3.34*10^{-3}$	$7.01*10^{-4}$
MP467	Outlet	118	32.3	8.35	15.0	$4.18*10^{-4}$	$3.50*10^{-3}$	118	32.3	8.35	15.0	$1.42*10^{-2}$	$7.21*10^{-4}$
	Outfall	118	32.3	89.8	15.0	$2.19*10^{-2}$	$4.26*10^{-4}$	115	26.6	89.8	15.0	$2.19*10^{-2}$	$4.26*10^{-4}$
MP495	Outlet	113	32.3	171	15.0	$1.46*10^{-3}$	$2.15*10^{-3}$	113	26.4	171	15.0	$2.67*10^{-2}$	$4.71*10^{-4}$
	Outfall	113	26.4	171	15.0	$2.67*10^{-2}$	$4.71*10^{-4}$	115	26.6	89.8	15.0	$1.73*10^{-2}$	$4.46*10^{-4}$
MP814	Outlet	118	32.3	8.35	15.0	$1.27*10^{-2}$	$1.66*10^{-3}$	115	26.6	89.8	15.0	$5.01*10^{-2}$	$4.65*10^{-3}$
	Outfall	115	26.6	89.8	15.0	$1.15*10^{-1}$	$1.03*10^{-3}$	115	26.6	89.8	15.0	$2.09*10^{-3}$	$1.77*10^{-3}$
MP840	Outlet	118	32.3	8.35	15.0	$9.19*10^{-3}$	$2.85*10^{-3}$	118	32.3	8.35	15.0	$7.73*10^{-3}$	$1.92*10^{-3}$
	Outfall	115	26.6	89.8	15.0	$1.25*10^{-3}$	$2.06*10^{-3}$	115	26.6	89.8	15.0	$2.09*10^{-3}$	$2.30*10^{-3}$

[1] γ_{sat}, ϕ', c', ϕ^b, τ_c, and k_d refers to the soil's saturated unit weight, friction angle, cohesion, phi b, critical shear stress, and erodibility coefficient, respectively.

MP495 did not erode to an outfall, and samples were collected where the channel stopped (End). MP458 eroded to a culvert that had severe downstream erosion. Runoff from an adjacent neighborhood discharged into the channel immediately downslope of the culvert, and it was not possible to isolate the hydraulic impacts of the runoff flowing from the pipe outlet to the culvert. Per recommendations by Brunner (2022), cross-sectional data for MP458 were not collected within a distance four times the width of the channel (15 ft) from the culvert to model only the pipe outlet's hydraulic impacts. Refer to Objective Five for more details regarding how the banks' τ_c and k_d were identified.

The banks' saturated unit weight (γ_{sat}), friction angle (ϕ'), cohesion (c'), and phi b (ϕ^b) were estimated using the banks' known soil textures and erodibility parameters (CEIWR-HEC, 2015) (Table 3). Soil characteristics were assigned to cross-sections without data using site photos and the cross-section's proximity to a cross-section with known soil data. The channel bed gradations were interpolated in HEC-RAS, and groundwater elevations were estimated using Web Soil Survey (USDA, 2015). Method of slices was selected as the bank failure method, and static ground water was chosen for the ground water method.

Water temperature was not measured, and United States Geological Survey (USGS) stream stations were not located near the sites (Merriman et al., 2017). Air temperature data collected from nearby North Carolina State Climate Office (NCSCO) weather stations (NCSCO, 2022) served as a substitution. While temperatures in stormwater runoff fluctuate throughout the storm (Jones and Hunt, 2010) and are influenced by watershed characteristics (Jones et al., 2012), these NCSCO data were the best available estimates for this parameter.

The channel soil texture determined which transport function, sorting, and fall velocity methods were used to simulate the existing channel and swales without check dams' sediment transport capacities. The channel beds were mostly comprised of sand and silt, which resulted in each model using the Laursen (Copeland) transport function and Copeland (Ex7) sorting method (Brunner, 2022). Every model also used the Soulsby fall velocity method and a computational time step of one minute (Brunner, 2022). The Soulsby method considers grain size and density as well as water viscosity. Influent sediment data were not available to develop a rating curve or sediment load time series, which resulted in each model using the Equilibrium Load as the sediment boundary condition. Equilibrium Load calculates the sediment transport capacity for each time step and grain class at the upstream cross-section and uses these capacities as the load time series for the downstream cross-section. Default computational steps and tolerances were used except for the bed change options. Veneer (equal vertical)

deposition was allowed to occur along the overbanks or floodplains. Brunner (2022) reported it is common for models to allow for deposition along the overbanks. Assessment data included in Objective Two determined the depth of potential erosion at each modeled cross-section (Figure 8).

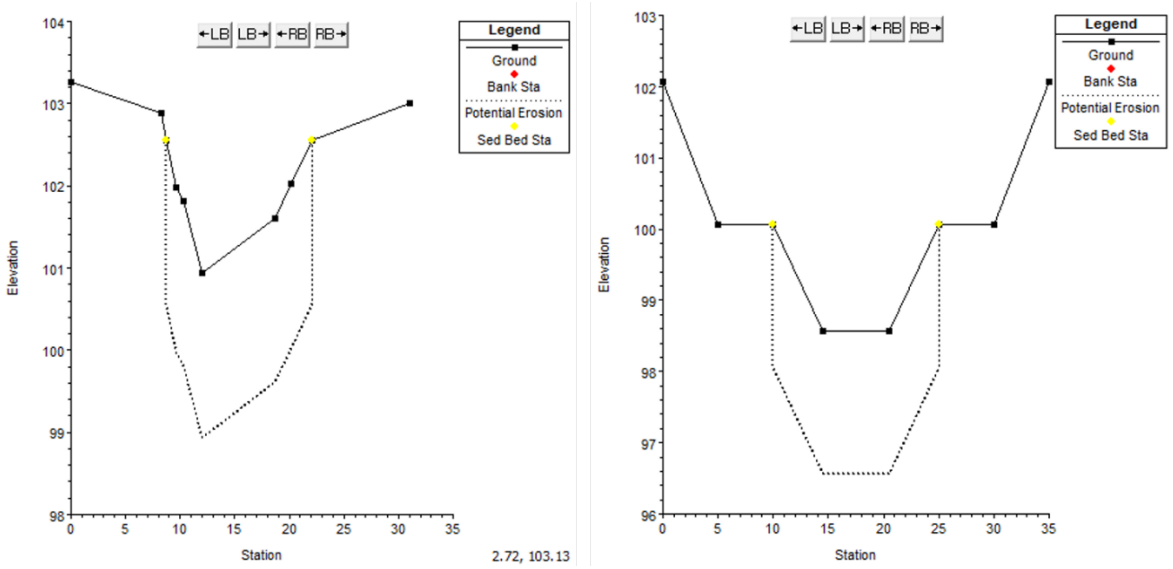

Figure 8. Cross-section plots of existing channel (left) and proposed swale (right)

The swales retrofitted with well-established vegetation, rip-rap, or check dams were designed using the pipe outlets' watershed characteristics, average channel bed slope, SwaleMod 1.0.3 (Anderson et al., 2015), and the minimum design criteria (MDC) established by the North Carolina Department of Environmental Quality (NC DEQ) for treatment swales (NC DEQ, 2020). If the flow conveyance discharge required a bottom width greater than 6 ft, the bottom width was limited to this threshold. Table 4 summarizes the proposed swale designs, and Table 5 includes the channel roughness coefficients assigned to each design (Brunner, 2022). For consistency, the proposed designs included the floodplain roughness coefficients and soil characteristics representing the existing conditions. The proposed check dams had a top width of 2 ft, side slope of 4:1 (H:V), and spaced such that the base of the upstream check dam was at the same elevation as the top of downstream check dam (Figure 9) (Powell, 2015; Purvis, 2018; Winston et al., 2019). The check dams were placed at the correct station along the channel using the RAS Mapper option in HEC-RAS (USACE, 2022).

Table 5. Summary of proposed swale designs for monitored sites

Parameter/Site	MP458	MP459	MP467	MP495	MP814	MP840
Bottom width (ft)	6.0	6.0	3.0	3.0	6.0	6.0
Top width (ft)	15.0	15.0	12.0	12.0	21	15
Side slope (H:V)	3:1					
Swale length (ft)	404	226	633	99	404	821
Longitudinal slope (ft/ft)	0.032	0.058	0.024	0.024	0.024	0.028
Freeboard (ft)	0.50					
Maximum swale depth (ft)	1.0	1.0	1.0	1.0	2.0	1.0

Table 6. Summary of channel roughness coefficients for design scenarios (Brunner, 2022)

Design scenario	Channel roughness coefficient ($s/ft^{1/3}$)	Roughness coefficient description
Rip-rap swale	0.07	Cobbles with large boulders
Vegetated swale; Un-maintained vegetated swale with check dams	0.14	Excavated earthen channel with dense brush at high stage
Maintained vegetated swale with check dams	0.03	Winding excavated earthen channel with grass and some weeds

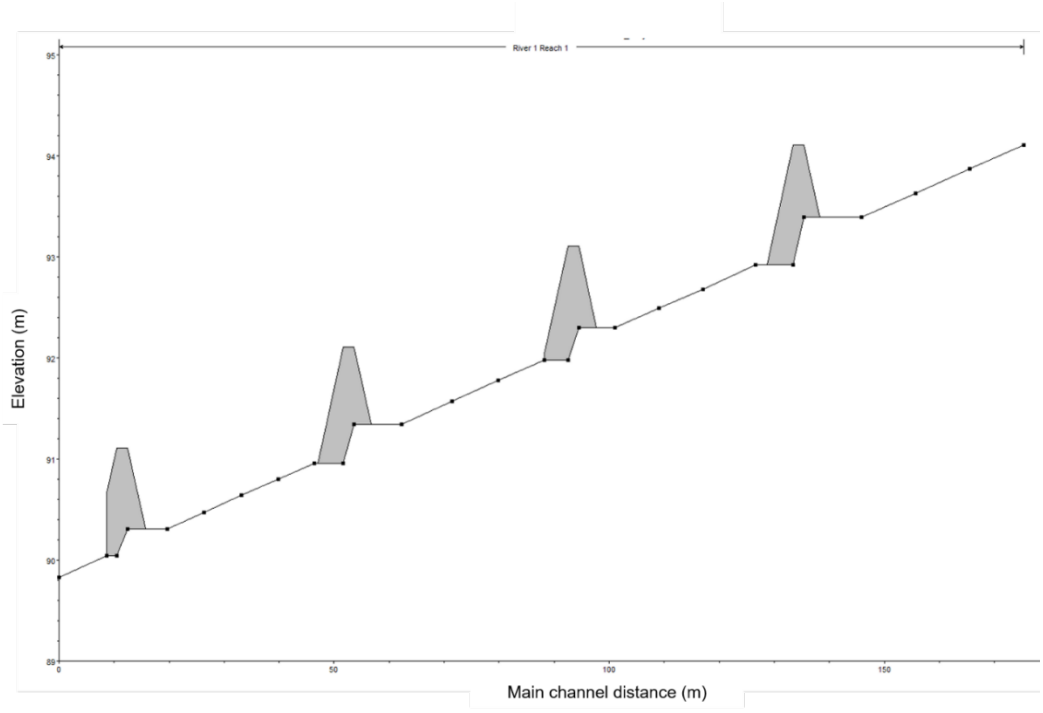

Figure 9. Longitudinal profile of swale with check dams

For each storm event, the calculated shear stress (τ) at the outlet, middle, and outfall or end cross-sections was compared between the existing conditions and proposed designs using the 1D steady models. Current design tools, such as SwaleMod (Anderson et al., 2015), for swales use this parameter as a factor of safety (FOS). Sediment mass balances were compared between the existing conditions and alternative lining swales using the 1D quasi-unsteady models. The differences between the predicted influent and effluent sediment volumes determined if the proposed designs reduced or increased erosion. The proposed design that mitigated τ and sediment loss the most was identified as the design with the greatest potential to limit erosion downslope of pipe outlets.

Objective Seven

The costs associated with the proposed designs were estimated using data from NCDOT, Hunt et al. (2021), and previous bid documents for NC State University construction projects. The average unit cost for each line item is included Table 7. Excavation quantities were estimated using the swale's cross-sectional area and length. Rip-rap, sod, and geotextile fabric quantities were estimated using the swale's length and wetted perimeter for the maximum flow depth. The maintenance and planting associated with the maintained and un-maintained swales, respectively, were estimated using the swale's length. Unit costs for check dam installation and maintenance were not available for the analyses. The analyses also did not consider costs associated with grading or maintenance easements.

Table 7. Estimated mean unit costs for proposed designs (Hunt et al., 2021)

Item	**Mean unit cost**
Mobilization ($)	18,753
Excavation ($/yd^3)	275
Rip-rap ($/ton)	67
Geotextile ($/yd^2)	4
Sod ($/lf)	77
Plants ($/lf)	8
Annual mowing ($/lf)	38
Pre-formed scour hole ($)	4,772

Objective Eight

The final predictive equations and decision trees for the occurrence and magnitude of erosion were compiled into a Microsoft Excel-based tool. The tool also includes the bankfull regional curves associated with each physiographic region of North Carolina. The tool is available as a separate document from the report.

Results and Discussion

Objective Two

Assessments

Forty-eight of the 60 assessed sites had erosion downslope of the pipe outlet and only 12 sites exhibited no signs of erosion. Data were collected from a minimum of two cross-sections to a maximum of nine cross-sections. Channel and bank soil textures were mostly sandy loam or silt loam. The length of downslope erosion ranged from 0 to 7,431 ft, and the total estimated volume of eroded soil was between 0 and 4,102 yd^3 (Table 6). The median depth to the channel's confining layer was approximately 0.30 m. BEHI scores were as low as 0 (very low) and as high as 59 (extreme). The majority of BEHI scores and depths to confining layers indicate the channels are at risk of widening and incising.

Table 8. Summary of assessments

Parameter	Minimum	Mean	Median	Maximum
Length of downslope erosion (ft)	0	885	410	7,431
Estimated total volume of eroded soil (yd^3)	0	290	94.0	4,102
Top of bank cross-sectional area (ft^2)	0	16.2	9.35	162
Top of bank width (ft)	0	10.9	8.90	44.0
Maximum depth (ft)	0	2.48	2.05	6.95
Depth to confining layer (ft)	0	1.52	1.00	4.60
Bank erosion hazard index (BEHI)	Very low (0)	High (32.6)	High (32.8)	Extreme (59.0)
Channel bank bulk density (lb/ft^3)	33.1	74.5	74.0	111
Channel bank median approximate unconfined compressive strength (ton/ft^2)	0.16	1.12	1.00	4.00

The pipe diameters for the assessed sites were between 1.0 and 4.0 ft. The watersheds draining to the pipes ranged from 0.22 to 112 ac, and up to 106 ac of these watersheds were comprised of non-highway areas (Table 7). The amount of impervious area within the watersheds ranged between 0 and 15.4 ac, and the composite CN ranged from 43 to 94. On average, the maximum velocities for the 1-yr and 10-yr, 24-hr storms were 5.98 and 30.4 ft/s, respectively. The ratio of the maximum permissible velocity to the peak velocity was between 0.34 and 6.40. The only defining characteristic between sites that did or did not exhibit erosion was the downslope vegetative conditions. Sites that did not experience any erosion had heavy stands of herbaceous and grass vegetation and a lack of trees clustered together (Figure 10). On average, HSG B soils comprised 57% of the soils at the erosion-free sites. The combination of well-established vegetation, soils that tend to infiltrate, and lack of clustered trees to concentrate flow most likely kept runoff diffused and reduced the potential for downslope

erosion (Haghnazari et al., 2015; Jia et al., 2020). Refer to Appendix D for summaries of the field collected and desktop data.

Table 9. Summary of characteristics for assessed sites (Homer et al., 2020; Malcom, 1989; NC DPS, 2016; NOAA, 2006; USDA, 2015; USDA-NRCS, 2004; USGS, 2018)

Parameter	Minimum	Mean	Median	Maximum
Pipe outlet watershed area (ac)	0.22	11.8	2.99	112
Non-highway (offsite) area within pipe outlet watershed (ac)	0	10.4	1.46	106
Impervious area within pipe outlet watershed (ac)	0	1.70	0.50	15.4
Composite curve number (CN) for pipe outlet watershed	43	74	77	94
Duration of runoff 1-yr, 24-hr storm (hr)	1.67	5.21	3.23	30.7
Peak discharge 1-yr, 24-hr storm (ft^3/s)	0.01	10.2	2.87	80.5
Maximum velocity 1-yr, 24-hr storm (ft/s)	1.20	5.98	5.60	13.6
Duration of runoff 10-yr, 24-hr storm (hr)	1.83	4.15	3.47	12.1
Peak discharge 10-yr, 24-hr storm (ft^3/s)	0.44	30.4	10.8	258
Maximum velocity 10-yr, 24-hr storm (ft/s)	2.11	8.35	7.87	16.0
Maximum permissible velocity/peak 1-yr, 24-hr velocity	0.34	2.22	2.05	5.46
Maximum permissible velocity/peak 10-yr, 24-hr velocity	0.70	3.10	3.08	6.40
Radial distance of pipe outlet to stream (ft)	7.84	1,044	669	4,544
Departure (ft)	0	17.8	16.2	73.8

Figure 10. Assessed sites free of downslope erosion

Objectives Three and Four

Occurrence of erosion

Thirty-five of the 60 sites eroded to the outfall and received a “false” or 0 response. Both watershed characteristics and downslope soil conditions influenced the prediction of erosion occurrence of downslope erosion (Figure 11). The most important factors dividing the data into the correct responses (erosion vs. no erosion occurring to the outfall location) are the ratio between the maximum permissible velocity and the peak velocity for the 1-yr, 24-hr storm event and the percentage of sand and clay in the channel banks immediately downslope of the pipe outlet. It is not surprising these predictors would have the most influence on splitting the data into the correct response categories. The ratio of maximum velocities incorporates other factors that greatly influence discharge and thus the shear stress (τ) applied to the soil (e.g., watershed area, CN). Additionally, flows for higher frequency storm events (e.g., 2-yr, 24-hr) have more erosion potential than storms with lower frequencies (Hawley et al., 2017; Roesner et al., 2001; Rohrer & Roesner, 2006; Tillinghast et al., 2011). Soils with pore size distributions favoring macropores (e.g., sands) tend to have higher infiltration rates, which helps to reduce the risk of degradation (Hillel, 2003). The risk of soil detachment also decreases with increasing clay content. Similar to the velocity ratio, pipe diameters are influenced by factors that affect τ (e.g.,

discharge). HSG D soils tend to be less permeable, which reduces the potential for infiltration (NRCS, 2007).

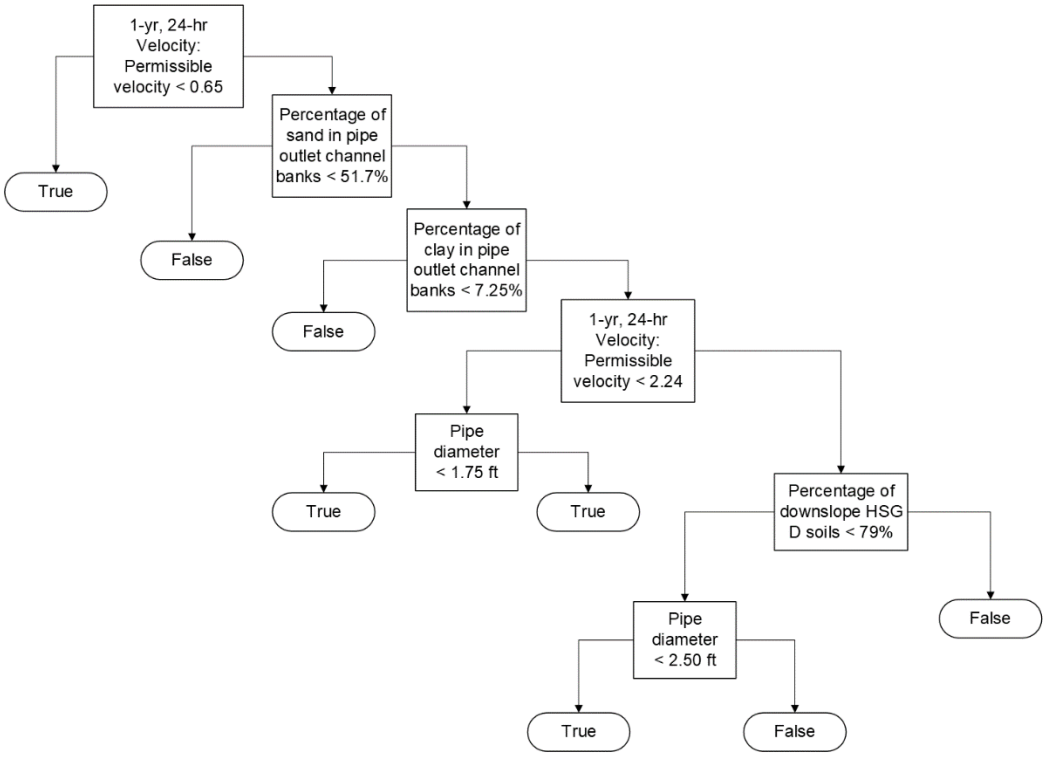

Figure 11. Decision tree for the occurrence of erosion downslope of pipe outlets (note true refers to no erosion occurs to the outfall)

The first split corresponding to pipe diameter resulted in the same predicted responses because of increased node purity (James et al., 2000). Node purity refers to the homogeneity of the responses, and higher node purity increases certainty in the predicted responses. The Gini index as well as entropy are measures of node purity, and decision tree algorithms use these parameters to evaluate the quality of a split. A small Gini index or entropy indicates the node mostly includes observations from a single class. This pipe diameter split does not indicate the decision tree cannot be used to predict the occurrence of erosion to an outfall. The decision tree had an 8% misclassification error during training and an accuracy and precision of 62.5% and 50%, respectively, during testing. These metrics would most likely improve with the use of additional data during model development (James et al., 2000; Kotsiantis, 2013).

The PCA resulted in 22 PCs comprised of the predictors included in Table 3, and the first eight components explained approximately 80% of the data variability (Figure 12). Ideally, the first few components would have explained most of the variability (Faraway, 2016; James et al., 2000).This suggests the PCA may not have included predictors that could have better

explained data variability. These predictors include the age of the pipe installation at the time of assessment, changes to the watershed between the design and assessment phases (e.g., development), and the downslope conditions at the time of the pipe installation. Previous research has shown the extent of erosion varies with time, changes to the landscape, and rainfall patterns (Shellberg et al., 2013; Sidorchuk, 1999; Vanmaercke et al., 2016). Design plans and maintenance records associated with the assessed sites were not available to include in the analyses. The extensive vegetative cover downslope of the pipes prevented the opportunity to digitally quantify downslope conditions over time (Ghimire et al., 2006; Maugnard et al., 2014). Additionally, it was difficult to identify the sites in aerial imagery from the 1990s and earlier to quantify the downslope vegetative cover. The photos had poor resolution and did not include any distinguishable landmarks.

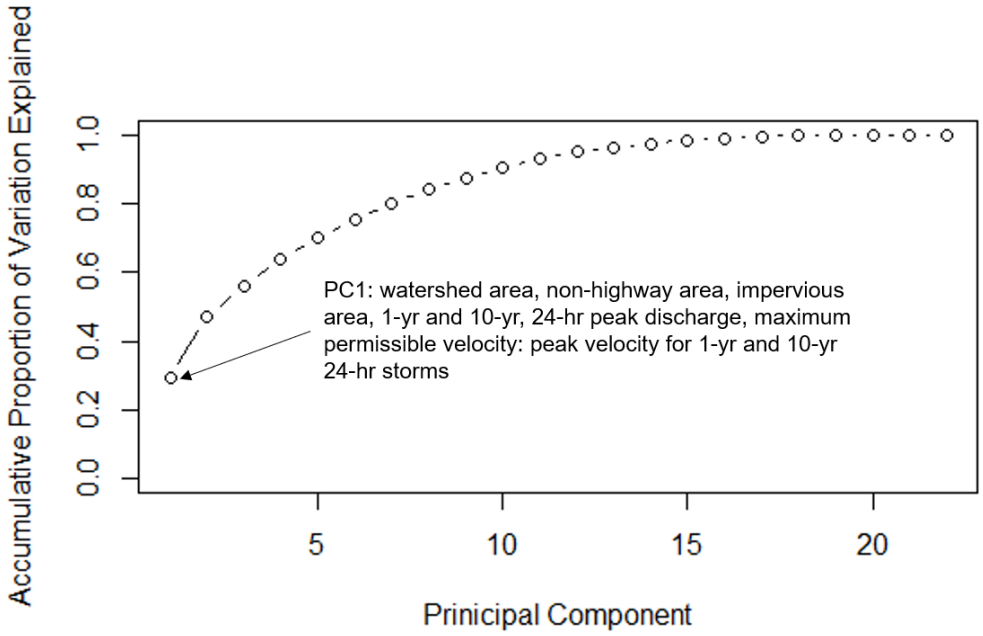

Figure 12. Principal components proportion of variance explained with key predictors for PC1 shown

PC coefficients and a threshold of 0.25 determined the most influential predictors in each PC. Influential predictors for PC1 included watershed and hydrologic characteristics that either directly (e.g., peak velocity) or indirectly (e.g., impervious area) affect erosion. These characteristics also had some of the most variability (Table 7). Predictors that repeatedly had PC coefficients with a magnitude greater than or equal to 0.25 included the percentage of HSG soils, ρ_b, percentage of sand and clay in the pipe outlet's channel banks, duration of the 10-yr,

24-hr storm, departure, watershed area, and the pipe outlet's radial distance to the stream (Table 8). These predictors either describe the soils' resistance to detachment or influence erosion (Bledsoe, 2002; Hillel, 2003; Nehrke & Roesner, 2004; Pomeroy et al., 2008; Roesner et al., 2001; Rohrer & Roesner, 2006). The influential predictors also support the use of velocity ratios and the banks' sand and clay content in the decision tree to optimize the partitioning of data into response categories. The eight components used in the logistic regression model to predict the occurrence of erosion stopping before reaching the outfall location were not significant (p-value > 0.05). The model only had an accuracy, specificity, and sensitivity of 50% when used with the testing dataset. The model most likely underperformed due to missing predictors and the components failing to capture the relationship between the predictors and response (Faraway, 2016; James et al., 2000).

Table 10. Summary of principal components used in logistic regression model

Predictor	PC1	PC2	PC3	PC4	PC5	PC6	PC7	PC8
Pipe diameter (ft)	-0.16	-0.12	**0.28**	0.15	-0.02	**0.42**	**-0.44**	-0.12
Watershed area for pipe outlet (ac)	**-0.36**	-0.08	-0.01	-0.08	0.08	**-0.36**	-0.10	0.01
Non-highway (offsite) area within pipe outlet's watershed (ac)	**-0.35**	-0.08	-0.02	-0.09	0.05	**-0.37**	-0.11	0.01
Impervious area within pipe outlet's watershed (ac)	**-0.28**	0.11	-0.06	-0.16	0.24	0.05	**0.25**	-0.01
Radial distance of pipe outlet to stream (ft)	0.15	-0.01	0.41	**0.29**	0.18	-0.17	0.00	**-0.39**
Percentage HSG A soils downslope of pipe outlet (%)	-0.10	**-0.33**	**-0.34**	**0.25**	0.14	0.15	0.11	-0.04
Percentage HSG B soils downslope of pipe outlet (%)	-0.09	**-0.32**	0.24	**-0.29**	-0.21	-0.02	-0.19	0.05
Percentage HSG C soils downslope of pipe outlet (%)	-0.02	0.09	0.23	**0.26**	**-0.29**	-0.18	**0.46**	**0.26**
Percentage HSG D soils downslope of pipe outlet (%)	0.13	**0.34**	-0.24	0.00	**0.33**	0.09	-0.18	-0.21
Curve number (CN) for pipe outlet's watershed	0.04	**0.45**	0.01	0.05	-0.02	0.08	0.18	-0.06
Peak discharge 1-yr, 24-hr storm (ft^3/s)	**-0.32**	0.24	0.11	-0.16	0.11	0.07	0.13	0.01
Peak discharge 10-yr, 24-hr storm (ft^3/s)	**-0.37**	0.14	0.10	-0.12	0.06	-0.08	0.01	0.01
Duration of runoff for 1-yr, 24-hr storm (hr)	-0.19	**-0.31**	**-0.29**	0.18	0.10	-0.15	-0.01	-0.02
Duration of runoff for 10-yr, 24-hr storm (hr)	-0.17	-0.14	-0.07	0.12	**0.30**	0.10	**0.31**	**-0.25**
Median approximate unconfined compressive strength at pipe outlet banks (ton/ft^2)	0.02	-0.20	**0.29**	0.01	0.15	**0.27**	0.16	**0.50**
Median Manning's n of channel banks at pipe outlet ($s/ft^{1/3}$)	-0.23	-0.15	0.15	0.22	0.04	**0.40**	0.20	-0.17
Median bulk density of channel banks at pipe outlet (lb/ft^3)	0.04	0.13	0.02	**0.44**	**0.40**	-0.17	**-0.36**	**0.48**
Median percentage of sand in pipe outlet channel banks (%)	-0.16	0.09	**-0.25**	**0.36**	-0.22	0.02	0.11	0.20
Median percentage of clay in pipe outlet channel banks (%)	0.07	-0.04	**0.28**	-0.22	**0.51**	-0.04	0.15	0.16
Departure (ft)	0.09	-0.10	**0.29**	**0.29**	0.00	**-0.37**	0.08	**-0.28**
Maximum permissible velocity/ peak 1-yr, 24-hr velocity	**-0.27**	**0.33**	0.14	0.10	-0.12	0.06	-0.07	-0.03
Maximum permissible velocity/ peak 10-yr, 24-hr velocity	**-0.33**	0.13	0.10	0.20	-0.14	0.07	-0.23	-0.02

Note: bold values indicate principal component (PC) coefficients greater than 0.25; HSG refers to hydrologic soil group

Magnitude of erosion

Soil and vegetative data were collected from 109 cross-sections downslope of the 60 pipe outlets. The $Area_{TOB}/Area_{BKFUL}$, $Width_{TOB}/Width_{BKFUL}$, $Depth_{TOB}/Depth_{BKFUL}$, and $Volume_{ERORDED}/Length_{CHNL}$ ratios were 5.29, 7.33, 7.74, and 0.04, respectively (Table 9). Appendix E includes the predictors used in the regression and decision tree analyses.

Table 11. Summary of magnitude of erosion

Parameter	Minimum	Mean	Median	Maximum	Standard deviation
$Width_{TOB}/Width_{BKFUL}$	0	11.04	7.33	68.81	7.09
$Area_{TOB}/Area_{BKFUL}$	0	13.62	5.29	160.20	18.92
$Depth_{TOB}/Depth_{BKFUL}$	0	9.74	7.74	36.56	1.51
$Volume_{ERODED}/Length_{CHNL}$	0	0.07	0.04	0.63	0.44

Note TOB, BKFUL, and CHNL refers to top of bank, bankfull, and channel, respectively

Figure 13 includes the Q-Q plots for each final regression model. The plots suggest the regression equations did not fully explain the data variability, particularly for the gullies' estimated volume of eroded soil.

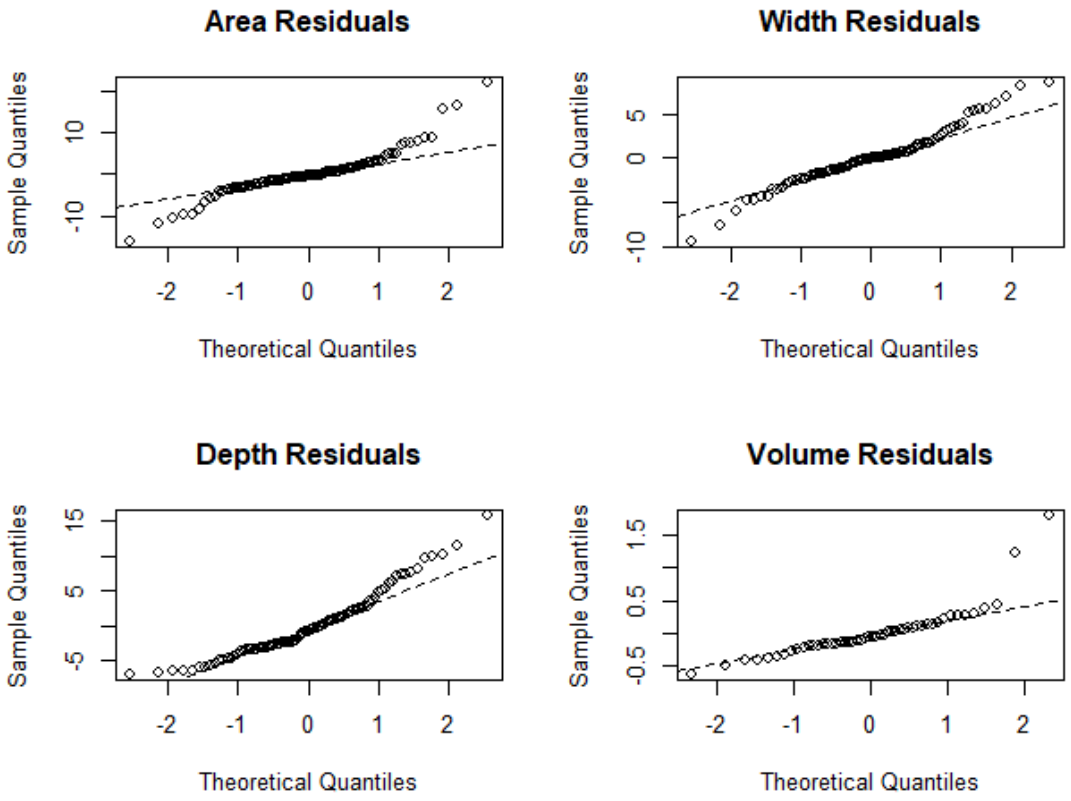

Figure 13. Q-Q plots of residuals for $Area_{TOB}/Area_{BKFUL}$ (Area), $Width_{TOB}/Width_{BKFUL}$ (Width), $Depth_{TOB}/Depth_{BKFUL}$ (Depth), and $Volume_{ERODED}/Length_{CHNL}$ (Volume) regression equations

The final regression model predicting the magnitude of erosion in terms of $Area_{TOB}/Area_{BKFUL}$ includes the radial distance of the pipe outlet to the stream, percentage of HSG C and D soils downslope of the pipe outlet, CN for the pipe outlet's watershed, and the duration of runoff for the 10-yr, 24-hr storm event (Equation 14). The NRMSE for the model and testing data was 0.07; values closer to zero indicate the model was a better fit to the data. This NRMSE suggest model performance could improve with additional predictors that were not quantified at each cross-section during the site assessments (e.g., soil texture).

$$A_{TOB}/A_{BKFUL} = 12.11 - 8.93*R + 10.33*C + 24.74*D - 21.08*CN - 9.28*D_{10} \quad \text{Equation 15}$$

Where:
A_{TOB}/A_{BKFUL} = cross-sectional area top of bank/bankfull cross-sectional area (ft^2/ft^2)
R = scaled radial distance of pipe outlet to stream (ft)
C = scaled percentage of HSG C soils downslope of pipe outlet (%)
D = scaled percentage of HSG D soils downslope of pipe outlet (%)
CN = scaled composite CN for pipe outlet watershed (unitless)
D_{10} = scaled duration of runoff for 10-yr, 24-hr storm event (hr)

The decision tree predicting $Area_{TOB}/Area_{BKFUL}$ includes the approximate unconfined compressive strength of the channel banks, peak discharge for the 10-yr, 24-hr event, and percentage of downslope HSG D soils (Figure 14). The decision tree most likely associated smaller $Area_{TOB}/Area_{BKFUL}$ ratios with 10-yr, 24-hr peak discharges greater than 12.86 ft^3/s because the peak discharge for the pipe outlet's watershed was included as a predictor for each cross-section measured along the length of the channel. The NRMSE for the decision tree and testing dataset was 0.09. This slightly larger value suggests the regression equation (Equation 14) explains variability among the $Area_{TOB}/Area_{BKFUL}$ ratios somewhat better than the decision tree.

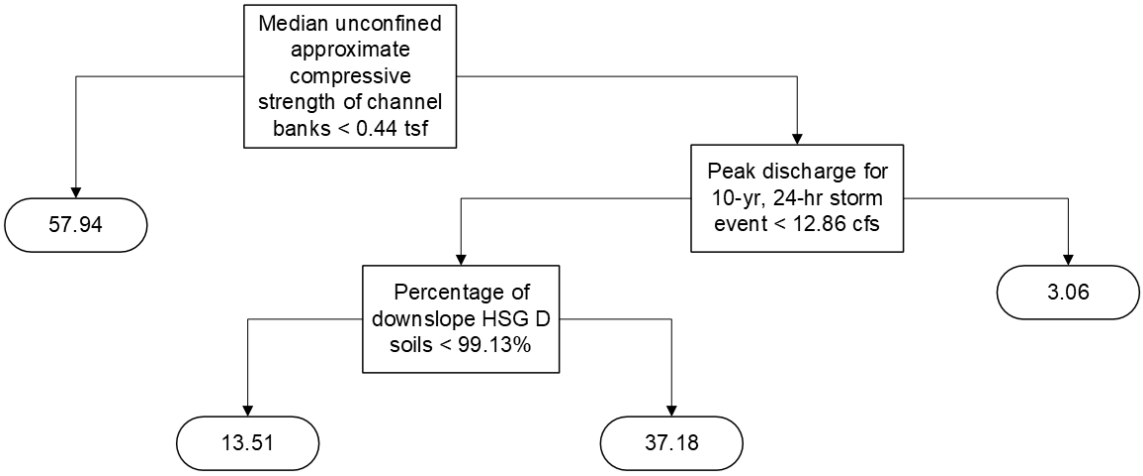

Figure 14. Decision tree for $Area_{TOB}/Area_{BKFUL}$ for gullies downslope of pipe outlets

The final regression equation and decision tree predicting $Width_{TOB}/Width_{BKFUL}$ had similar predictors as the model and decision tree estimating $Area_{TOB}/Area_{BKFUL}$. The models most likely had similar predictors because the channel's cross-sectional area includes the width at the top of bank. Additional predictors for the $Width_{TOB}/Width_{BKFUL}$ regression equation include the radial distance from the stream and percentage of HSG A and B soils (Equation 15). The NRMSE for regression equation was 0.09.

$$W_{TOB}/W_{BKFUL} = 10.82 - 3.90*R - 5.69*A - 14.40*B - 3.33*C - 13.84*CN - 7.30*D_{10} \quad \text{Equation 16}$$

Where:
W_{TOB}/W_{BKFUL} = width at top of bank/bankfull width (ft/ft)
R = scaled radial distance of pipe outlet to stream (ft)
A = scaled percentage of HSG A soils downslope of pipe outlet (%)
B = scaled percentage of HSG b soils downslope of pipe outlet (%)
C = scaled percentage of HSG D soils downslope of pipe outlet (%)
CN = scaled composite CN for pipe outlet watershed (unitless)
D_{10} = scaled duration of runoff for 10-yr, 24-hr storm event (hr)

Additional variables in the final decision tree predicting $Width_{TOB}/Width_{BKFUL}$ include the duration of the 1-yr, 24-hr storm event, pipe diameter, and radial distance from the stream (Figure 15). The NRMSE for the decision tree was 0.17, which suggests the decision tree does not explain the variability among the $Width_{TOB}/Width_{BKFUL}$ ratios as well as the regression equation.

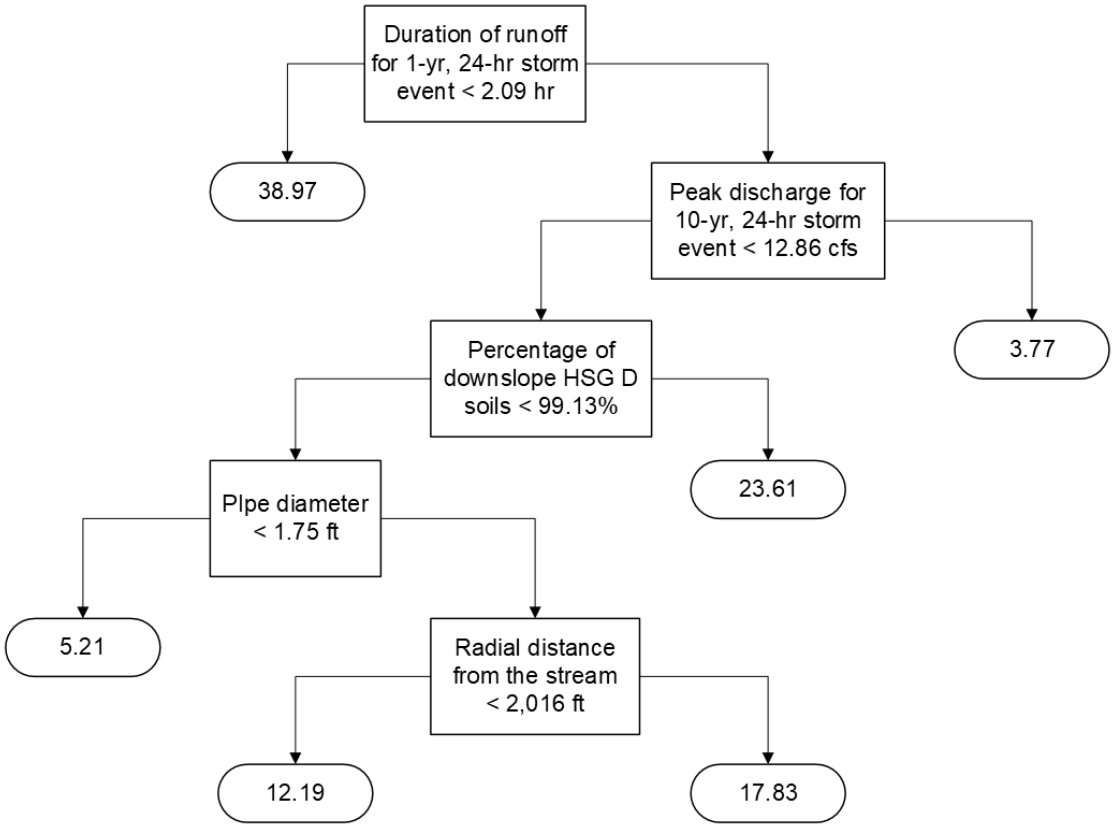

Figure 15. Decision tree for $Width_{TOB}/Width_{BKFUL}$ for gullies downslope of pipe outlets

The final regression equation predicting the magnitude of erosion in terms of $Depth_{TOB}/Depth_{BKFUL}$ includes the pipe outlet's watershed area and composite CN, percentage of downslope HSG B soils, duration of runoff for the 10-yr, 24-hr storm event, radial distance from the stream, and the distance between the cross-section of interest and the pipe outlet (Equation 16). The distance between the cross-section and pipe outlet indirectly describes headcut migration. As expected, cross-sections closer to the stream tended to be deeper due to this migration. The final decision tree includes the pipe outlet's watershed area, non-highway (offsite) and impervious areas within the watershed, pipe diameter, pipe outlet's radial distance from the stream, duration of runoff for 10-yr, 24-hr storm event, and the median Manning's n and approximate unconfined compressive strength for the cross-section of interest's channel banks (Figure 16). Typically, a soil's critical shear stress or shear strength describes the soil's resistance to detachment (Hillel, 2003; Léonard & Richard, 2004; Partheniades, 1965). However, Liu et al. (1999) and Robinson & Hanson (1995) found that soils, especially cohesive soils, with higher compressive strength have less risk of detachment. The decision tree most likely associated larger depth ratios with smaller radial distances and off-site areas because

these characteristics were used as predictors for every cross-section, and cross-sections near the stream were deeper due to headcut migration. The NRMSE for the regression equation and decision tree was 0.21 and 0.17, respectively. This suggests the data collected during the site assessments better predicts the magnitude of erosion in terms of cross-sectional area and width than depth.

$$D_{TOB}/D_{BKFUL} = 8.90 - 2.09*W - 1.86*R - 3.54*B - 3.35*CN - 2.56*D_{10} + 1.95*DI \quad \text{Equation 17}$$

Where:
D_{TOB}/D_{BKFUL} = maximum depth at top of bank/bankfull mean depth (ft/ft)
W = scaled pipe outlet watershed area (ac)
R = scaled radial distance of pipe outlet to stream (ft)
B = scaled percentage of HSG B soils downslope of pipe outlet (%)
CN = scaled composite CN for pipe outlet watershed (unitless)
D_{10} = scaled duration of runoff for 10-yr, 24-hr storm event (hr)
DI = scaled distance between cross-section and pipe outlet (ft)

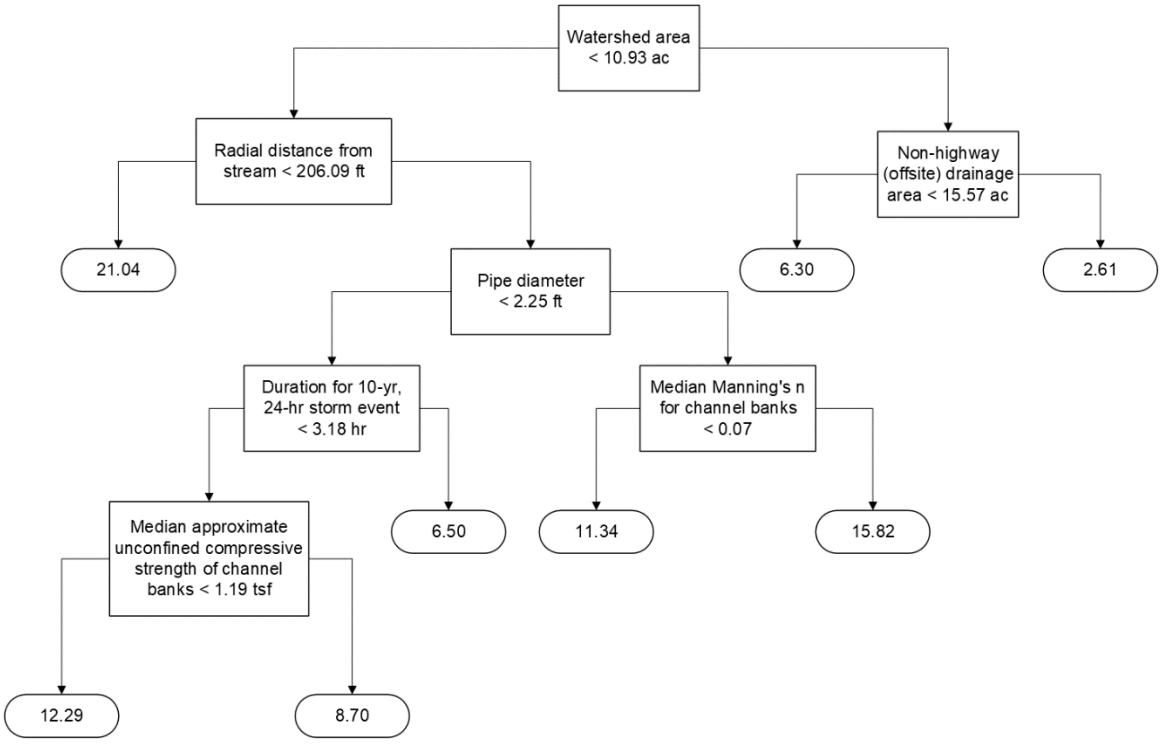

Figure 16. Decision tree for $Depth_{TOB}/Depth_{BKFUL}$ for gullies downslope of pipe outlets

The final regression model predicting erosion in terms of $Volume_{ERODED}/Length_{CHNL}$ includes the peak discharges for the 1-yr and 10-yr, 24-hr storm events as well as the ratios between the permissible velocity and the peak velocities for these storm events (Equation 17).

The NRMSE using the testing dataset was 0.17. The predictors in the final decision tree included the median ρ_b and percentage of clay in the pipe outlet channel banks, and the pipe outlet's radial distance to the stream (Figure 17). The NRMSE for the decision tree was 0.07 and indicates this model was a better fit for the data compared to the regression equation.

$$Volume_{ERODED}/Length_{CHNL} = 0.32 + 0.67*QP_1 - 0.60*QP_{10} - 0.60*V_1 + 0.60*V_{10} \quad \text{Equation 18}$$

Where:
$Volume_{ERODED}/Length_{CHNL}$ = estimated volume of erosion/channel length (yd^3/ft)
QP_1 = scaled peak discharge for the 1-yr, 24-hr storm event (ft^3/s)
QP_{10} = scaled peak discharge for the 10-yr, 24-hr storm event (ft^3/s)
V_1 = scaled max. peak velocity for the 1-yr, 24-hr storm event: permissible velocity
V_{10} = scaled max. peak velocity for the 10-yr, 24-hr storm event: permissible velocity

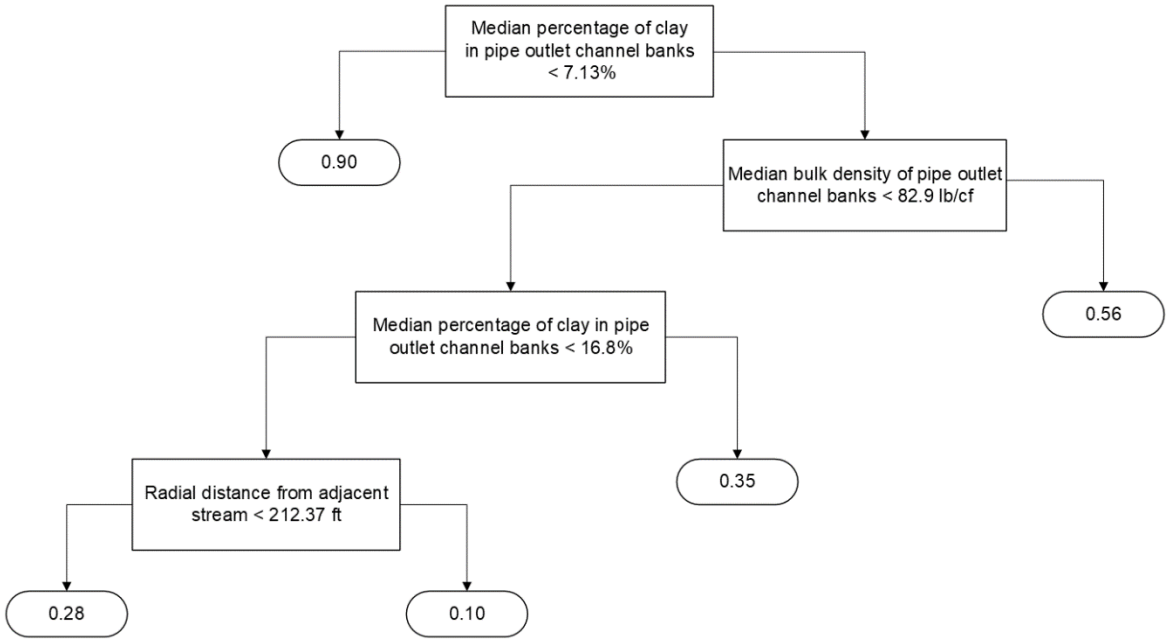

Figure 17. Decision tree for $Volume_{ERODED}/Length_{CHNL}$ for gullies downslope of pipe outlets

The regression equations and decision trees predicting the magnitude of erosion in terms of cross-sectional dimensions and volume used a combination of watershed, hydrologic, and downslope soil characteristics that influence channel instability. Recurring predictors include the duration of runoff and peak discharge for the 10-yr, 24-hr storm event, percentage of downslope HSG soils, radial distance of the pipe outlet from the stream, and the pipe outlet watershed's CN and impervious area. Numerous studies have shown impervious areas directly influence channel degradation (Baruch et al., 2018; Booth & Jackson, 1997; Burns et al., 2015;

Morse et al., 2003; Schueler et al., 2009; Vietz et al., 2014; Walsh et al., 2005a, 2005b). Channel instability concomitantly increases with the amount of impervious area, particularly areas directly connected to streams by stormwater drainage networks. Runoff duration and discharge, particularly for lower frequency storm events (e.g., 1-yr, 24-hr), also have a direct impact on streambank instability (Bledsoe, 2002; Hawley et al., 2017; Nehrke & Roesner, 2004; Pomeroy et al., 2008; Roesner et al., 2001; Rohrer & Roesner, 2006; Tillinghast et al., 2011). The regression equations and decision trees used the duration of runoff for the 1-yr and 10-yr, 24-hr storm events. The average duration of runoff for both storm events is comparable (Table 7). It is likely the duration of runoff for both storm events exceeded the soil's allowable erosional hours (Tillinghast et al., 2011), thus increasing the risk of channel degradation.

CNs and HSGs indirectly influence channel stability. CNs are the combination of a watershed's infiltration, surface topography, interception, and depressional storage characteristics (Chin, 2021; Ponce & Hawkins, 1996). Higher CNs represent landscapes more likely to produce runoff, which increases the risk of channel instability (Schueler et al., 2009; Walsh et al., 2005b). HSGs provide a general description of a soil's capacity to infiltrate; HSG C and D soils tend to infiltrate less compared to HSG A and B soils (NRCS, 2007). Infiltration is a key factor influencing runoff volume and discharge as well as the risk of soil degradation (Hillel, 2003; Hopkins et al., 2015, 2020). The radial distance to a stream is not a factor influencing stream channel instability. However, the regression equations and decision trees herein predict the magnitude of erosion caused by gullies. Gullies are the result of migrating headcuts (Bennett & Wells, 2019; Bull & Kirkby, 1997). Headcuts are miniature waterfall and plunge pools and migrate upwards when backward eddies force flow against the foot of the soil's headwall (Bennett & Wells, 2019; Douglas-Mankin et al., 2020; Flores-Cervantes et al., 2006). A pipe outlet near a stream reduces the distance, and possibly the time, for a headcut to migrate to the outlet and cause erosion. The radial distance accounts for this relationship.

Table 10 summarizes the NRMSEs for the regression equations and decision trees. Apart from $Depth_{TOB}/Depth_{BKFUL}$ and V_{ERODED}/L_{CHNL}, the regression equations performed as well if not better than the decision trees. Because decision trees find patterns within datasets to optimize performance, they generally perform better when built with larger datasets (Hastie et al., 2009; Kotsiantis, 2013; Myles et al., 2004). It is possible the decision trees for $Depth_{TOB}/Depth_{BKFUL}$ and V_{ERODED}/L_{CHNL} performed better than the respective regression equations because these erosion metrics had the smallest standard deviations (Table 5), which

may have allowed the trees to identify patterns within the data that the linear regression equations could not capture.

Table 12. Summary of NRMSEs for regression equations and decision trees

Parameter	Regression equation	Decision tree
$Area_{TOB}/Area_{BKFUL}$	0.07	0.09
$Width_{TOB}/Width_{BKFUL}$	0.09	0.17
$Depth_{TOB}/Depth_{BKFUL}$	0.21	0.17
$Volume_{ERODED}/Length_{CHNL}$	0.17	0.07

Note TOB, BKFUL, and CHNL refer to top of bank, bankfull, and channel, respectively

The influential predictors in the decision trees for the cross-sectional dimensions did not hold the expected relationships between channel instability and impervious area and peak discharge. This was caused by characteristics for the pipe outlet's watershed being used as predictors for every cross-section along the channel. The generalized linear mixed effects model used to build the regression equations accounted for repeated predictors, and the decision tree predicting the volume of eroded soil did not include repeated measurements along the channel. These results suggest decisions tree predicting cross-sectional dimensions for channels should only be built and tested using data unique to each cross-section.

The NRMSEs and residuals (Figure 13) suggest the equations and trees may be missing predictors that better explain the variability in the data. These predictors include the amount of time that has occurred between the installation of the pipe and the assessment, how the watershed has changed since the design phase (e.g., increased development), and the downslope conditions at the time of the pipe installation. Research has shown erosion varies over time and is susceptible to changes to rainfall patterns and the landscape (Shellberg et al., 2013; Sidorchuk, 1999; Vanmaercke et al., 2016). Extensive vegetative cover downslope of the pipes prevented the downslope conditions from being quantified over time using aerial imagery (Ghimire et al., 2006; Maugnard et al., 2014). Design plans and surveys detailing the watershed characteristics and downslope soil conditions were not available to include in the analyses. The models would also improve if data influencing soil degradation (e.g., percent sand/clay, ρ_b) had been collected at each cross-section. Soil texture and ρ_b, were only collected at the outlet, intermediate, and outfall cross-sections.

Kinnell (2017) compared erosion simulated by the USLE, RUSLE2, and USLE-M models to measured data using NSEs. The performance of these existing models cannot be directly compared to the performance of the regression equations and decision trees. However, if the models are compared in terms of meeting or exceeding the respective threshold for good performance, the regression equations developed for $Area_{TOB}/Area_{BKFUL}$ and $Width_{TOB}/Width_{BKFUL}$ as well as the decision tree for $Volume_{ERODED}/Length_{CHNL}$ appear to be as reliable as the USLE,

RUSLE2, and USLE-M (with observed runoff data) models. This indicates designers could use these equations and decision tree to determine the optimal discharge points for pipe outlets to minimize downslope erosion or help identify existing pipe outlets that may need re-stabilization.

Objective Five

Rainfall and hydrology

Monitoring occurred from July 2021 to August 2022. However, due to equipment damage from a 2.99 in storm, monitoring at MP458 and MP459 stopped July 2022 (Figure 18). Debris from overhanging vegetation often clogged the tipping bucket and compromised rainfall data. Additionally, battery failure and wires cut by routine mowing caused a loss of data. MP458 and MP459 were most affected by these issues. Due to proximity (8 mi), rainfall data collected at MP467 was substituted for missing MP458 and MP459 rainfall data. The nearest weather station maintained by the North Carolina State Climate Office (NCSCO) was 9 mi away. The minimum number of storm events recorded was 57, and rainfall ranged from 0.10 to 5.42 in. Antecedent dry periods varied between 0.26 and 30 days, and the average rainfall intensity ranged from 0.02 to 1.37 in/hr (Table 11).

Figure 18. MP459 equipment buried by sediment transported during 2.99 in storm

Table 13. Description of rainfall characteristics

Parameter/Site	MP458[a]	MP459[a]	MP467	MP495	MP814	MP840
Monitoring period	07/21-07/22		07/21-08/22			
Number of storms	70		73	67	57	63
Rainfall depth (in)						
Minimum	0.10		0.10	0.11	0.10	0.10
Mean	0.65		0.73	0.74	0.80	0.56
Median	0.43		0.43	0.47	0.54	0.37
Maximum	2.99		4.24	4.24	5.42	3.68
Peak 5-min intensity (in/hr)						
Minimum	0.12		0.12	0.12	0.12	0.12
Mean	1.36		1.55	1.54	1.91	1.17
Median	1.08		1.14	1.08	1.68	0.60
Maximum	4.56		8.34	8.34	5.64	4.14
Average intensity (in/hr)						
Minimum	0.02		0.02	0.02	0.02	0.02
Mean	0.21		0.21	0.20	0.22	0.17
Median	0.09		0.10	0.08	0.12	0.10
Maximum	1.14		1.37	1.37	0.92	0.92
Duration (hr)						
Minimum	0.25		0.27	0.33	0.29	0.17
Mean	5.89		6.26	6.86	6.68	5.72
Median	4.37		4.67	4.97	4.30	4.23
Maximum	18.60		19.63	19.40	30.83	30.83
Antecedent dry period (day)						
Minimum	0.26		0.26	0.26	0.35	0.26
Mean	4.90		5.23	5.07	7.20	6.11
Median	4.43		4.43	3.98	5.71	4.60
Maximum	24.03		27.87	17.64	29.70	24.08

[a] Due to monitoring issues 67% of rainfall statistics include data collected at MP467

Table 13 summarizes the runoff characteristics for the pipe outlets. The measured runoff volumes ranged from $1.00*10^2$ to $7.20*10^5$ ft^3, and peak discharges varied between 0.04 and 83 ft^3/s. Runoff discharged from the pipes occurred for up to 26 hours. Measured water levels in MP458 and MP840 exceeded the pipe diameter two and five times, respectively; the peak 5-minute intensities associated with these events were at least 0.71 in/hr. Despite the watersheds' impervious coverage and dominant HSGs that tend to be less permeable, runoff did not occur for every monitor-able storm event (including up to 3.86 in). No clear threshold existed among the rainfall characteristics for runoff to occur. Appendix F provides for a summary of each storm event.

Table 14. Description of runoff characteristics

Site	Number of runoff events	Runoff volume (ft^3)	Peak discharge (ft^3/s)	Runoff duration (hr)
MP458	38	$3.07*10^3$-$1.01*10^6$	0.43-79	1.87 - 26
MP459	42	$1.98*10^2$-$7.20*10^5$	0.12-81	0.43 - 23
MP467	34	$1.10*10^4$-$4.93*10^5$	3.3-83	0.80 - 22
MP495	54	$1.00*10^2$-$6.22*10^5$	0.04-13	0.20 - 23
MP814	51	$3.91*10^2$-$4.70*10^5$	0.16-43	0.83 - 24
MP840	37	$4.43*10^2$-$1.95*10^5$	0.13-82	0.33 - 21

Hydraulic impacts

Table 13 summarizes the potential maximum τ_a and ε for storms using 1D steady flow analyses. The potential τ_a among the six sites ranged between 0.04 and 1.6 lb/ft^2. The τ_a exceeded the τ_c by a factor of at least 2.21, and the maximum potential ε was $4.5*10^{-2}$ in/s. As expected, sites with higher k_d experienced larger potential ε. Hoomehr et al. (2018) conducted a flume study with loam soil samples to identify the effects of water temperature, pH, and road salts on ε for cohesive soils and found the ε were between 0 and $1.97*10^{-2}$ in/s. Except for MP840, the potential ε are within the range reported by Hoomehr et al. (2018).

Table 15. Description of potential maximum erosion rates using 1D steady flow analyses

Site	Number of runoff events	Potential applied shear stress (lb/ft^2)	Applied: Critical shear stress	Potential maximum erosion rate (in/s)
MP458	38	0.12-0.64	43-227	$1.3*10^{-3}$-$7.6*10^{-3}$
MP459	42	0.04-0.79	2-44	$6.1*10^{-5}$-$2.1*10^{-3}$
MP467	34	0.17-0.71	23-97	$4.2*10^{-3}$-$1.8*10^{-2}$
MP495	54	0.15-0.67	10-44	$2.2*10^{-3}$-$1.1*10^{-2}$
MP814	51	0.22-0.57	7-18	$7.1*10^{-3}$-$2.0*10^{-2}$
MP840	37	0.11-1.6	13-186	$2.9*10^{-3}$-$4.5*10^{-2}$

For MP458 and MP814, more than half of the maximum potential τ_a were associated with discharges less than the peak discharges. For low flow rates, contractions (narrowing) or expansions (widening) of the channel will increase and decrease the energy grade line slope, respectively (Brunner 2022). Increases in the energy grade line slope will result in higher τ_a (Equation 14). At MP458 and MP814, the cross-section immediately downslope of the pipe outlet cross-section was much narrower than the pipe outlet cross-section, which explains why the maximum τ_a was generally associated with flows less than the peak discharge (Figure 19).

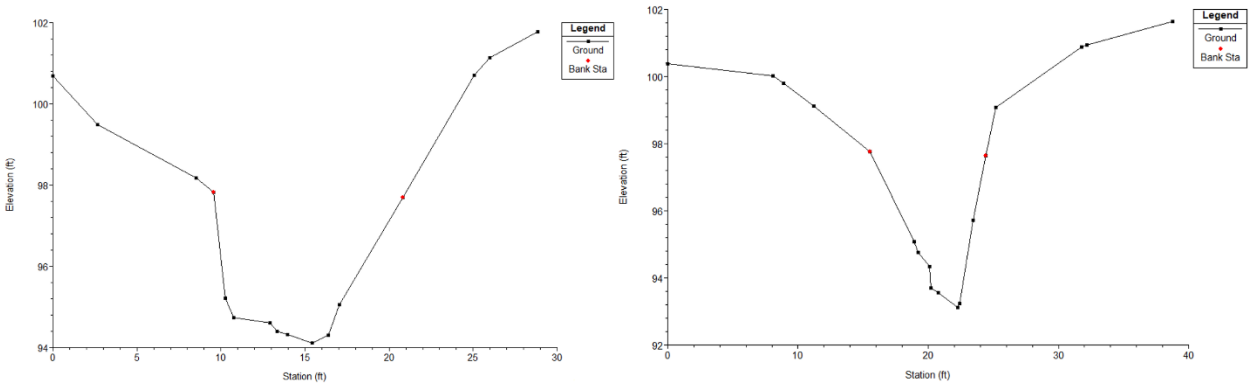

Figure 19. MP814 pipe outlet cross-section (left) and immediate downslope cross-section (right)

Except for MP495 and MP814, the models were too unstable for 1D unsteady flow simulations. Brunner (2022) reported flow regimes with high velocities and/or rapid changes in velocity and depth increase model instability. Model instability also increases with steep slopes, low flows, and downstream boundary conditions that cause abrupt changes in the WSE or approach the critical depth (Brunner, 2022). Per Rosgen (1994), steep streams have a channel bed slope greater than 0.04 ft/ft, and moderately steep streams have a bed slope between 0.02 and 0.04 ft/ft. HEC-RAS's default solution for routing is subcritical flow (Brunner, 2022). If the flow depth is at or below critical depth, the unsteady model will often overestimate the flow depth at the upstream cross-section and possibly underestimate the downstream cross-section's depth. Brunner (2022) recommends increasing channel roughness, adding or removing cross-sections, including or increasing baseflow, and adjusting the computational intervals or channel slope to increase model stability. These recommendations failed to improve model stability for MP458, MP459, MP467, and MP840. The models were most likely unstable due to the channels' slope (Table 1) (Figure 20 through Figure 23), low flows (Table 13), and varying cross-sectional geometry. During the 1D steady flow analyses for these sites, the WSEs were often at or below the critical depth, and the model assumed critical depth to complete the simulations. Appendix I includes the geometry file associated with each model.

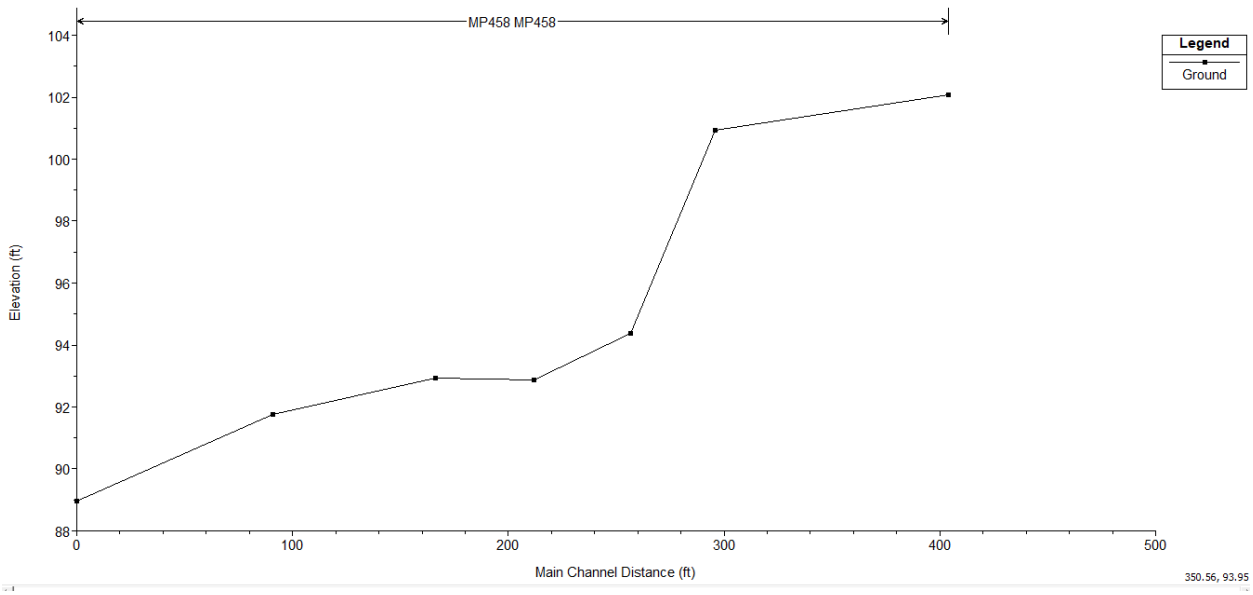

Figure 20. Longitudinal profile of MP458 channel bed

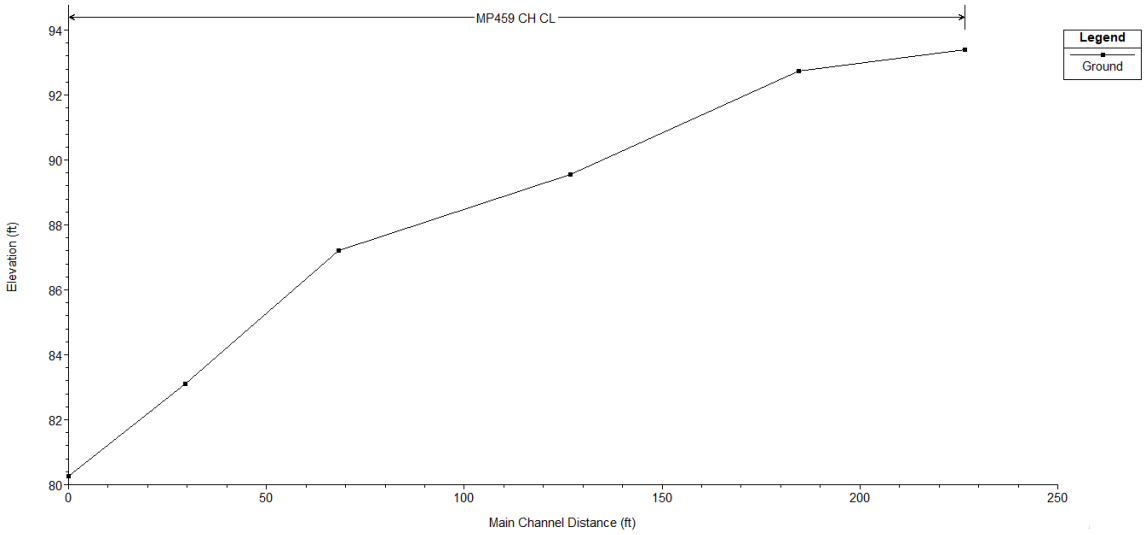

Figure 21. Longitudinal profile of MP459 channel bed

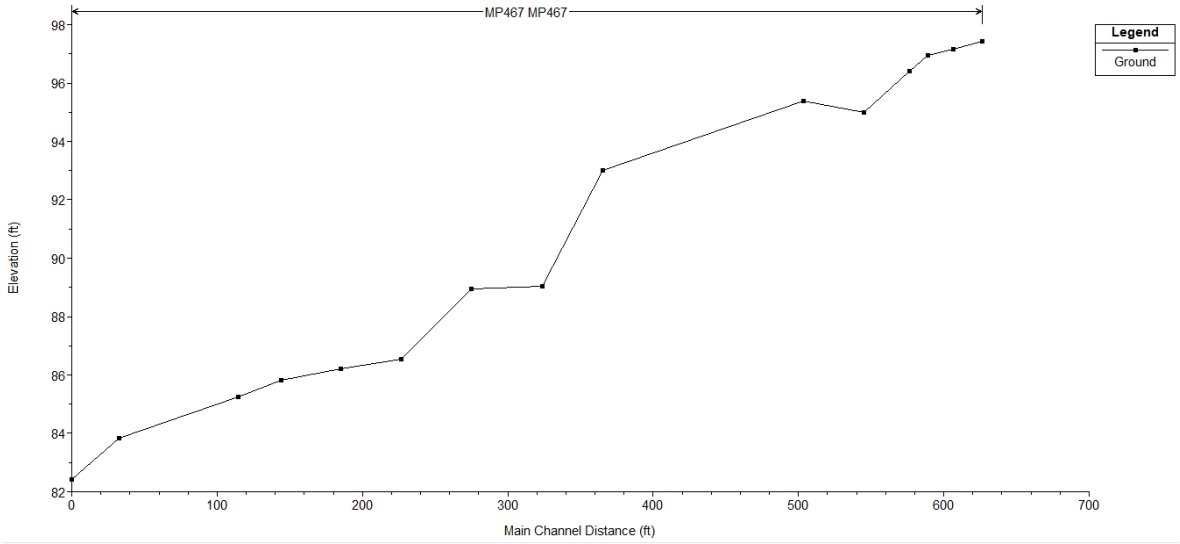

Figure 22. Longitudinal profile of MP467 channel bed

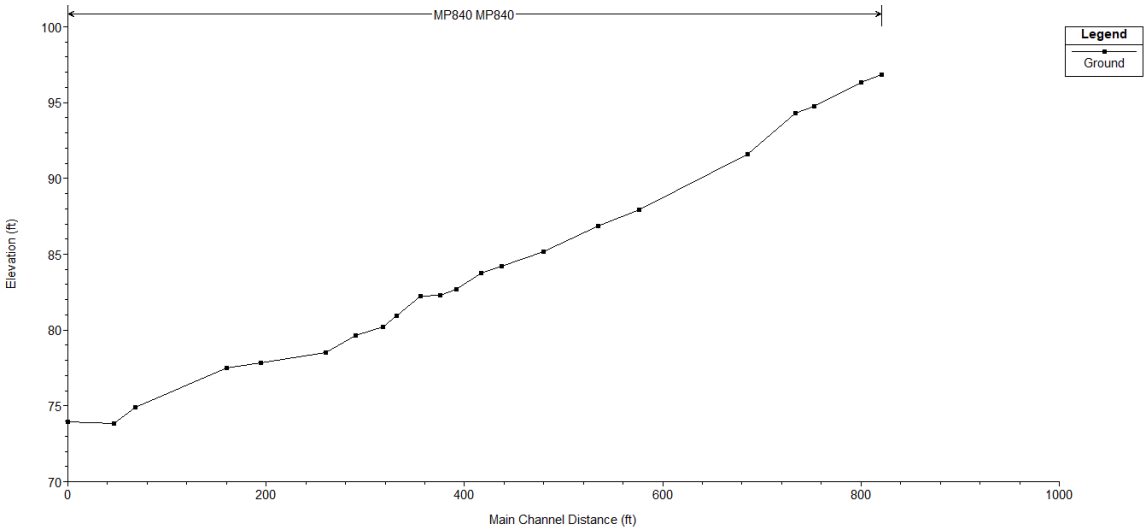

Figure 23. Longitudinal profile of MP840 channel bed

Table 15 summarizes the potential 1D unsteady flow τ_a and ε that had an overall volume accounting error of one percent or less. The potential maximum ε ranged from 0.01 to 0.17 in/s, and the limited results suggest the steady flow analyses may be under-predicting ε associated with pipe outlets draining highway and non-highway areas. However, more studies are needed to verify this conclusion. The channels downslope of the pipe outlets extended past the NCDOT ROW. A lack of property owner cooperation prevented flow from being measured downslope of the pipe outlets. This also prevented the use of erosion pins and repeated surveys of permanent cross-sections to validate the potential ε (Beck et al., 2018; Hancock & Lowry, 2015; Harden et al., 2009; Luffman et al., 2015; Myers et al., 2019; Palmer et al., 2014; Zaimes et al., 2021;

Zaimes & Schultz, 2015). Additional flow and erosion data would have allowed for the calibration and validation of the HEC-RAS models, thus improving model stability and confidence in the results (Bennett et al., 2013; Brunner, 2022; Krause et al., 2005; Ritter & Muñoz-Carpena, 2013). However, the simulated ε indicate designers should include the erodibility of the soils downslope of the pipe discharge points in their hydraulic analyses. Over time, the τ_a could cause additional sediment loss if a gully forms downslope of the pipe outlet.

Table 16. Description of potential maximum erosion rates using 1D unsteady flow analyses

Site	Number of storm events with stable simulations	Potential applied shear stress (lb/ft^2)	Applied: Critical shear stress	Potential maximum erosion rate (in/s)
MP495	45	4.4-10	295-702	0.07-0.17
MP814	5	0.28-1.1	9-36	0.01-0.04

Table 16 summarizes the measured peak velocities of storm events with runoff. The peak velocities ranged from 0.56 to 20 ft/s, and these velocities exceeded the permissible velocities by at most a factor of eight. None of the storms that occurred during the monitoring period exceeded the 10-yr, 24-hr rainfall depth (NOAA, 2006); yet the measured velocities exceeded the permissible velocity between 10 and 44 times during this period. The actual age of the monitored sites is unknown but aerial imagery suggests four of the six pipes were installed within 15 years of this study (Google, 2022). The estimated volume of eroded soil downslope of the outlets was between 22 and 774 yd^3 (Table 1). The magnitude of erosion downslope of the outlets and the reoccurring exceedance of the permissible velocity suggest designers should limit the velocity for 1-yr, 24-hr storm to reduce erosion potential. Research has shown flows associated with higher frequency storm events have more erosion potential than storms with lower frequencies (Hawley et al., 2017; Pomeroy et al., 2008; Roesner et al., 2001; Rohrer & Roesner, 2006; Tillinghast et al., 2011). This new velocity threshold may require designers to minimize pipe slopes or use elements of spillway designs (e.g., Saint Anthony Falls stilling basin) to meet regulations. Refer to Appendix F for a summary of the peak velocity, expected τ_a, and ε associated with each storm event.

Table 17. Description of measured peak velocities

Site	Number of runoff events	Peak velocity (ft/s)	Peak: Permissible velocity	Number of times permissible velocity exceed
MP458	38	4.3-20	2-8	37
MP459	42	0.56-4.9	0.2-2	10
MP467	34	1.9-4.2	1-2	20
MP495	54	2.2-11	1-3	42
MP814	51	2.2-10	1-3	46
MP840	37	2.9-18	1-7	37

TSS

A minimum of nine water quality samples were collected from the pipe outlets (Table 17). The average TSS concentrations ranged from 15.1 to 153 mg/L, and the median concentrations are within the range of TSS concentrations sampled from highway bridge decks in North Carolina (Winston et al., 2015; Wu et al., 1998).

Table 18. Summary of TSS data from pipe outlets

Site	Number of samples	Minimum (mg/L)	Mean (mg/L)	Median (mg/L)	Maximum (mg/L)
MP458	11	8.21	15.1	13.4	25.7
MP459	10	4.87	43.2	21.8	107
MP467	14	47.5	153	123	339
MP495	23	5.34	15.4	13.6	38.0
MP814	15	13.2	74.1	47.9	213[a]
MP840	9	8.86	24.5	25.9	64.2

TSS concentrations sampled from four of the six sites exceeded the North Carolina surface water standard for non-trout waters (*15A NCAC 02B .0101*, 2019) more than 50% of the time (Table 18; Figure 24). The sources of TSS were most likely the extensive traffic on the adjacent highways and road degradation (Charters et al., 2016; Sansalone & Buchberger, 1996; Thomson et al., 1997). For MP467, bank instability near the monitoring equipment was almost certainly an additional source of TSS (Voli et al., 2013). Throughout monitoring, unstable undercuts were evident at this site (Figure 25), and bank erosion hazard index (BEHI) assessments indicated the channel banks were at very high or extreme risk of eroding (Rosgen, 2001) (Appendix E). MP458 and MP495 most likely had the smallest exceedance probabilities due to their watershed characteristics. MP495 had the lowest average annual daily traffic (62,500 vehicles per day), and MP458's watershed was only 11% impervious. Refer to Appendix F for full details regarding the raw TSS data.

Table 19. Exceedance probabilities for TSS standard (*15A NCAC 02B .0101*, 2019)

Site	Exceedance probability (%)
MP458	24
MP459	57
MP467	100
MP495	19
MP814	70
MP840	56

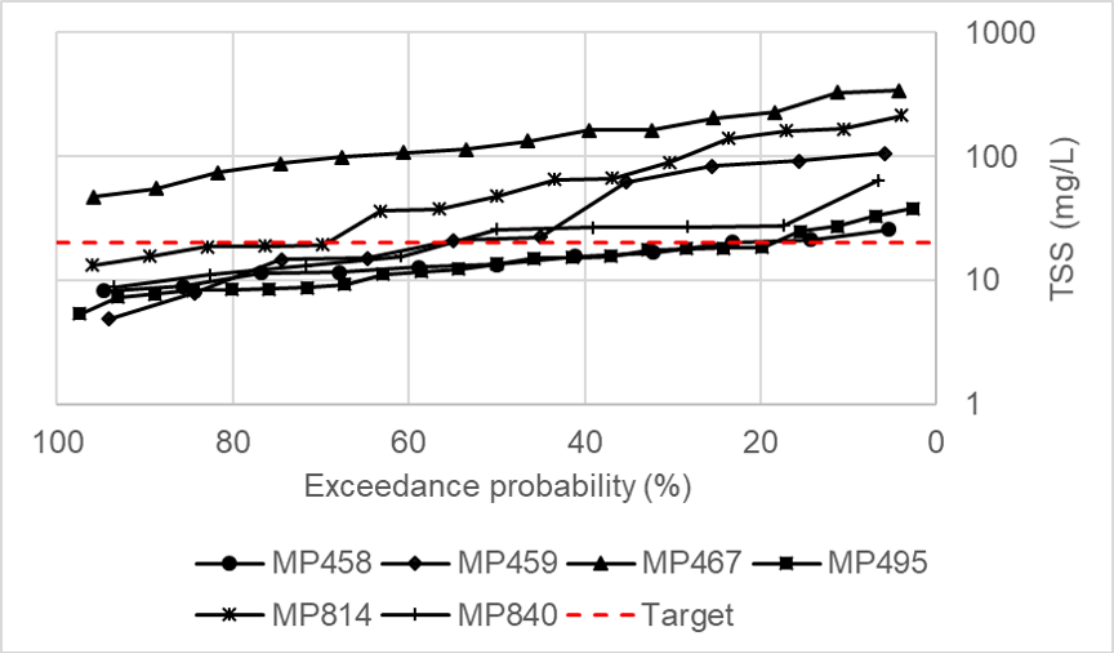

Figure 24. Exceedance probabilities for TSS standard (*15A NCAC 02B .0101*, 2019)

Figure 25. Evidence of unstable undercuts at MP467

Objective Six

1D steady analyses

Table 19 through Table 24 summarize the estimated maximum τ for the sites' existing conditions at the outlet, middle, and outfall or end cross-sections. Across the sites, the simulated maximum τ at the outlets ranged from 0.05 to 1.40 lb/ft^2 and from 0 and 1.61 lb/ft^2 for the middle cross-sections. The estimated τ at the outfall or end cross-sections varied between 0.06 and1.99 lb/ft^2. Except for two simulations, the predicted τ exceeds the sites' τ_c (Table 4). Flow was not measured at the channel outfall, and neither erosion pins nor repeated surveys of permanent cross-sections were included in the study to calibrate and validate the models representing the sites' existing conditions (Daly et al., 2015; Mohammed-Ali et al., 2021). These data would have improved confidence in the model results; however, site assessments taken over multiple visits confirmed erosion rather than deposition was most likely occurring.

Table 20. Summary of maximum shear stresses for MP458 existing conditions

Event	Outlet shear stress (lb/ft^2)	Middle shear stress (lb/ft^2)	Outfall shear stress (lb/ft^2)
87.5th	0.15	1.24	0.71
75th	0.59	1.42	0.87
50th	0.26	1.61	1.24
25th	0.36	1.61	1.66
12.5th	0.59	1.54	1.99
1-yr, 24-hr	0.32	0.55	0.06
10-yr, 24-hr	0.54	1.15	0.63

Table 21. Summary of maximum shear stresses for MP459 existing conditions

Event	Outlet shear stress (lb/ft^2)	Middle shear stress (lb/ft^2)	Outfall shear stress (lb/ft^2)
87.5^{th}	0.06	0.27	0.25
75^{th}	0.11	0.38	0.31
50^{th}	0.18	0.52	0.50
25^{th}	0.35	0.78	0.88
12.5^{th}	0.50	0.92	1.03
1-yr, 24-hr	0.05	0.29	0.25
10-yr, 24-hr	0.32	0.73	0.82

Table 22. Summary of maximum shear stresses for MP467 existing conditions

Event	Outlet shear stress (lb/ft^2)	Middle shear stress (lb/ft^2)	Outfall shear stress (lb/ft^2)
87.5th	0.83	0.06	0.49
75th	0.88	0.07	0.52
50th	1.04	0.11	0.61
25th	0.92	0.08	0.54
12.5th	1.40	0.29	0.95
1-yr, 24-hr	0.62	0.03	0.34
10-yr, 24-hr	0.76	0.04	0.44

Table 23. Summary of maximum shear stresses for MP495 existing conditions

Event	Outlet shear stress (lb/ft^2)	Middle shear stress (lb/ft^2)	Outfall shear stress (lb/ft^2)
87.5th	0.31	0.31	0.31
75th	0.32	0.33	0.32
50th	0.38	0.41	0.34
25th	0.59	0.55	0.44
12.5th	0.42	0.45	0.36
1-yr, 24-hr	0.51	0.48	0.39
10-yr, 24-hr	0.65	0.58	0.45

Table 24. Summary of maximum shear stresses for MP814 existing conditions

Event	Outlet shear stress (lb/ft^2)	Middle shear stress (lb/ft^2)	Outfall shear stress (lb/ft^2)
87.5th	0.45	0	0.46
75th	0.57	0.01	0.58
50th	0.55	0.02	0.80
25th	0.57	0.04	0.98
12.5th	0.56	0.05	1.00
1-yr, 24-hr	0.55	0.20	1.52
10-yr, 24-hr	0.53	0.42	1.90

Table 25. Summary of maximum shear stresses for MP840 existing conditions

Event	Outlet shear stress (lb/ft^2)	Middle shear stress (lb/ft^2)	Outfall shear stress (lb/ft^2)
87.5th	0.11	0.18	0.15
75th	0.24	0.24	0.21
50th	0.30	0.31	0.25
25th	0.45	0.33	0.32
12.5th	0.60	0.38	0.36
1-yr, 24-hr	0.83	0.52	0.50

10-yr, 24-hr	1.13	0.70	0.67

Table 25 includes the comparisons between the maximum τ for the existing conditions and the proposed swale designs. Across the sites, the maintained swales retrofitted with check dams reduced τ the most. In general, the models for this particular design reduced the hydraulic radius and energy grade line slope, which caused the reductions in τ (Equation 14). The estimated τ suggest the average channel bed slope does not influence the designs' effectiveness at mitigating downslope erosion.

Table 26. Comparison between existing conditions and proposed designs with regards to shear stress

Scenario	Site/Storm event[a]	Outlet shear stress (lb/ft^2)[b]							Middle shear stress (lb/ft^2)							Outfall/end shear stress (lb/ft^2)						
		1	2	3	4	5	6	7	1	2	3	4	5	6	7	1	2	3	4	5	6	7
Rip-rap swale	MP458	+	+	+	+	+	-	+	-	-	-	-	+	-	-	-	-	-	-	-	-	-	-
	MP459	+	+	+	+	+	+	+	+	+	+	+	+	-	+	+	+	+	+	+	+	-	+
	MP467	-	-	-	-	+	-	-	+	+	+	+	+	+	+	+	+	+	+	+	+	+	+
	MP495	+	+	+	+	+	+	+	+	+	+	+	+	+	+	+	+	+	+	+	+	+	+
	MP814	-	-	+	+	+	+	+	+	+	+	+	+	+	+	+	-	-	-	+	+	+	+
	MP840	-	-	-	-	-	-	-	-	-	-	-	+	+	+	-	-	-	-	+	+	+	+
Un-maintained vegetated swale	MP458	+	+	+	+	+	-	+	-	-	-	+	+	-	-	+	+	+	+	+	-	+	
	MP459	+	+	+	+	+	+	+	+	+	+	+	+	+	+	+	+	+	+	+	+	+	
	MP467	+	+	+	+	+	-	+	+	+	+	+	+	+	+	+	+	+	+	+	+	+	
	MP495	+	+	+	+	+	+	+	+	+	+	+	+	+	+	+	+	+	+	+	+	+	
	MP814	+	+	+	+	+	+	+	+	+	+	+	+	+	+	+	+	+	+	+	+	+	
	MP840	+	-	+	-	-	+	+	-	-	-	+	+	+	+	-	+	+	+	+	+	+	
Maintained vegetated swale with check dams	MP458	+	-	+	+	+	-	-	-	-	-	-	-	-	-	-	-	-	-	-	-	-	
	MP459	+	+	+	+	+	+	+	-	-	-	-	-	-	-	-	-	-	-	-	-	-	
	MP467	-	-	-	-	-	-	-	-	-	-	-	+	-	-	-	-	-	-	-	-	-	
	MP495	-	-	-	-	-	-	-	-	-	-	-	-	-	-	-	-	-	-	+	-	-	+
	MP814	-	-	-	-	-	+	+	+	+	+	+	+	+	+	-	-	-	-	-	-	-	
	MP840	-	-	-	-	-	-	-	-	-	-	-	-	-	-	-	-	-	-	-	-	-	
Un-maintained vegetated swale with check dams	MP458	+	+	+	+	+	-	+	-	-	-	-	+	-	-	+	+	+	+	+	-	+	
	MP459	+	+	+	+	+	+	+	-	-	-	+	+	-	+	+	+	+	+	+	+	+	
	MP467	+	+	+	+	+	+	+	+	+	+	+	+	+	+	+	+	+	+	+	+	+	
	MP495	+	+	+	+	+	+	+	+	+	+	+	+	+	+	+	+	+	+	+	+	+	
	MP814	+	+	+	+	+	+	+	+	+	+	+	+	+	+	+	+	+	+	+	+	+	
	MP840	+	+	+	+	-	+	+	-	-	-	-	-	+	+	-	+	+	+	+	+	+	

[a] Storm events 1 through 7 represent the 87.5th, 75th, 50th, 25th, 12.5th, 1-yr, 24-hr, and 10-yr, 24-hr storms, respectively.

[b] "+" refers to an increase and "-" refers to a decrease in shear stress.

Sediment Transport

Table 26 through Table 31 summarize the estimated sediment transport for the sites' existing conditions. The models predicted that erosion would occur for most, if not all, of the simulated storm events. For MP840, the model was not able to simulate all of the storm events. The model predicted the channel at the outfall would be filled with sediment despite adjusting the transport function, sorting, and fall velocity methods. Deposition was present throughout the channel, the channel narrowed as it approached the outfall, and the distance between the top of bank and toe of slope at the outfall was minimal (Figure 26). Brunner (2022) reported narrow and/or low bank stations can cause the model to predict sediment filling in the channel.

Table 27. Summary of sediment transport for MP458 existing conditions

Storm event	Sediment (ft^3)		Erosion/deposition
	Volume in	Volume out	
87.5^{th}	1,457	2,015	Erosion
75^{th}	1,002	1,695	Erosion
50^{th}	5,386	7,144	Erosion
25^{th}	39,836	42,217	Erosion
12.5^{th}	8,033	5,374	Deposition
1-yr, 24-hr	$1.73*10^{-1}$	0	Deposition
10-yr, 24-hr	462	895	Erosion

Table 28. Summary of sediment transport for MP459 existing conditions

Storm event	Sediment (ft^3)		Erosion/deposition
	Volume in	Volume out	
87.5^{th}	0	0.48	Erosion
75^{th}	0	111	Erosion
50^{th}	0	279	Erosion
25^{th}	1,126	2,355	Erosion
12.5^{th}	2,417	4,262	Erosion
1-yr, 24-hr	0	$3.30*10^{-3}$	Erosion
10-yr, 24-hr	1,458	2,941	Erosion

Table 29. Summary of sediment transport for MP467 existing conditions

Storm event	Sediment (ft^3)		Erosion/deposition
	Volume in	Volume out	
87.5th	10	223	Erosion
75th	11	307	Erosion
50th	75	1,086	Erosion
25th	73	1,336	Erosion
12.5th	293	3,712	Erosion
1-yr, 24-hr	1.17	0.90	Deposition
10-yr, 24-hr	7	90	Erosion

Table 30. Summary of sediment transport for MP495 existing conditions

Storm event	Sediment (ft^3)		Erosion/deposition
	Volume in	Volume out	
87.5th	0.15	0.25	Erosion
75th	0.22	1.26	Erosion
50th	0.19	0.62	Erosion
25th	2.49	4.91	Erosion
12.5th	2.35	6.34	Erosion
1-yr, 24-hr	1.42	1.86	Erosion
10-yr, 24-hr	7	12	Erosion

Table 31. Summary of sediment transport for MP814 existing conditions

Storm event	Sediment (ft^3)		Erosion/deposition
	Volume in	Volume out	
87.5th	1	5	Erosion
75th	4	40	Erosion
50th	34	336	Erosion
25th	1,152	2,759	Erosion
12.5th	1,353	1,503	Erosion
1-yr, 24-hr	20,835	22,192	Erosion
10-yr, 24-hr	90,343	94,068	Erosion

Table 32. Summary of sediment transport for MP840 existing conditions

Storm event	Sediment (ft^3)		Erosion/deposition
	Volume in	Volume out	
87.5^{th}	-	-	-
75^{th}	-	-	-
50^{th}	0	0.10	Erosion
25^{th}	0.01	6.96	Erosion
12.5^{th}	0.33	317	Erosion
1-yr, 24-hr	4.67	202	Erosion
10-yr, 24-hr	-	-	-

Figure 26. MP840 channel sediment deposition (left) and outfall bank (right)

Table 32 through Table 37 include the estimated sediment transport for the swales lined with rip-rap or well-established vegetation. Table 38 summarizes the comparisons between the sediment mass balances for the existing conditions and lined swales without check dams. The models predicted both linings would generally result in less erosion compared to the existing channels. The sediment transport results also support the τ predictions from the 1D steady analyses. Ideally, the models would have predicted equilibrium conditions where the influent and effluent sediment volumes were equal. Four of the seven simulated storm events had equilibrium conditions for the MP840 swales without check dams.

Table 33. Summary of sediment transport for MP458 swales without check dams

Storm event	Rip-rap swale sediment (ft^3)		Rip-rap swale erosion/ deposition	Vegetated swale sediment (ft^3)		Vegetated swale erosion/ deposition
	Volume in	Volume out		Volume in	Volume out	
87.5^{th}	11,581	10,954	Deposition	2,611	2,539	Deposition
75^{th}	8,100	8,068	Deposition	1,867	1,849	Deposition
50^{th}	44,853	44,808	Deposition	10,119	9,868	Deposition
25^{th}	309,600	300,570	Deposition	72,497	71,054	Deposition
12.5^{th}	16,111	16,127	Erosion	3,470	3,437	Deposition
1-yr, 24-hr	2	1	Deposition	92	27	Deposition
10-yr, 24-hr	3,750	3,724	Deposition	908	897	Deposition

Table 34. Summary of sediment transport for MP459 swales without check dams

Storm event	Rip-rap swale sediment (ft^3)		Rip-rap swale erosion/ deposition	Vegetated swale sediment (ft^3)		Vegetated swale erosion/ deposition
	Volume in	Volume out		Volume in	Volume out	
87.5^{th}	$2.90*10^{-3}$	79	Erosion	0	25	Erosion
75^{th}	$2.66*10^{-2}$	318	Erosion	$1.40*10^{-3}$	103	Erosion
50^{th}	$6.02*10^{-2}$	248	Erosion	$4.10*10^{-3}$	76	Erosion
25^{th}	13,552	13,439	Deposition	2,710	2,775	Erosion
12.5^{th}	18,789	18,981	Erosion	4,044	4,113	Erosion
1-yr, 24-hr	0	4	Erosion	0	2	Erosion
10-yr, 24-hr	12,159	12,238	Erosion	3,220	3,279	Erosion

Table 35. Summary of sediment transport for MP467 swales without check dams

Storm event	Rip-rap swale sediment (ft^3)		Rip-rap swale erosion/ deposition	Vegetated swale sediment (ft^3)		Vegetated swale erosion/ deposition
	Volume in	Volume out		Volume in	Volume out	
87.5^{th}	$3.61*10^{-2}$	45	Erosion	0	19	Erosion
75^{th}	$4.60*10^{-2}$	62	Erosion	$5.50*10^{-3}$	25	Erosion
50^{th}	3	226	Erosion	$3.94*10^{-2}$	79	Erosion
25^{th}	$3.75*10^{-1}$	279	Erosion	$5.78*10^{-2}$	104	Erosion
12.5^{th}	13,489	13,797	Erosion	2,239	2,201	Deposition
1-yr, 24-hr	0	1	Erosion	0	1	Erosion
10-yr, 24-hr	$2.00*10^{-2}$	23	Erosion	0	8	Erosion

Table 36. Summary of sediment transport for MP495 swales without check dams

Storm event	Rip-rap swale sediment (ft^3)		Rip-rap swale erosion/ deposition	Vegetated swale sediment (ft^3)		Vegetated swale erosion/ deposition
	Volume in	Volume out		Volume in	Volume out	
87.5^{th}	$3.30*10^{-3}$	$4.69*10^{-2}$	Erosion	0	$2.56*10^{-2}$	Erosion
75^{th}	$5.30*10^{-3}$	$6.31*10^{-2}$	Erosion	0	$3.27*10^{-2}$	Erosion
50^{th}	$6.10*10^{-3}$	$1.45*10^{-1}$	Erosion	0	$7.26*10^{-2}$	Erosion
25^{th}	$2.67*10^{-2}$	$6.22*10^{-1}$	Erosion	0	6	Erosion
12.5^{th}	$7.64*10^{-2}$	1	Erosion	0	$6.78*10^{-1}$	Erosion
1-yr, 24-hr	$9.30*10^{-3}$	$2.99*10^{-1}$	Erosion	0	$1.35*10^{-1}$	Erosion
10-yr, 24-hr	$3.85*10^{-2}$	$8.92*10^{-1}$	Erosion	0	25	Erosion

Table 37. Summary of sediment transport for MP814 swales without check dams

Storm event	Rip-rap swale sediment (ft^3)		Rip-rap swale erosion/ deposition	Vegetated swale sediment (ft^3)		Vegetated swale erosion/ deposition
	Volume in	Volume out		Volume in	Volume out	
87.5th	$1.64*10^{-2}$	$1.87*10^{-1}$	Erosion	0	$1.13*10^{-1}$	Erosion
75th	$1.87*10^{-2}$	$3.19*10^{-1}$	Erosion	0	1	Erosion
50th	$3.41*10^{-1}$	308	Erosion	1,454	1,472	Erosion
25th	21,035	20,920	Deposition	4,543	4,443	Deposition
12.5th	3,133	3,039	Deposition	677	665	Deposition
1-yr, 24-hr	15,716	15,522	Deposition	3,524	3,640	Erosion
10-yr, 24-hr	44,837	45,322	Erosion	9,469	9,778	Erosion

Table 38. Summary of sediment transport for MP840 swales without check dams

Storm event	Rip-rap swale sediment (ft^3)		Rip-rap swale erosion/ deposition	Vegetated swale sediment (ft^3)		Vegetated swale erosion/ deposition
	Volume in	Volume out		Volume in	Volume out	
87.5th	0	0	Equilibrium	0	0	Equilibrium
75th	0	0	Equilibrium	0	0	Equilibrium
50th	0	0	Equilibrium	0	0	Equilibrium
25th	0	0.43	Erosion	0	3	Erosion
12.5th	$1.34*10^{-2}$	284	Erosion	0	120	Erosion
1-yr, 24-hr	$1.24*10^{-2}$	155	Erosion	0	82	Erosion
10-yr, 24-hr	0	0	Equilibrium	0	0	Equilibrium

Table 39. Comparisons of sediment mass balances between existing conditions and swales without check dams

Design	Site	Storm event						
		87.5th	**75th**	**50th**	**25th**	**12.5th**	**1-yr, 24-hr**	**10-yr, 24-hr**
Rip-rap swale	MP458	Deposition	Deposition	Deposition	Deposition	Erosion	Less deposition	Deposition
	MP459	Erosion	Erosion	Erosion	Deposition	Erosion	Erosion	Erosion
	MP467	Less erosion	Less erosion	Less erosion	Less erosion	Less erosion	Erosion	Less erosion
	MP495	Erosion	Less erosion	Less erosion	Less erosion	Less erosion	Less erosion	Less erosion
	MP814	Less erosion	Less erosion	Erosion	Deposition	Deposition	Deposition	Less erosion
	MP840	N/A	N/A	Less erosion	Less erosion	Erosion	Less erosion	N/A
Vegetated swale	MP458	Deposition	Deposition	Deposition	Deposition	Deposition	Deposition	Deposition
	MP459	Erosion	Erosion	Erosion	Erosion	Erosion	Erosion	Erosion
	MP467	Less erosion	Less erosion	Less erosion	Less erosion	Deposition	Erosion	Less erosion
	MP495	Erosion	Less erosion	Less erosion	More erosion	Less erosion	Less erosion	More erosion
	MP814	Less erosion	Less erosion	Less erosion	Deposition	Deposition	Less erosion	Less erosion
	MP840	N/A	N/A	Equilibrium	Erosion	Less erosion	Less erosion	N/A

Note for MP840 the model predicted the existing channel filled with sediment at the outfall for the 87.5th, 75th, and 10-yr, 24-hr storm events

These preliminary results suggest turf grass swales with check dams may mitigate the potential for erosion downslope of pipe outlets. Studies have demonstrated swales retrofitted with check dams can reduce peak discharges and increase soil conservation (Davis et al., 2012; Lucas-Borja et al., 2018, 2021; Winston et al., 2019). Additionally, observations made during the site assessments for Objective Two, and previous research have shown vegetation can reduce soil detachment (Allen et al., 2018; Cerdá & Doerr, 2005; Smith et al., 2021; Zhao et al., 2016). Ultimately, field-scale studies should validate these results before design standards for pipe outlets are revised.

Objective Seven

Table 40 includes the estimated construction and maintenance costs for the proposed and typical outlet designs. The predicted costs for the rip-rap and un-maintained vegetated swales were comparable; these costs ranged between $30,575 and $161,906. The maintained vegetated swales had the highest costs ($41,314 to $244,343), and all the designs were significantly more expensive than the pre-formed scour holes. However, the results from Objectives Two and Five suggest pre-formed scour holes do not limit erosion downslope of pipe outlets. Designers should consider allocating more construction funds to downslope protection strategies to help reduce the potential of gully formation. Appendix L provides the costs associated with swale's line item.

Table 40. Estimated construction and maintenance costs for proposed designs

Site	Rip-rap swale	Maintained vegetated swale[1]	Un-maintained vegetated swale	Pre-formed scour hole
MP458	$86,626	$129,710	$86,492	$4,772
MP459	$56,729	$80,886	$56,654	
MP467	$95,263	$163,879	$96,103	
MP495	$30,575	$41,314	$30,707	
MP814	$161,906	$203,639	$160,421	
MP840	$156,820	$244,343	$156,549	

[1] Costs include annual maintenance without considering inflation
Note costs associated with check dam installation and maintenance are not included.

Summary and conclusions

Sediment pollution is a worldwide concern, and stormwater conveyance networks contribute to stream degradation and instability either through direct discharges or by causing gullies downslope of pipe outlets. To limit erosion downslope of pipe outlets in North Carolina, current regulations require designers to limit the peak velocity for the 10-yr, 24-hr storm event to the downslope soil's permissible velocity, otherwise the conveyance system must be redesigned

(*15A NCAC 04B .0109*, 1992; Fortier & Scobey, 1926). Recommendations to become compliant include using energy dissipators, installing stormwater control measures (SCMs), and replacing impervious areas with vegetation. However, the effectiveness of this design standard is not well documented. This study assessed 60 pipe outlets draining highway and non-highway areas in North Carolina to identify which watershed and downslope characteristics influence the severity of erosion caused by pipe outlets as well as the effectiveness of the current standard. Tools to predict the magnitude of erosion downslope of pipe outlets were calibrated and validated using these assessment data. This study also monitored six of the assessed sites for hydrologic, hydraulic, and water quality impacts and used these data to model proposed designs to limit downslope erosion.

Objective Two

- Of the 60 assessed pipe outlets, 12 did not exhibit any signs of erosion. The lack of erosion was attributed to well-established vegetation, minimal to no clusters of trees, and a high percentage of HSG B soils downslope of the outlets.
- The maximum length and estimated volume of downslope erosion was 7,431 ft and 4,102 yd^3, respectively. The median length and volume of erosion was 410 ft and 94 yd^3, respectively. The median BEHI score and depth to confining layer was 32.8 (high) and 1.0 ft, respectively which suggests assessed channels are at risk of widening and incising.
- These data suggest the current practice of limiting the peak 10-yr, 24-hr velocity to the permissible velocity for downslope soil conditions does not sufficiently reduce the potential for overland erosion. Designers should also consider the vegetative cover and percentage of higher infiltrating soils downslope of the discharge point as well as limiting the peak velocity for the 1-yr, 24-hr storm event to the downslope soil's permissible velocity. Research has shown flows associated with higher frequency storm events have more erosion potential than storms with lower frequencies (Hawley et al., 2017; Pomeroy et al., 2008; Roesner et al., 2001; Rohrer & Roesner, 2006; Tillinghast et al., 2011).

Objectives Three and Four

- Both the decision tree and logistic regression model fitted with PCA components indicated that watershed characteristics and downslope soil conditions influence the occurrence of erosion downslope of pipe outlets. Characteristics affecting the occurrence of erosion were primarily the downslope percentage of sand and clay in the

pipe outlets' channel banks, peak velocities for the 1-yr and 10-yr, 24-hr storm, and percentage of downslope HSG A/B/C/D soils.

- The ratio between the maximum permissible velocity and peak velocity for the 1-yr, 24-hr storm and the percentage of sand and clay in the banks immediately downslope of the pipe outlet were the most important predictors for the decision tree predicting the occurrence of erosion. The decision tree had an accuracy and precision of 62.5% and 50%, respectively, during testing.
- Eight components explained approximately 80% of the data variation. Most of the influential predictors within these components were related to the downslope soil conditions and factors affecting erosion (e.g., departure, duration of runoff). These components were not significant (p-value > 0.05), and the logistic regression model predicting the occurrence of erosion only had a 50% accuracy when used with the testing dataset. The logistic regression model's poor performance was most likely due to missing temporal predictors that could have better explained data variability. These predictors include the age of the pipe installation at the time of assessment, changes to the watershed between the design and assessment phases, and the downslope conditions at the time of the pipe installation.
- Recurring variables for the models predicting the magnitude of erosion include the duration of runoff and peak discharge for the 10-yr, 24-hr storm event, percentage of downslope HSG soils, radial distance of the pipe outlet from the stream, and the pipe outlet watershed's CN and impervious area. These significant predictors also support the conclusion drawn for Objective Two; designers should account for soil characteristics downslope of discharge points in addition to hydrologic factors such as runoff duration and discharge when designing stormwater conveyance systems.
- Model performance for predicting the magnitude of erosion was evaluated using NRMSEs and Q-Q plots of the residuals. The NRMSEs for the $Area_{TOB}/Area_{BKFUL}$, $Width_{TOB}/Width_{BKFUL}$, $Depth_{TOB}/Depth_{BKFUL}$, and $Volume_{ERODED}/Length_{CHNL}$ regression equations were 0.07, 0.09, 0.21, and 0.29, respectively. The NRMSEs for the decision trees predicting erosion in terms of cross-sectional area, width, depth, and volume were 0.10, 0.09, 0.21, 0.03, respectively. Aside from $Volume_{ERODED}/Length_{CHNL}$, the regression equations performed as well if not better than the decision trees. This was mostly like due to the size of the dataset (Hastie et al., 2009; Kotsiantis, 2013; Myles et al., 2004). The NRMSEs and Q-Q plots indicated the data collected for this study were better suited

to predict $Area_{TOB}/Area_{BKFUL}$ and $Width_{TOB}/Width_{BKFUL}$ than $Depth_{TOB}/Depth_{BKFUL}$, and $Volume_{ERODED}/Length_{CHNL}$ using regression equations.

- Similar to the logistic regression model predicting the occurrence of erosion, the NRMSEs and Q-Q plots indicate the equations and decision trees predicting the magnitude of erosion need additional predictors to explain the variability in the data (e.g., downslope conditions at the time of pipe installation). Future studies should also collect data that influences soil degradation (e.g., percent sand/clay) at every cross-section along the channel.
- The regression equations developed for $Area_{TOB}/Area_{BKFUL}$ and $Width_{TOB}/Width_{BKFUL}$ as well as the decision tree for $Volume_{ERODED}/Length_{CHNL}$ appear to be as reliable as existing erosion models (USLE, RUSLE2, USLE-M). Designers could use these equations and decision tree to optimize the location of pipe outlets to minimize downslope erosion or identify which existing pipe outlets may require re-stabilization. Additionally, these predictive tools may assist with designing the footprint of an RSC as current guidance focuses on ensuring the design conveys extreme storm events (e.g., 100-yr) (Anne Arundel County Department of Public Works, 2022; WV DEP, 2012). Refined RSC footprints could help reduce construction costs and or the need for an easement.

Objective Five

- The hydraulic impacts of the pipe outlets were quantified using the maximum ε estimated from HEC-RAS 6.2 (USACE, 2022) 1D steady and unsteady flow simulations. Except for MP495 and MP814, the models were too unstable for unsteady flow analyses. The potential maximum ε simulated in steady flow analyses ranged from $1.3*10^{-3}$ to $4.5*10^{-2}$ in/s per storm event. The limited results from the unsteady flow analyses suggest steady flow analyses may under-predict ε associated with pipe outlets. This study did not include erosion pins or re-survey permanent cross-sections to validate simulated ε, and flow was not monitored throughout the channel to verify the duration of the potential maximum ε. These data would have improved model stability and performance as well as better quantified the impacts of the estimated ε. However, the results indicate designers should include the erodibility of the soils downslope of the pipe discharge points in their hydraulic analyses. Over time, the τ_a could cause additional sediment loss if a gully forms downslope of the pipe outlet.
- The hydraulic impacts of the pipe outlets were also quantified using peak velocities. The peak velocities ranged from 0.56 to 20 ft/s and exceeded the permissible velocity at least

10 times during the monitoring period despite none of the storms having rainfall depths greater the sites' 10-yr, 24-hr rainfall depth (NOAA, 2006). The magnitude of erosion downslope of the monitored sites and the reoccurring exceedance of the permissible velocity supports the conclusion drawn for Objective Two; designers should consider limiting the 1-yr, 24-hr storm peak velocity to reduce erosion potential.

- Monitoring occurred from July 2021 to August 2022 and at least 57 storm events per site were recorded. Rainfall ranged from 0.10 to 5.42 in, and runoff volumes were between $1.00*10^2$ to $7.20*10^5$ ft^3. The largest recorded peak discharge was 83 ft^3/s. TSS data were collected from at least nine storm events per site. TSS concentrations leaving the outlets ranged from 4.87 to 339 mg/L and exceeded water quality standards for TSS more than 50% of the time. Based on this study, pipe outlets draining highway and non-highway areas require additional treatment to meet regulations.

Objective Six

- The 1D steady models representing the existing conditions predicted the maximum τ at the outlet cross-sections ranged from 0.05 to 1.40 lb/ft^2 and from 0 and 1.61 lb/ft^2 for the middle cross-sections. The estimated τ at the outfall or end cross-sections varied between 0.06 and1.99 lb/ft^2. The models predicted the τ_c was exceeded throughout the simulated storm events. The 1D quasi-unsteady models predicted erosion would occur for most, if not all, of the sites. Multiple site visits suggest erosion is most likely occurring, and these results suggest the existing sites are at risk of continued de-stabilization.
- Across the sites, the maintained swales retrofitted with check dams reduced τ the most. The sediment mass balances for the rip-rap and vegetated swales indicate these swales would generally result in less erosion compared to the existing channels. These preliminary results suggest turf grass swales with check dams may mitigate the potential for erosion downslope of pipe outlets. Previous research has demonstrated swales retrofitted with check dams can mitigate erosion (Lucas-Borja et al., 2018, 2021). However, the feasibility of establishing vegetation in swales that would be constructed in wooded areas is questionable. The swales would require easements wide enough to avoid the turf grass growing in shade.
- Swales typically convey runoff from highways which increases the likelihood of designers accepting this proposed design. Ultimately, field-scale studies should validate these results before design standards for pipe outlets draining highway and non-highway

areas are revised. Future studies should also consider RSCs and step pool systems without media as potential designs to limit erosion downslope of pipe outlets. Previous studies have demonstrated field-scale RSCs mitigate peak discharges and runoff volumes while stabilizing eroded outfalls (Cizek et al., 2017, 2018; Koryto et al., 2017; Thompson et al., 2020), and Thompson et al. (2018) has shown RSCs have the potential to minimize erosive velocities.

Objective Seven

- The expected costs for the rip-rap swales ranged from $30,575 to $161,906 while the estimated costs for the un-maintained vegetated swales were between $30,707 and $156,549. Costs for the maintained vegetated swales were from $41,314 to $244,343. The cost of a pre-formed scour hole was $4,772. Construction and maintenance costs for check dams were not included in the analyses. Additionally, costs associated with grading and maintenance easements were not considered.
- Results from Objectives Two and Five indicate pre-formed scour holes do not limit erosion downslope of pipe outlets, and future research is needed to determine which design(s) will limit erosion downslope of pipe outlets. However, designers should consider using these estimated costs to project future allocations of construction funds to downslope protection.

Recommendations for future work

Controlling stormwater runoff to limit degradation in streams and other water bodies is a long-standing issue (Bledsoe, 2002; Schueler et al., 2009). This study has contributed towards the efforts to mitigate flow-caused erosion but has also yielded questions that future research will need to address.

This study lacked temporal predictors that would have further refined the study's conclusions and improved the accuracy of model prediction. Future studies should evaluate the severity of downslope erosion for pipe outlets with known ages to quantify the impacts over time. These studies should also include repeated surveys of permanent cross-sections and erosion pin measurements to quantify the channels' ε. Relationships should be established between the measured ε and watershed and downslope characteristics to help designers identify how quickly erosion may occur and/or the magnitude of erosion that can occur, given certain site conditions. These data would also help calibrate and validate the proposed CEM. Other states, such as Maryland, that focus on limiting erosion downslope of pipe outlets may

also consider calibrating and validating the proposed CEM to help optimize resources designated for rehabilitating eroding channels.

Future studies should consider quantifying the minimum width and length and the maximum slope of well-established or non-clumping grassed and herbaceous vegetation needed to minimize the hydraulic impacts of runoff discharged by pipe outlets. These studies should identify which types of vegetation provide the most resistance to soil detachment, if a combination of grasses and a typical riparian buffer dissipates flow, and how often should the vegetation be maintained to continue providing resistance to erosion. The studies also may consider evaluating the effects of using a level-spreader upslope of the vegetation or rehabilitating downslope soils with compost or permeable media to decrease the risk of downslope erosion. Studies focused on rehabilitating downslope soils should also identify the minimum width, length, and depth of rehabilitation needed to limit erosion.

More efforts should be directed towards determining which discharge threshold limits erosion. Previous studies have advocated for limiting discharges to the critical discharge (Q_c) to increase the likelihood that stormwater management preserves stream stability (Hawley et al. 2017; Hawley & Vietz, 2016; Lammers et al., 2020; Tillinghast et al., 2011; Wooten et al., 2022). Limiting flow to the Q_c will reduce the risk of disrupting streams' natural flow regimes and sediment transport capacities. Future efforts should develop methods to predict the Q_c for pipe outlets; this may include using the Q_c for nearby streams or the Q_c for soils downslope of pipe outlets. Studies may also consider developing new pipe outlet configurations or implementing elements of spillway designs (e.g., Saint Anthony Falls stilling basin) to reduce the risk of downslope erosion (Figure 19). Prior to implementation, field collected data should be simulated with the altered conveyance system to better understand the feasibility of the system to safely convey runoff under different runoff conditions. Studies monitoring the field-scale designs should use repeated surveys of permanent cross-sections and erosion pin measurements to evaluate the effectiveness of the proposed designs.

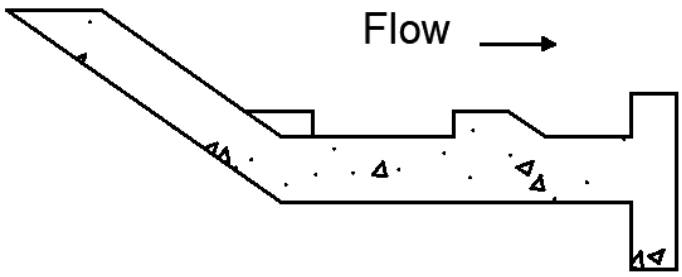

Figure 27. Side profile view of Saint Anthony Falls stilling basin (Blaisdell, 1948)

Future studies focused on the stability of and water quality in channels downslope of pipe outlets should monitor for cross-sectional and water level as well as water quality changes at the outfall. These data will improve the results of models representing the channels, identify how long τ occurs within the channel, and determine how water quality improves. Studies should determine which maintenance regimens and types of vegetation reduce erosion optimize the designs' potential to limit erosion. Additional future research includes evaluating how well stream restoration techniques (e.g., toe wood, rock vanes) help stabilize channels caused by pipe erosion and if channels designed per the predictive equations remain stable. States that use RSCs for stormwater management may also consider evaluating how well the predictive equations improve RSC design.

References

15A NCAC 02B .0101. (2019). http://reports.oah.state.nc.us/ncac/title%2015a%20-%20environmental%20quality/chapter%2002%20-%20environmental%20management/subchapter%20b/subchapter%20b%20rules.pdf

15A NCAC 04B .0109. (1992). http://reports.oah.state.nc.us/ncac/title%2015a%20-%20environmental%20quality/chapter%2004%20-%20sedimentation%20control/subchapter%20b/15a%20ncac%2004b%20.0109.pdf

Ackers, P., & White, W.R. (1973). Sediment transport: New approach and analysis. *Journal of Hydraulics Division*, 99(HY11). https://doi.org/10.1061/jyceaj.0003791

Aksoy, H., & Kavvas, M. L. (2005). A review of hillslope and watershed scale erosion and sediment transport models. *Catena*, *64*(2–3). https://doi.org/10.1016/j.catena.2005.08.008

Allen, D. C., Wynn-Thompson, T. M., Kopp, D. A., & Cardinale, B. J. (2018). Riparian plant biodiversity reduces stream channel migration rates in three rivers in Michigan, U.S.A. *Ecohydrology*, *11*(4). https://doi.org/10.1002/eco.1972

Allmanová, Z., Vlcková, M., Jankovský, M., Allman, M., & Hlavatá, H. (2019). Predicting the annual erosion rates on a small stream by the BANCS model. *Soil and Water Research*, *14*(4). https://doi.org/10.17221/58/2018-SWR

Allmanová, Z., Vlčková, M., Jankovský, M., Allman, M., & Merganič, J. (2021). How can stream bank erosion be predicted on small water courses? Verification of BANCS model on the Kubrica watershed. *International Journal of Sediment Research*, *36*(3). https://doi.org/10.1016/j.ijsrc.2020.10.008

Al-Madhhachi, A. T., Fox, G. A., Hanson, G. J., Tyagi, A. K., & Bulut, R. (2014). Mechanistic Detachment Rate Model to Predict Soil Erodibility Due to Fluvial and Seepage Forces. *Journal of Hydraulic Engineering*, *140*(5). https://doi.org/10.1061/(asce)hy.1943-7900.0000836

Al-Madhhachi, A. T., Hanson, G. J., Fox, G. A., Tyagi, A. K., & Bulut, R. (2013a). Deriving parameters of a fundamental detachment model for cohesive soils from flume and jet erosion tests. *Transactions of the ASABE*, *56*(2).

Al-Madhhachi, A. T., Hanson, G. J., Fox, G. A., Tyagi, A. K., & Bulut, R. (2013b). Measuring soil erodibility using a laboratory "mini" jet. *Transactions of the ASABE*, *56*(3). https://doi.org/10.13031/trans.56.9742

Amiri-Tokaldany, E., Darby, S. E., & Tosswell, P. (2003). Bank stability analysis for predicting reach scale land loss and sediment yield. *Journal of the American Water Resources Association*, *39*(4). https://doi.org/10.1111/j.1752-1688.2003.tb04414.x

Anne Arundel County Department of Public Works. (2022). *Regenerative step pool storm conveyance (SPSC)*. https://www.aacounty.org/departments/public-works/wprp/restoration/step-pool-conveyance-systems/

APHA. (2005). Standard Methods for the Examination of Water and Wastewater. *Standard Methods*. https://doi.org/ISBN 9780875532356

ASTM. (2014). ASTM C136 / C136M - 14 Standard Test Method for Sieve Analysis of Fine and Coarse Aggregates. *ASTM International, West Conshohocken*.

ASTM D7263. (2021). Standard Test Methods for Laboratory Determination of Density and Unit Weight of Soil Specimens | Engineering360. *United States: American Society for Testing and Material.*

ASTM D7928. (2021). Standard Test Method for Particle-Size Distribution (Gradation) of Fine-Grained Soils Using the Sedimentation (Hydrometer) Analysis. *ASTM International*, *May 2016*.

Autodesk. (2019). *Autodesk Civil 3D 2020* (23.1). https://www.autodesk.com/products/civil-3d/overview?term=1-YEAR&tab=subscription

Barrett, M.E., Walsh, P.M., Malina, J.F., & Charbeneau, R.J. (1998). Performance of vegetative controls for treating highway runoff. *Journal of Environmental Engineering*, *124*(11). https://doi.org/10.1061/(asce)0733-9372(1998)124:11(1121)

Baruch, E. M., Voss, K. A., Blaszczak, J. R., Delesantro, J., Urban, D. L., & Bernhardt, E. S. (2018). Not all pavements lead to streams: Variation in impervious surface connectivity affects urban stream ecosystems. *Freshwater Science*, *37*(3). https://doi.org/10.1086/699014

Beck, W., Isenhart, T., Moore, P., Schilling, K., Schultz, R., & Tomer, M. (2018). Streambank alluvial unit contributions to suspended sediment and total phosphorus loads, walnut Creek, Iowa, USA. *Water (Switzerland)*, *10*(2). https://doi.org/10.3390/w10020111

Bennett, N.D., Croke, B.F.W., Guariso, G., Guillaume, J.H.A., Hamilton, S.H., Jakeman, A.J., Marsili-Libelli, S., Newham, L.T.H., Norton, J.P., Perrin, C., Pierce, S.A., Robson, B., Seppelt, R., Voinov, A.A., Fath, B.D., & Andreassian, V. (2013). Characterising performance of environmental models. *Environmental Modelling and Software*, *40*. https://doi.org/10.1016/j.envsoft.2012.09.011

Bennett, S. J., Alonso, C.V., Prasad, S. N., & Römkens, M. J. M. (2000). Experiments on headcut growth and migration in concentrated flows typical of upland areas. *Water Resources Research*, *36*(7). https://doi.org/10.1029/2000WR900067

Bennett, S. J., & Wells, R. R. (2019). Gully erosion processes, disciplinary fragmentation, and technological innovation. *Earth Surface Processes and Landforms*, *44*(1). https://doi.org/10.1002/esp.4522

Biedenharn, D. S., Watson, C. C., Smith, J. B., & Hubbard, L. C. (2004). *Application of regional sediment approach to Hickahala Creek Watershed, Northern Mississippi*.

Bigham, K. A., Moore, T. L., Vogel, J. R., & Keane, T. D. (2018). Repeatability, Sensitivity, and Uncertainty Analyses of the BANCS Model Developed to Predict Annual Streambank Erosion Rates. *Journal of the American Water Resources Association*, *54*(2). https://doi.org/10.1111/1752-1688.12615

Blaisdell, F.W. (1948). Development and hydraulic design, Saint Anthony Falls Stilling basin. *Transactions of the American Society of Civil Engineers*, *113*(1). https://doi.org/10.1061/taceat.0006103

Blaisdell, F. W., Anderson, C. L., & Hebaus, G. G. (1981). Ultimate dimensions of local scour (erosion). *Journal of the Hydraulics Division, ASCE*, *107*(HY3, Proc. Paper, 16144).

Bledsoe, B. P. (2002). Stream Erosion Potential and Stormwater Management Strategies. *Journal of Water Resources Planning and Management*, *128*(6). https://doi.org/10.1061/(asce)0733-9496(2002)128:6(451)

Bledsoe, B.P., Baker, D., Nelson, P., Rosburg, T., Sholtes, J., Stroth, T., United States. Federal Highway Administration, National Academies of Sciences, E., National Cooperative Highway Research Program, & American Association of State Highway and Transportation Officials. (2017). *Guidance for design hydrology for stream restoration and channel stability*.

Bledsoe, B. P., Stein, E. D., Hawley, R. J., & Booth, D. (2012). Framework and Tool for Rapid Assessment of Stream Susceptibility to Hydromodification. *Journal of the American Water Resources Association*, *48*(4). https://doi.org/10.1111/j.1752-1688.2012.00653.x

Booth, D. B., & Fischenich, C. J. (2015). A channel evolution model to guide sustainable urban stream restoration. *Area*, *47*(4). https://doi.org/10.1111/area.12180

Booth, D.B., & Jackson, C.R. (1997). Urbanization of aquatic systems: Degradation thresholds, stormwater detection, and the limits of mitigation. Journal of the American Water Resources Association, 33(5). https://doi.org/10.1111/j.1752-1688.1997.tb04126.x

Bracken, L. J., & Croke, J. (2007). The concept of hydrological connectivity and its contribution to understanding runoff-dominated geomorphic systems. *Hydrological Processes*, *21*(13). https://doi.org/10.1002/hyp.6313

Brunner, G., Savant, G., & Heath, R. E. (2020). *Modeler application guidance for steady vs. unsteady, and 1D vs 2D vs 3D hydraulic modeling*. https://www.hec.usace.army.mil/publications/TrainingDocuments/TD-41.pdf

Brunner, G. W. (2022). HEC-RAS User's Manual. *US Army Corps of Engineers Hydrologic Engineering Center*.

Bryan, R. B. (2000). Soil erodibility and processes of water erosion on hillslope. *Geomorphology*, *32*(3–4). https://doi.org/10.1016/S0169-555X(99)00105-1

Bull, L. J., & Kirkby, M. J. (1997). Gully processes and modelling. *Progress in Physical Geography*, *21*(3). https://doi.org/10.1177/030913339702100302

Burns, M.J., Walsh, C.J., Fletcher, T.D., Ladson, A.R., & Hatt, B.E. (2015). A landscape measure of urban stormwater runoff effects is a better predictor of stream condition than a suite of hydrologic factors. Ecohydrology, 8(1). https://doi.org/10.1002/eco.1497

Cerdà, A., & Doerr, S.H. (2005). Influence of vegetation recovery on soil hydrology and erodibility following fire: An 11-year investigation. *International Journal of Wildland Fire*, *14*(4). https://doi.org/10.1071/WF05044

Charters, F.J., Cochrane, T.A., & O'Sullivan, A.D. (2016). Untreated runoff quality from roof and road surfaces in a low intensity rainfall climate. *Science of the Total Environment*, *550*. https://doi.org/10.1016/j.scitotenv.2016.01.093

Chin, D.A. (2021). Deficiencies in the curve number method. Journal of Irrigation and Drainage Engineering, 147(5). https://doi.org/10.1061/(asce)ir.1943-4774.0001552

Cizek, A. R., Hunt, W. F., Winston, R. J., & Lauffer, M. S. (2017). Hydrologic Performance of Regenerative Stormwater Conveyance in the North Carolina Coastal Plain. *Journal of Environmental Engineering*, *143*(9). https://doi.org/10.1061/(asce)ee.1943-7870.0001198

Cizek, A. R., Hunt, W. F., Winston, R. J., Waickowski, S. E., Narayanaswamy, K., & Lauffer, M. S. (2018). Water Quality and Hydrologic Performance of a Regenerative Stormwater Conveyance in the Piedmont of North Carolina. *Journal of Environmental Engineering*, *144*(8). https://doi.org/10.1061/(asce)ee.1943-7870.0001344

Clark, L.A., & Wynn, T.M. (2007). Methods for Determining Streambank Critical Shear Stress and Soil Erodibility: Implications for Erosion Rate Predictions. *Transactions of the ASABE*, *50*(1). https://doi.org/10.13031/2013.22415

Cluer, B., & Thorne, C. (2014). A stream evolution model integrating habitat and ecosystem benefits. *River Research and Applications*, *30*(2). https://doi.org/10.1002/rra.2631

CEIWR-HEC. (2015). *HEC-RAS USDA-ARS bank stability & toe erosion model (BSTEM)*.

Dabney, S.M., Shields, F.D., Temple, D.M., & Langendoen, E.J. (2004). Erosion processes in gullies modified by establishing grass hedges. *Transactions of the American Society of Agricultural Engineers*, *47*(5). https://doi.org/ 10.13031/2013.17634

Dagenais, D., Thomas, I., & Paquette, S. (2017). Siting green stormwater infrastructure in a neighbourhood to maximise secondary benefits: lessons learned from a pilot project. *Landscape Research*, *42*(2). https://doi.org/10.1080/01426397.2016.1228861

Daly, E. R., Fox, G. A., Al-Madhhachi, A. T., & Miller, R. B. (2013). A scour depth approach for deriving erodibility parameters from jet erosion tests. *Transactions of the ASABE*, *56*(6). https://doi.org/10.13031/trans.56.10350

Daly, E. R., Fox, G. A., Enlow, H. K., Storm, D. E., & Hunt, S. L. (2015). Site-scale variability of streambank fluvial erodibility parameters as measured with a jet erosion test. *Hydrological Processes*, *29*(26). https://doi.org/10.1002/hyp.10547

Damte, F., G_Mariam, B., Ayana, M. T., Lohani, T. K., Dhiman, G., & Shabaz, M. (2021). Computing the sediment and ensuing its erosive activities using HEC-RAS to surmise the flooding in Kulfo River in Southern Ethiopia. *World Journal of Engineering*, *18*(6). https://doi.org/10.1108/WJE-01-2021-0002

Daren Harmel, R., Haan, C. T., & Dutnell, R. C. (1999). Evaluation of Rosgen's streambank erosion potential assessment in northeast Oklahoma. *Journal of the American Water Resources Association*, *35*(1). https://doi.org/10.1111/j.1752-1688.1999.tb05456.x

Doll, B. A., Kurki-Fox, J.J., & Line, D.E. (2020). A framework for planning and evaluating the role of urban stream restoration for improving transportation resilience to extreme rainfall events. *Water (Switzerland)*, *12*(6). https://doi.org/10.3390/w12061620

Doll, B. A., Kurki-Fox, J.J., Page, J.L., Nelson, N.G., & Johnson, J.P. (2020). Flood flow frequency analysis to estimate potential floodplain nitrogen treatment during overbank flow events in urban stream restoration projects. *Water (Switzerland)*, *12*(6). https://doi.org/10.3390/W12061568

Doll, B.A., Wise-Frederick, D.E., Buckner, C.M., Wilkerson, S.D., Harman, W.A., Smith, R.E., & Spooner, J. (2002). Hydraulic geometry relationships for urban streams throughout the Piedmont of North Carolina. *Journal of the American Water Resources Association*, *38*(3). https://doi.org/10.1111/j.1752-1688.2002.tb00986.x

Douglas-Mankin, K.R., Roy, S.K., Sheshukov, A.Y., Biswas, A., Gharabaghi, B., Binns, A., Rudra, R., Shrestha, N.K., & Daggupati, P. (2020). A comprehensive review of ephemeral gully erosion models. In *Catena* (Vol. 195). https://doi.org/10.1016/j.catena.2020.104901

Driscoll, E.D., Palhegyi, G.E., Strecker, E.W., & Shelley, P.E. (1989). *Analysis of storm event characteristics for selected rainfall gauges throughout the United States*.

Dutta, S. (2016). Soil erosion, sediment yield and sedimentation of reservoir: A review. Modeling Earth Systems and Environment, 2(3). https://doi.org/10.1007/s40808-016-0182-y

Engelund, F., & Hansen, E. (1967). *A monograph on sediment transport in alluvial streams*. http://resolver.tudelft.nl/uuid:81101b08-04b5-4082-9121-861949c336c9

ESRI. (2019). *ArcGIS* (10.7.1). https://www.esri.com/en-us/store/overview

Faraway, J.J. (2016). Extending the Linear model with R. *Extending the Linear Model with R*. https://doi.org/10.1201/b21296

Flores-Cervantes, J.H., Istanbulluoglu, E., & Bras, R.L. (2006). Development of gullies on the landscape: A model of headcut retreat resulting from plunge pool erosion. *Journal of Geophysical Research: Earth Surface*, *111*(1). https://doi.org/10.1029/2004JF000226

Fortier, S., & Scobey, F.C. (1926). Permissible Canal Velocities. *Transactions of the American Society of Civil Engineers*, *89*(1). https://doi.org/10.1061/taceat.0003574

Fox, G.A., Guertault, L., Castro-Bolinaga, C., & Swanson, A. (2022). Guidance on applied pressure heads for quantifying cohesive soil erodibility with a jet erosion test (JET). *Journal of the American Society of Agricultural and Biological Engineers*, *65*(6). https://doi.org/10.13031/ja.14884

Fox, G. A., Wilson, G. V., Simon, A., Langendoen, E.J., Akay, O., & Fuchs, J.W. (2007). Measuring streambank erosion due to ground water seepage: Correlation to bank pore water pressure, precipitation and stream stage. *Earth Surface Processes and Landforms*, *32*(10). https://doi.org/10.1002/esp.1490

Ghimire, S.K., Higaki, D., & Bhattarai, T.P. (2006). Gully erosion in the Siwalik Hills, Nepal: Estimation of sediment production from active ephemeral gullies. *Earth Surface Processes and Landforms*, *31*(2). https://doi.org/10.1002/esp.1320

Google. (2022). *Google Earth Pro* (7.3.4).

Gordon, L.M., Bennett, S.J., Bingner, R.L., Theurer, F.D., & Alsono, C.V. (2007). Simulating ephemeral gully erosion in AnnAGNPS. *Transactions of the American Society of Agricultural and Biological Engineers*, *50*(3).

Haghiabi, A. H., & Zaredehdasht, E. (2012). Evaluation of HEC-RAS ability in erosion and sediment transport forecasting. *World Applied Sciences Journal*, *17*(11).

Haghnazari, F., Shahgholi, H., & Feizi, M. (2015). Factors affecting the infiltration of agricultural soils: review. *International Journal of Agronomy and Agricultural Research*, *6*(5).

Hancock, G. R., & Lowry, J. B. C. (2015). Hillslope erosion measurement-a simple approach to a complex process. *Hydrological Processes*, *29*(22). https://doi.org/10.1002/hyp.10608

Hanson, G. J. (1990). Surface erodibility of earthen channels at high stresses. Part II - Developing an in situ testing device. *Transactions of the American Society of Agricultural Engineers*, *33*(1). https://doi.org/10.13031/2013.31306

Hanson, G. J., & Cook, K. R. (1997). Development of excess shear stress parameters for circular jet testing. *Paper - American Society of Agricultural Engineers*, *2*.

Hanson, G. J., & Cook, K. R. (2004). Apparatus, test procedures, and analytical methods to measure soil erodibility in situ. *Applied Engineering in Agriculture*, *20*(4).

Hanson, G. J., Robinson, K. M., & Cook, K. R. (2002). Scour below an overfall: Part II. Prediction. *Transactions of the American Society of Agricultural Engineers*, *45*(4). https://doi.org/10.13031/2013.9948

Hanson, G. J., & Simon, A. (2001). Erodibility of cohesive streambeds in the loess area of the Midwestern USA. *Hydrological Processes*, *15*(1). https://doi.org/10.1002/hyp.149

Han, Y., Lau, S.-L., Kayhanian, M., & Stenstrom, M.K. (2006). Characteristics of highway stormwater runoff. *Water Environment Research*, *78*(12). https://doi.org/10.2175/106143006x95447

Harden, C. P., Foster, W., Morris, C., Chartrand, K. J., & Henry, E. (2009). Rates and processes of streambank erosion in tributaries of the Little River, Tennessee. *Physical Geography*, *30*(1). https://doi.org/10.2747/0272-3646.30.1.1

Harman, W. (2000). *Finding bankfull stage in North Carolina streams*. https://content.ces.ncsu.edu/finding-bankfull-stage-in-north-carolina-streams

Harman, W. A., Jennings, G. D., Patterson, J. M., Clinton, D. R., Slate, L. O., Jessup, A. G., Everhart, J. R., Smith, R. E., Olsen, D. S., & Potyondy, J. P. (1999). Bankfull hydraulic geometry relationships for North Carolina streams. *Wildlife Hydrology*, *1978*.

Harman, W. A., Wise, D. E., Walker, M. A., Morris, R., Cantrell, M. A., Clemmons, M., Jennings, G. D., Clinton, D., & Patterson, J. (2014). Bankfull regional curves for North Carolina mountain streams. *Water Resources in Extreme Environments, Proceedings*, *2000*(1).

Harrelson, C.C., Rawlins, C.L., & Potyondy, J.P. (1994). Stream channel reference sites: an illustrated guide to field technique. *General Technical Report - US Department of Agriculture, Forest Service*, *RM-245*.

Hastie, T., Tibshirani, R., & Friedman, J. (2009). Springer Series in Statistics The elements of statistical learning - data mining, inference, and prediction. *Springer* (Vol. 2).

Hawley, R. J., Bledsoe, B. P., Stein, E. D., & Haines, B. E. (2012). Channel Evolution Model of Semiarid Stream Response to Urban-Induced Hydromodification. *Journal of the American Water Resources Association*, *48*(4). https://doi.org/10.1111/j.1752-1688.2012.00645.x

Hawley, R.J., Goodrich, J.A., Korth, N.L., Rust, C.J., Fet, E.V., Frye, C., MacMannis, K. R., Wooten, M.S., Jacobs, M., & Sinha, R. (2017). Detention outlet retrofit improves the functionality of existing detention basins by reducing erosive flows in receiving channels. *Journal of the American Water Resources Association*, *53*(5). https://doi.org/10.1111/1752-1688.12548

Hawley, R. J., MacMannis, K. R., Wooten, M. S., Fet, E. v., & Korth, N. L. (2020). Suburban stream erosion rates in northern Kentucky exceed reference channels by an order of magnitude and follow predictable trajectories of channel evolution. *Geomorphology*, *352*. https://doi.org/10.1016/j.geomorph.2019.106998

Hawley, R.J., & Vietz, G.J. (2016). Addressing the urban stream disturbance regime. *Freshwater Science*, *35*(1). https://doi.org/10.1086/684647

Hillel, D. (2003). Introduction to Environmental Soil Physics. In *Introduction to Environmental Soil Physics*. https://doi.org/10.1016/B978-0-12-348655-4.X5000-X

Homer, C., Dewitz, J., Jin, S., Xian, G., Costello, C., Danielson, P., Gass, L., Funk, M., Wickham, J., Stehman, S., Auch, R., & Riitters, K. (2020). Conterminous United States land cover change patterns 2001–2016 from the 2016 National Land Cover Database. *ISPRS Journal of Photogrammetry and Remote Sensing*, *162*. https://doi.org/10.1016/j.isprsjprs.2020.02.019

Hoomehr, S., Akinola, A.I., Wynn-Thompson, T., Garnand, W., & Eick, M.J. (2018). Water temperature, pH, and road salt impacts on the fluvial erosion of cohesive streambanks. *Water (Switzerland)*, *10*(3). https://doi.org/10.3390/w10030302

Hopkins, K.G., Bhaskar, A.S., Woznicki, S.A., & Fanelli, R.M. (2020). Changes in event-based streamflow magnitude and timing after suburban development with infiltration-based stormwater management. Hydrological Processes, 34(2). https://doi.org/10.1002/hyp.13593

Hopkins, K.G., Morse, N.B., Bain, D.J., Bettez, N.D., Grimm, N.B., Morse, J.L., Palta, M.M., Shuster, W.D., Bratt, A.R., & Suchy, A.K. (2015). Assessment of regional variation in streamflow responses to urbanization and the persistence of physiography. Environmental Science and Technology, 49(5). https://doi.org/10.1021/es505389y

Huang, C., Wells, L. K., & Norton, L. D. (1999). Sediment transport capacity and erosion processes: Model concepts and reality. *Earth Surface Processes and Landforms*, *24*(6). https://doi.org/10.1002/(SICI)1096-9837(199906)24:6<503::AID-ESP972>3.0.CO;2-T

Hunt, W.F., Waickowski, S.E., & Lord, W.G. (2021). *Maintenance costs of stormwater control measures (SCMs) in North Carolina*. https://repository.lib.ncsu.edu/handle/1840.20/39523

Ismail, J., & Ravichandran, S. (2008). RUSLE2 model application for soil erosion assessment using remote sensing and GIS. *Water Resources Management*, *22*(1). https://doi.org/10.1007/s11269-006-9145-9

James, G., Witten, D., Hastie, T., & Tibshirani, R. (2000). An introduction to statistical learning. *Current medicinal chemistry, 7*(10). https://doi.org/10.1007/978-1-4614-7138-7

Jia, C., Sun, B., Yu, X., & Yang, X. (2020). Analysis of runoff and sediment losses from a sloped roadbed under variable rainfall intensities and vegetation conditions. *Sustainability (Switzerland)*, *12*(5). https://doi.org/10.3390/su12052077

Jollife, I.T., & Cadima, J. (2016). Principal component analysis: A review and recent developments. *Philosophical Transactions of the Royal Society A: Mathematical, Physical and Engineering Sciences, 374*(2065). https://doi.org/10.1098/rsta.2015.0202

Joseph, V.R. (2022). Optimal ratio for data splitting. *Statistical Analysis and Data Mining: The ASA Data Science Journal*, *15*(4), 531–538.

Karamigolbaghi, M., Ghaneeizad, S. M., Atkinson, J. F., Bennett, S. J., & Wells, R. R. (2017). Critical assessment of jet erosion test methodologies for cohesive soil and sediment. *Geomorphology*, *295*. https://doi.org/10.1016/j.geomorph.2017.08.005

Kayhanian, M., Fruchtman, B.D., Gulliver, J.S., Montanaro, C., Ranieri, E., & Wuertz, S. (2012). Review of highway runoff characteristics: Comparative analysis and universal implications. *Water Research*, *46*(20). https://doi.org/10.1016/j.watres.2012.07.026

Kayhanian, M., Suverkropp, C., Ruby, A., & Tsay, K. (2007). Characterization and prediction of highway runoff constituent event mean concentration. *Journal of Environmental Management*, *85*(2). https://doi.org/10.1016/j.jenvman.2006.09.024

Khanal, A., & Fox, G.A. (2017). Detachment characteristics of root-permeated soils from laboratory jet erosion tests. *Ecological Engineering*, *100*. https://doi.org/10.1016/j.ecoleng.2016.10.081

Khanal, A., Fox, G.A., & Al-Madhhachi, A. T. (2016a). Variability of Erodibility Parameters from Laboratory Mini Jet Erosion Tests. *Journal of Hydrologic Engineering*, *21*(10). https://doi.org/10.1061/(asce)he.1943-5584.0001404

Khanal, A., Klavon, K.R., Fox, G.A., & Daly, ER. (2016b). Comparison of linear and nonlinear models for cohesive sediment detachment: Rill erosion, hole erosion test, and streambank erosion studies. *Journal of Hydraulic Engineering*, *142*(9). https://doi.org/10.1061/(asce)hy.1943-7900.0001147

Kinnell, P.I.A. (2008). Sediment delivery from hillslopes and the universal soil loss equation: Some perceptions and misconceptions. Hydrological Processes, 22(16). https://doi.org/10.1002/hyp.6903

Kinnell, P. I. A. (2017). A comparison of the abilities of the USLE-M, RUSLE2 and WEPP to model event erosion from bare fallow areas. *Science of the Total Environment*, *596–597*. https://doi.org/10.1016/j.scitotenv.2017.04.046

Klavon, K., Fox, G., Guertault, L., Langendoen, E., Enlow, H., Miller, R., & Khanal, A. (2017). Evaluating a process-based model for use in streambank stabilization: insights on the Bank Stability and Toe Erosion Model (BSTEM). *Earth Surface Processes and Landforms*, *42*(1). https://doi.org/10.1002/esp.4073

Koryto, K. M., Hunt, W. F., & Page, J. L. (2017). Hydrologic and water quality performance of regenerative stormwater conveyance installed to stabilize an eroded outfall. *Ecological Engineering*, *108*. https://doi.org/10.1016/j.ecoleng.2017.04.041

Kotsiantis, S.B. (2013). Decision trees: A recent overview. *Artificial Intelligence Review, 39*(4). https://doi.org/10.1007/s10462-011-9272-4

Kranz, C.N., McLaughlin, R.A., Johnson, A., Miller, G., & Heitman, J.L. (2020). The effects of compost incorporation on soil physical properties in urban soils – A concise review. Journal of Environmental Management, 261. https://doi.org/10.1016/j.jenvman.2020.110209

Krause, P., Boyle, D.P., & Bäse, F. (2005). Comparison of different efficiency criteria for hydrological model assessment. *Advances in Geosciences*, *5*. https://doi.org/10.5194/adgeo-5-89-2005

Laflen, J.M., Elliot, W.J., Flanagan, D.C., Meyer, C.R., & Nearing, M.A. (1997). WEPP-predicting water erosion using a process-based model. *Journal of Soil and Water Conservation*, *52*(2)

Lammers, R. W., Dell, T. A., & Bledsoe, B. P. (2020). Integrating stormwater management and stream restoration strategies for greater water quality benefits. *Journal of Environmental Quality*, *49*(3). https://doi.org/10.1002/jeq2.20047

Langendoen, E.J., & Simon, A. (2008). Modeling the Evolution of Incised Streams. II: Streambank Erosion. *Journal of Hydraulic Engineering*, *134*(7). https://doi.org/10.1061/(asce)0733-9429(2008)134:7(905)

Langendoen, E.J., & Ursic, M. (2016). *Bank stability and toe erosion model* (Version 5.4). USDA Agricultural Research Service. https://www.ars.usda.gov/southeast-area/oxford-ms/national-sedimentation-laboratory/watershed-physical-processes-research/research/bstem/overview/

Laursen, E.M. (1958). The total sediment load of streams. *Journal of the Hydraulic Division*, *84*(HY1). https://doi.org/10.1061/jyceaj.0000158

Léonard, J., & Richard, G. (2004). Estimation of runoff critical shear stress for soil erosion from soil shear strength. Catena, 57(3). https://doi.org/10.1016/j.catena.2003.11.007

Leopold, L. B., & Maddock, T. Jr. (1953). The Hydraulic Geometry of Stream Channels and Some Physiographic Implications. In *Geological Survey Professional Paper 252*.

Lindow, N., Fox, G.A., & Evans, R.O. (2009). Seepage erosion in layered stream bank material. *Earth Surface Processes and Landforms*, *34*(12). https://doi.org/10.1002/esp.1874

Line, D.E., & Hunt, W.F. (2009). Performance of a bioretention area and a level spreader-grass filter strip at two highway sites in North Carolina. *Journal of Irrigation and Drainage Engineering*, *135*(2). https://doi.org/10.1061/(asce)0733-9437(2009)135:2(217)

Litschert, S.E., & MacDonald, L.H. (2009). Frequency and characteristics of sediment delivery pathways from forest harvest units to streams. *Forest Ecology and Management*, *259*(2). https://doi.org/10.1016/j.foreco.2009.09.038

Liu, H., Cleveland, T.G., & Wang, K.H. (1999). Laboratory tests of erosion dependence on properties of soils and rainfall. *Journal of the American Water Resources Association*, *35*(1). https://doi.org/10.1111/j.1752-1688.1999.tb05461.x

Liu, Y., Yang, W., Yu, Z., Lung, I., & Gharabaghi, B. (2015). Estimating Sediment Yield from Upland and Channel Erosion at A Watershed Scale Using SWAT. *Water Resources Management*, *29*(5). https://doi.org/10.1007/s11269-014-0729-5

Luell, S.K., Hunt, W.F., & Winston, R.J. (2011). Evaluation of undersized bioretention stormwater control measures for treatment of highway bridge deck runoff. *Water Science and Technology*, *64*(4). https://doi.org/10.2166/wst.2011.736

Luffman, I.E., Nandi, A., & Spiegel, T. (2015). Gully morphology, hillslope erosion, and precipitation characteristics in the Appalachian Valley and Ridge province, southeastern USA. *Catena*, *133*. https://doi.org/10.1016/j.catena.2015.05.015

Mahalder, B., Schwartz, J.S., Palomino, A.M., & Zirkle, J. (2018). Estimating erodibility parameters for streambanks with cohesive soils using the mini jet test device: A comparison of field and computational methods. *Water (Switzerland)*, *10*(3). https://doi.org/10.3390/w10030304

Mahalder, B., Schwartz, J. S., Wynn-Thompson, T.M., Palomino, A.M., & Zirkle, J. (2022). Comparison of erodibility parameters for cohesive streambank soils between in situ jet test device and laboratory conduit flume. *Journal of Hydraulic Engineering*, *148*(1). https://doi.org/10.1061/(asce)hy.1943-7900.0001938

Malcom, H.R. (1989). *Elements of urban stormwater design*. North Carolina State University.

Marois, D.E., & Mitsch, W.J. (2017). A mangrove creek restoration plan utilizing hydraulic modeling. *Ecological Engineering*, *108*. https://doi.org/10.1016/j.ecoleng.2017.06.063

Marshall, S., Pettigrove, V., Carew, M., & Hoffmann, A. (2010). Isolating the impact of sediment toxicity in urban streams. *Environmental Pollution*, *158*(5). https://doi.org/10.1016/j.envpol.2009.11.019

Maugnard, A., Van Dyck, S., & Bielders, C L. (2014). Assessing the regional and temporal variability of the topographic threshold for ephemeral gully initiation using quantile regression in Wallonia (Belgium). *Geomorphology*, *206*. https://doi.org/10.1016/j.geomorph.2013.10.007

McCool, D.K., & Williams, J.D. (2008). Soil erosion by water. In S. E. Jorgensen & B. D. Fath (Eds.), *Ecological Processes* (1st ed., Vol. 4, pp. 3284–3290). Elsevier B.V.

MDOT SHA. (2018). *Alternative headwater channel and outfall crediting protocol*. https://www.roads.maryland.gov/OED/2018-02-26_Rev%202018-03-20%20Alternative%20Headwater%20Channel%20and%20Outfall%20Crediting%20Protocol.pdf

Metcalf, C. K., Wilkerson, S. D., & Harman, W. A. (2009). Bankfull regional curves for north and northwest Florida streams. *Journal of the American Water Resources Association*, *45*(5). https://doi.org/10.1111/j.1752-1688.2009.00364.x

Meyer-Peter, E., & Müller, R. (1948). Formulas for bedload transport. *Proceedings of the 2nd International Association for Hydro-Environment Engineering and Research meeting*. http://resolver.tudelft.nl/uuid:4fda9b61-be28-4703-ab06-43cdc2a21bd7

Moore, C. E., Loheide, S. P., Lowry, C. S., & Lundquist, J. D. (2014). Instream restoration to improve the ecohydrologic function of a subalpine meadow: Pre-implementation modeling with HEC-RAS. *Journal of the American Water Resources Association*, *50*(4). https://doi.org/10.1111/jawr.12155

Morse, C. C., Huryn, A. D., & Cronan, C. (2003). Impervious surface area as a predictor of the effects of urbanization on stream insect communities in Maine, U.S.A. In *Environmental Monitoring and Assessment* (Vol. 89, Issue 1). https://doi.org/10.1023/A:1025821622411

Myers, D. T., Rediske, R. R., & McNair, J. N. (2019). Measuring streambank erosion: A comparison of erosion pins, total station, and terrestrial laser scanner. *Water (Switzerland)*, *11*(9). https://doi.org/10.3390/w11091846

Myles, A.J., Feudale, R.N., Liu, Y., Woody, N.A., & Brown, S.D. (2004). An introduction to decision tree modeling. *Journal of Chemometrics, 18*(6). https://doi.org/10.1002/cem.873

Nachtergaele, J., Poesen, J., Vandekerckhove, Oostwoud Wijdenes, D., & Roxo, M. Testing the ephemeral gully erosion model (EGEM) for two Mediterranean environments. (2001). *Earth Surface Processes and Landforms*, *26*(1). https://doi-org.prox.lib.ncsu.edu/10.1002/1096-9837(200101)26:1%3C17::AID-ESP149%3E3.0.CO;2-7

NC DEQ. (2017). *North Carolina stormwater control measure crediting document*. https://deq.nc.gov/about/divisions/energy-mineral-and-land-resources/stormwater/stormwater-program/stormwater-design

NC DEQ. (2022). *North Carolina 2022 303(D) list*. https://deq.nc.gov/about/divisions/water-resources/water-planning/modeling-assessment/water-quality-data-assessment/integrated-report-files

NCDOT. (2022, August 8). *GIS data layers*. https://connect.ncdot.gov/resources/gis/pages/gis-data-layers.aspx

NC DPS. (2016, July 31). *Elevation data download*. https://sdd.nc.gov/NCIDLogin.aspx

Nehrke, S. M., & Roesner, L. A. (2004). Effects of Design Practice for Flood Control and Best Management Practices on the Flow-Frequency Curve. *Journal of Water Resources Planning and Management*, *130*(2). https://doi.org/10.1061/(asce)0733-9496(2004)130:2(131)

NOAA. (2006, July 31). *Precipitation-frequency atlas of the United States, Ohio River Basin and surrounding states (Delaware, District of Columbia, Illinois, Indiana, Kentucky, Maryland, New Jersey, North Carolina, Ohio, Pennsylvania, South Carolina, Tennessee, Virginia, West Virginia)*. https://hdsc.nws.noaa.gov/hdsc/pfds/pfds_map_cont.html

NRCS. (2007). Chapter 7 hydrologic soil groups. *USDA Natural Resource Conservation Service National Engineering Handbook - Part 630 Hydrology*.

O'Driscoll, M., Clinton, S., Jefferson, A., Manda, A., & McMillan, S. (2010). Urbanization effects on watershed hydrology and in-stream processes in the southern United States. In *Water (Switzerland)* (Vol. 2, Issue 3). https://doi.org/10.3390/w2030605

Opher, T., & Friedler, E. (2010). Factors affecting highway runoff quality. *Urban Water Journal, 7*(3). https://doi.org/10.1080/15730621003782339

Osman, A. M., & Thorne, C. R. (1988). Riverbank Stability Analysis. I: Theory. *Journal of Hydraulic Engineering*, *114*(2). https://doi.org/10.1061/(asce)0733-9429(1988)114:2(134)

Owoputi, L. O., & Stolte, W. J. (1995). Soil detachment in the physically based soil erosion process: a review. *Transactions - American Society of Agricultural Engineers*, *38*(4). https://doi.org/10.13031/2013.27927

Palmer, J. A., Schilling, K. E., Isenhart, T. M., Schultz, R. C., & Tomer, M. D. (2014). Streambank erosion rates and loads within a single watershed: Bridging the gap between temporal and spatial scales. *Geomorphology*, *209*. https://doi.org/10.1016/j.geomorph.2013.11.027

Papanicolaou, A.T.N., Elhakeem, M., Krallis, G., Prakash, S., & Edinger, J. (2008). Sediment transport modeling review- current and future developments. *Journal of Hydraulic Engineering*, *134*(1). https://doi.org/10.1061/(asce)0733-9429(2008)134:1(1)

Partheniades, E. (1965). Erosion and deposition of cohesive soils. Journal of the Hydraulics Division, 91(1). https://doi.org/10.1061/jyceaj.0001165

Paul, M. J., & Meyer, J. L. (2001). Streams in the urban landscape. In *Annual Review of Ecology and Systematics* (Vol. 32). https://doi.org/10.1146/annurev.ecolsys.32.081501.114040

Peacher, R.D., Lerch, R N., Schultz, R.C., Willett, C.D., & Isenhart, T.M. (2018). Factors controlling streambank erosion and phosphorus loss in claypan watersheds. *Journal of Soil and Water Conservation*, *73*(2). https://doi.org/10.2489/jswc.73.2.189

Pollen-Bankhead, N., & Simon, A. (2009). Enhanced application of root-reinforcement algorithms for bank-stability modeling. *Earth Surface Processes and Landforms*, *34*(4). https://doi.org/10.1002/esp.1690

Pollen-Bankhead, N., & Simon, A. (2010). Hydrologic and hydraulic effects of riparian root networks on streambank stability: Is mechanical root-reinforcement the whole story? *Geomorphology*, *116*(3–4). https://doi.org/10.1016/j.geomorph.2009.11.013

Pomeroy, C. A., Postel, N. A., O'Neill, P. A., & Roesner, L. A. (2008). Development of Storm-Water Management Design Criteria to Maintain Geomorphic Stability in Kansas City Metropolitan Area Streams. *Journal of Irrigation and Drainage Engineering*, *134*(5). https://doi.org/10.1061/(asce)0733-9437(2008)134:5(562)

Ponce, V.M., & Hawkins, R.H. (1996). Runoff curve number: Has it reached maturity? Journal of Hydrologic Engineering, 1(1). https://doi.org/10.1061/(asce)1084-0699(1996)1:1(11)

Prosser, I. P., & Rustomji, P. (2000). Sediment transport capacity relations for overland flow. *Progress in Physical Geography: Earth and Environment*, *24*(2). https://doi.org/10.1177/030913330002400202

Renard, K., Foster, G., Weesies, G., McCool, D., & Yoder, D. (1997). Predicting soil erosion by water: a guide to conservation planning with the Revised Universal Soil Loss Equation (RUSLE). In *Agricultural Handbook No. 703*.

Ritter, A., & Muñoz-Carpena, R. (2013). Performance evaluation of hydrological models: Statistical significance for reducing subjectivity in goodness-of-fit assessments. *Journal of Hydrology*, *480*. https://doi.org/10.1016/j.jhydrol.2012.12.004

Robinson, K.M., & Hanson, G.J. (1995). Large-scale headcut erosion testing. Transactions - American Society of Agricultural Engineers, 38(2). https://doi.org/10.13031/2013.27849

Roesner, L. A., Bledsoe, B. P., & Brashear, R. W. (2001). Are Best-Management-Practice Criteria Really Environmentally Friendly? *Journal of Water Resources Planning and Management*, *127*(3). https://doi.org/10.1061/(asce)0733-9496(2001)127:3(150)

Rohrer, C.A., & Roesner, L.A. (2006). Matching the critical portion of the flow duration curve to minimise changes in modelled excess shear. *Water Science and Technology*, *54*(6–7). https://doi.org/10.2166/wst.2006.590

Rosgen, D.L. (1994). A classification of natural rivers. *Catena*, *22*(3). https://doi.org/10.1016/0341-8162(94)90001-9

Rosgen, D.L. (2001). A Practical Method of Computing Streambank Erosion Rate. *Proceedings of the Seventh Federal Interagency Sedimentation Conference, March 25 to 29, 2001, Reno, Nevada*.

Rosgen, D.L. (2009). *A watershed assessment for river stability and sediment supply (WARSSS)* (D. Frantila, Ed.; 2nd ed.). Wildland Hydrology.

Rosgen, D. L. (2011). Natural channel design: Fundamental concepts, assumptions, and methods. *Geophysical Monograph Series*, *194*. https://doi.org/10.1029/2010GM000990

RStudio Team. (2021). RStudio™: Integrated development for R. *RStudio, Inc.,* Boston, MA.

Saatci, A. (1990). Velocity and depth of flow calculations in partially filled pipes. *Journal of Environmental Engineering*, *116*(6). https://doi.org/10.1061/(asce)0733-9372(1990)116:6(1202)

Sansalone, J.J., & Buchberger, S.G. (1996). Characterization of metals and solids in urban highway winter snow and spring rainfall-runoff. *Transportation Research Record*, *1523*. https://doi.org/10.3141/1523-18

Sass, C.K., & Keane, T.D. (2012). Application of Rosgen's BANCS Model for NE Kansas and the Development of Predictive Streambank Erosion Curves. *Journal of the American Water Resources Association*, *48*(4). https://doi.org/10.1111/j.1752-1688.2012.00644.x

Sathya, A., Thampi, S.G., & Chithra, N.R. (2021). Development of a framework for sand auditing of the Chaliyar River basin, Kerala, India using HEC-HMS and HEC-RAS model coupling. *International Journal of River Basin Management*. https://doi.org/10.1080/15715124.2021.1909604

Schueler, T.R., Fraley-McNeal, L., & Cappiella, K. (2009). Is Impervious Cover Still Important? Review of Recent Research. *Journal of Hydrologic Engineering*, *14*(4). https://doi.org/10.1061/(asce)1084-0699(2009)14:4(309)

Schultze, A.K., Gellert, G., Koenzen, U., Riecker, T., & Rittner, R. (2019). Systematic rehabilitation planning: a new decision support system for targeted morphological river restoration. *Water and Environment Journal*, *33*(1). https://doi.org/10.1111/wej.12384

Schumm, S.A., Harvey, M.D., & Watson, C.C. (1984). Incised channels: morphology, dynamics and control. In *Incised channels: morphology, dynamics and control.*

Shcherbakov, M.V., Brebels, A., Shcherbakova, N.L., Tyukov, A.P., Janovsky, T.A., & Kamaev, V.A. (2013). A survey of forecast error measures. World Applied Sciences Journal, 24(24). https://doi.org/10.5829/idosi.wasj.2013.24.itmies.80032

Shellberg, J.G., Brooks, A.P., & Rose, C.W. (2013). Sediment production and yield from an alluvial gully in Northern Queensland, Australia. *Earth Surface Processes and Landforms*, *38*(15). https://doi.org/10.1002/esp.3414

Shields, F.D., Lizotte, R.E., Knight, S.S., Cooper, C.M., & Wilcox, D. (2010). The stream channel incision syndrome and water quality. *Ecological Engineering*, *36*(1). https://doi.org/10.1016/j.ecoleng.2009.09.014

Sidorchuk, A. (1999). Dynamic and static models of gully erosion. *Catena*, *37*(3–4). https://doi.org/10.1016/S0341-8162(99)00029-6

Simon, A., & Collison, A.J.C. (2002). Quantifying the mechanical and hydrologic effects of riparian vegetation on streambank stability. *Earth Surface Processes and Landforms*, *27*(5). https://doi.org/10.1002/esp.325

Simon, A., Curini, A., Darby, S. E., & Langendoen, E. J. (2000). Bank and near-bank processes in an incised channel. *Geomorphology*, *35*(3–4). https://doi.org/10.1016/S0169-555X(00)00036-2

Simon, A., & Hupp, C. R. (1987). Channel evolution in modified alluvial streams. *Transportation Research Record*, *1151*.

Simon, A., Pollen-Bankhead, N., & Thomas, R. E. (2011). Development and application of a deterministic bank stability and toe erosion model for stream restoration. *Geophysical Monograph Series*, *194*. https://doi.org/10.1029/2010GM001006

Simon, A., & Rinaldi, M. (2000). Channel instability in the loess area of the midwestern United States. *Journal of the American Water Resources Association*, *36*(1). https://doi.org/10.1111/j.1752-1688.2000.tb04255.x

Simon, A., & Rinaldi, M. (2006). Disturbance, stream incision, and channel evolution: The roles of excess transport capacity and boundary materials in controlling channel response. *Geomorphology*, *79*(3–4). https://doi.org/10.1016/j.geomorph.2006.06.037

Simon, A., Thomas, R. E., & Klimetz, L. (2010). Comparison and experiences with field techniques to measure critical shear stress and erodibility of cohesive deposits. *Proceedings of the 2nd Joint Federal Inter-Agency Conference on Sedimentation and Hydrologic Modeling*.

Smith, D. J., Wynn-Thompson, T. M., Williams, M. A., & Seiler, J. R. (2021). Do roots bind soil? Comparing the physical and biological role of plant roots in fluvial streambank erosion: A mini-JET study. *Geomorphology*, *375*. https://doi.org/10.1016/j.geomorph.2020.107523

Stein, O. R., & Nett, D. D. (1997). Impinging jet calibration of excess shear sediment detachment parameters. *Transactions of the American Society of Agricultural Engineers*, *40*(6). https://doi.org/10.13031/2013.21421

Sweet, W. v., & Geratz, J. W. (2003). Bankfull hydraulic geometry relationships and recurrence intervals for North Carolina's Coastal Plain. *Journal of the American Water Resources Association*, *39*(4). https://doi.org/10.1111/j.1752-1688.2003.tb04411.x

Taguas, E.V., Yuan, Y., Bingner, R.L., & Gómez, J.A. (2012). Modeling the contribution of ephemeral gully erosion under different soil managements: A case study in an olive orchard microcatchment using the AnnAGNPS model. *Catena*, *98*. https://doi.org./10.1016/j.catena.2012.06.002

Thien, T.F., & Yeo, W.S. (2022). A comparative study between PCR, PLSR, and LW-PLS on the predictive performance at different data splitting ratios. *Chemical Engineering Communications*, *209*(11). https://doi.org/10.1080/00986445.2021.1957853

Thompson, J. M., Hathaway, J. M., & Schwartz, J. S. (2018). Three-Dimensional Modeling of the Hydraulic Function and Channel Stability of Regenerative Stormwater Conveyances. *Journal of Sustainable Water in the Built Environment*, *4*(3). https://doi.org/10.1061/jswbay.0000861

Thompson, J., Schwartz, J. S., & Hathaway, J. M. (2020). Performance Evaluation of a Regenerative Stormwater Conveyance System: Case Study in Knoxville, Tennessee. *Journal of Environmental Engineering*, *146*(7). https://doi.org/10.1061/(asce)ee.1943-7870.0001744

Thomsen, A.T.H., Nielsen, J.E., Riis, T., & Rasmussen, M.R. (2020). Hydraulic effects of stormwater discharge into a small stream. *Journal of Environmental Management*, *270*. https://doi.org/10.1016/j.jenvman.2020.110793

Tillinghast, E.D., Hunt, W.F., & Jennings, G.D. (2011). Stormwater control measure (SCM) design standards to limit stream erosion for Piedmont North Carolina. *Journal of Hydrology*, *411*(3–4). https://doi.org/10.1016/j.jhydrol.2011.09.027

Toffaleti, F.B. (1968). *A procedure for computation of the total river sand discharge and detailed distribution, bed to surface*. United States Army Corp of Engineers. http://hdl.handle.net/11681/1822

USACE. (2022). *HEC-RAS* (6.2). US Army Corps of Engineers.

USDA. (2015). *Web Soil Survey*. Natural Resources Conservation Service, United States Department of Agriculture.

USDA-NRCS. (2004). Estimation of direct runoff from storm rainfall. *National Engineering Handbook*.

USGS. (2018). National Hydrography Dataset. *The National Map*.

Valentin, C., Verstraeten, G., Nachtergaele, J., & Poesen, J. (2003). Gully erosion and environmental change: importance and research needs. *Catena*, *50*(2–4).

Vanmaercke, M., Poesen, J., van Mele, B., Demuzere, M., Bruynseels, A., Golosov, V., Bezerra, J. F. R., Bolysov, S., Dvinskih, A., Frankl, A., Fuseina, Y., Guerra, A. J. T., Haregeweyn, N., Ionita, I., Makanzu Imwangana, F., Moeyersons, J., Moshe, I., Nazari Samani, A., Niacsu, L., … Yermolaev, O. (2016). How fast do gully headcuts retreat? In *Earth-Science Reviews* (Vol. 154). https://doi.org/10.1016/j.earscirev.2016.01.009

Vericat, D., & Batalla, R. J. (2010). Sediment transport from continuous monitoring in a perennial Mediterranean stream. *Catena*, *82*(2). https://doi.org/10.1016/j.catena.2010.05.003

Vietz, G. J., Sammonds, M. J., Walsh, C. J., Fletcher, T. D., Rutherfurd, I. D., & Stewardson, M. J. (2014). Ecologically relevant geomorphic attributes of streams are impaired by even low levels of watershed effective imperviousness. *Geomorphology*, *206*. https://doi.org/10.1016/j.geomorph.2013.09.019

Violin, C. R., Cada, P., Sudduth, E. B., Hassett, B. A., Penrose, D. L., & Bernhardt, E. S. (2011). Effects of urbanization and urban stream restoration on the physical and biological structure of stream ecosystems. *Ecological Applications*, *21*(6). https://doi.org/10.1890/10-1551.1

Voli, M. T., Wegmann, K. W., Bohnenstiehl, D. W. R., Leithold, E., Osburn, C. L., & Polyakov, V. (2013). Fingerprinting the sources of suspended sediment delivery to a large municipal drinking water reservoir: Falls Lake, Neuse River, North Carolina, USA. *Journal of Soils and Sediments*, *13*(10). https://doi.org/10.1007/s11368-013-0758-3

Wahl, T. L. (2021). Methods for analyzing submerged jet erosion test data to model scour of cohesive soils. *Transactions of the ASABE*, *64*(3). https://doi.org/10.13031/TRANS.14212

Walsh, C. J., Fletcher, T. D., & Ladson, A. R. (2005a). Stream restoration in urban catchments through redesigning stormwater systems: Looking to the catchment to save the stream. *Journal of the North American Benthological Society*, *24*(3). https://doi.org/10.1899/04-020.1

Walsh, C. J., Fletcher, T. D., & Vietz, G. J. (2016). Variability in stream ecosystem response to urbanization: Unraveling the influences of physiography and urban land and water management. *Progress in Physical Geography*, *40*(5). https://doi.org/10.1177/0309133316671626

Walsh, C.J., Roy, A.H., Feminella, J.W., Cottingham, P.D., Groffman, P.M., & Morgan, R.P. (2005n). The urban stream syndrome: Current knowledge and the search for a cure. *Journal of the North American Benthological Society*, *24*(3). https://doi.org/10.1899/04-028.1

Watson, C. C., Biedenharn, D. S., & Bledsoe, B. P. (2002). Use of incised channel evolution models in understanding rehabilitation alternatives. *Journal of the American Water Resources Association*, *38*(1). https://doi.org/10.1111/j.1752-1688.2002.tb01542.x

Wischmeier, W., & Smith, D. (1978). Predicting rainfall erosion losses: a guide to conservation planning. U.S. Department of Agriculture Handbook No. 537. https://doi.org/10.1029/TR039i002p00285

Wilcock, P.R., & Crowe, J.C. (2003). Surface-based transport model for mixed-size sediment. *Journal of Hydraulic Engineering*, *129*(2). https://doi-org /10.1061/(ASCE)0733-9429(2003)129:2(120)

Willett, C.D., Lerch, R.N., Schultz, R.C., Berges, S.A., Peacher, R.D., & Isenhart, T.M. (2012). Streambank erosion in two watersheds of the central claypan region of Missouri, United States. *Journal of Soil and Water Conservation*, *67*(4). https://doi.org/10.2489/jswc.67.4.249

Williams, B. M., Hopkins, K. G., Metes, M. J., Jones, D. K., Gordon, S., & Hamilton, W. (2022). Tracking geomorphic changes after suburban development with a high density of green stormwater infrastructure practices in Montgomery County, Maryland. *Geomorphology*, *414*, 108399. https://doi.org/10.1016/j.geomorph.2022.108399

Williams, D.T., & Julien, P.Y. (1989). Applicability index for sand transport equations. *Journal of Hydraulic Engineering*, *115*(11). https://doi.org/10.1061/(asce)0733-9429(1989)115:11(1578)

Wilson, B. N. (1993a). Development of a fundamentally based detachment model. In *Transactions - American Society of Agricultural Engineers* (Vol. 36, Issue 4). https://doi.org/10.13031/2013.28441

Wilson, B. N. (1993b). Evaluation of a fundamentally based detachment model. In *Transactions - American Society of Agricultural Engineers* (Vol. 36, Issue 4). https://doi.org/10.13031/2013.28442

Winston, R.J., Lauffer, M.S., Narayanaswamy, K., McDaniel, A.H., Lipscomb, B.S., Nice, A.J., & Hunt, W.F. (2015). Comparing bridge deck runoff and stormwater control measure quality in North Carolina. *Journal of Environmental Engineering*, *141*(1). https://doi.org/10.1061/(asce)ee.1943-7870.0000864

Winston, R.J., Powell, J.T., & Hunt, W.F. (2019). Retrofitting a grass swale with rock check dams: hydrologic impacts. *Urban Water Journal*, *16*(6). https://doi.org/10.1080/1573062X.2018.1455881

Wischmeier, W., & Smith, D. (1978). Predicting rainfall erosion losses: a guide to conservation planning. In *U.S. Department of Agriculture Handbook No. 537*. https://doi.org/10.1029/TR039i002p00285

Wissler, A.D., Hunt, W F., & McLaughlin, R.A. (2020a). Hydrologic and water quality performance of two aging and unmaintained dry detention basins receiving highway stormwater runoff. *Journal of Environmental Management*, *255*. https://doi.org/10.1016/j.jenvman.2019.109853

Wissler, A.D., Hunt, W.F., & McLaughlin, R.A. (2020b). Water quality and hydrologic performance of two dry detention basins receiving highway stormwater runoff in the Piedmont region of North Carolina. *Journal of Sustainable Water in the Built Environment*, *6*(2). https://doi.org/10.1061/jswbay.0000915

Wolman, M. G., & Miller, J. P. (1960). Magnitude and Frequency of Forces in Geomorphic Processes. *The Journal of Geology*, *68*(1). https://doi.org/10.1086/626637

Wooten, M.S., Hawley, R.J., & Rust, C. (2022). Optimizing stormwater management to facilitate urban stream restoration via a science-based approach. *Freshwater Science*. https://doi.org/10.1086/721031

Woodward, D.E. (1999). Method to predict cropland ephemeral gully erosion. *Catena*, *37.* https://doi.org/ 10.1016/S0341-8162(99)00028-4

Wu, J.S., Allan, C.J., Saunders, W.L., & Evett, J.B. (1998). Characterization and pollutant loading estimation for highway runoff. *Journal of Environmental Engineering*, *124*(7). https://doi.org/10.1061/(asce)0733-9372(1998)124:7(584)

WV DEP. (2012). 4.2.7. Regenerative stormwater conveyance system (RSC). https://dep.wv.gov/WWE/Programs/stormwater/MS4/Pages/StormwaterManagementDesignandGuidanceManual.aspx

Yang, C.T. (1979). Unit stream power equations for total load. *Journal of Hydrology*, *40*(1-2). https://doi.org/10.1016/0022-1694(79)90092-1

Yang, C.T. (1984). Unit stream power equation for gravel. *Journal of Hydraulic Engineering*, *110*(12).

Yaw, M., Pizzi, D., AuBuchon, J., Gronewold, R., & Gibson, S. (2019). *Proceedings of SEDHYD2019: Conferences on sedimentation and hydrologic modeling* (Vol. 2). SEDHYD, Inc. https://www.sedhyd.org/2019/

Zaimes, G.N., & Schultz, R.C. (2012). Assessing riparian conservation land management practice impacts on gully erosion in Iowa. *Environmental Management*, *49*(5). https://doi.org/10.1007/s00267-012-9830-9

Zaimes, G.N., & Schultz, R.C. (2015). Riparian land-use impacts on bank erosion and deposition of an incised stream in north-central Iowa, USA. *Catena*, *125*. https://doi.org/10.1016/j.catena.2014.09.013

Zaimes, G.N., Schultz, R.C., & Tufekcioglu, M. (2009). Gully and stream bank erosion in three pastures with different management in southeast Iowa. *Journal of the Iowa Academy of Science*, *116*(1-4).

Zaimes, G., Tamparopoulos, A.E., Tufekcioglu, M., & Schultz, R.C. (2021). Understanding stream bank erosion and deposition in Iowa, USA: A seven year study along streams in different regions with different riparian land-uses. *Journal of Environmental Management*, *287*. https://doi.org/10.1016/j.jenvman.2021.112352